

SYNTHESIS OF BLOCK CONDUCTING COPOLYMERS OF CHOLESTERYL  
FUNCTIONALIZED THIOPHENE AND THEIR USE IN THE  
IMMOBILIZATION OF CHOLESTEROL OXIDASE

A THESIS SUBMITTED TO  
THE GRADUATE SCHOOL OF NATURAL AND APPLIED SCIENCES  
OF  
THE MIDDLE EAST TECHNICAL UNIVERSITY

BY

ALİ ÇIRPAN

IN PARTIAL FULFILLMENT OF THE REQUIREMENTS FOR THE DEGREE  
OF DOCTOR OF PHILOSOPHY  
IN  
THE DEPARTMENT OF CHEMISTRY

FEBRUARY 2004

Approval of the Graduate School of Natural and Applied Sciences.

---

Prof. Dr. Canan Özgen  
Director

I certify that this thesis satisfies all the requirements as a thesis for the degree of Doctor of Philosophy.

---

Prof. Dr. Hüseyin İşçi  
Head of the Department

This is to certify that we have read this thesis and that in our opinion it is fully adequate, in scope and quality, as a thesis for the degree of Doctor of Philosophy.

---

Prof. Dr. Levent Toppare  
Supervisor

Examining Committee Members

Prof. Dr. Levent Toppare

Prof. Dr. Hüseyin İşçi

Prof. Dr. Ahmet Önal

Prof. Dr. Duygu Kısakürek

Prof. Dr. Kadir Pekmez

## ABSTRACT

### SYNTHESIS OF BLOCK CONDUCTING COPOLYMERS OF CHOLESTERYL FUNCTIONALIZED THIOPHENE AND THEIR USE IN THE IMMOBILIZATION OF CHOLESTEROL OXIDASE

Çirpan, Ali

Ph.D., Department Chemistry

Supervisor: Prof. Dr. Levent Toppare

February 2004, 115 pages

Synthesis and characterization of conducting copolymers were achieved by using thiophene-3-yl acetic acid cholesteryl ester (CM) and poly (3-methylthienyl methacrylate) (PMTM). A new polythiophene containing a cholesteryl side chain in the  $\beta$ -position was chemically polymerized in nitromethane/carbon tetrachloride using  $\text{FeCl}_3$  as the oxidizing agent. Polymerization was also achieved by constant current electrolysis in dichloromethane. Subsequently, conducting copolymers of thiophene-3-yl acetic acid cholesteryl ester (CM), PCM1 (obtained from chemical polymerization method), PCM4 (obtained from constant current electrolysis) with pyrrole were synthesized. Thiophene functionalized

methacrylate monomer (MTM) was synthesized via esterification of the 3-thiophene methanol with methacryloyl chloride. The methacrylate monomer was polymerized by free radical polymerization in the presence of azobis (isobutyronitrile) (AIBN) as the initiator. Graft copolymers of poly (3-methylthienyl methacrylate)/polypyrrole, (PMTM2/PPy) and poly (3-methylthienyl methacrylate)/polythiophene, (PMTM2/PTh) were synthesized by constant potential electrolyses. PMTM2 coated Pt electrodes were utilized as the anode in the polymerization of pyrrole and thiophene. Moreover, oxidative polymerization of PMTM1 was studied by galvanostatic and chemical techniques. Characterizations of the samples were performed by CV, FTIR, NMR, DSC, TGA and SEM analyses. Electrical conductivities were measured by the four-probe technique.

Immobilization of invertase in conducting copolymer matrices, poly (3-methylthienyl methacrylate) with pyrrole and thiophene was achieved by constant potential electrolysis using the sodium dodecyl sulfate as the supporting electrolyte. Polythiophene was also used for immobilization matrices. Cholesterol oxidase has been immobilized in conducting copolymer of thiophene-3-yl acetic acid cholesteryl ester with polypyrrole (CM/PPy) and polypyrrole (PPy) by the electropolymerization method. *p*-Toluene sulfonic acid was used as a supporting electrolyte. Kinetic parameters (Kinetic parameters;  $V_{\max}$  and Michaelis-Menten constant;  $K_m$ ) and operational stability of enzyme electrodes were investigated. Surface morphology of the films was also examined.

Keywords: Electrochemical polymerization, conducting copolymers, enzyme immobilization, cholesterol oxidase, invertase.

## ÖZ

### KOLESTEROL FONKSİYONLU TİYOFEN İLE İLETKEN KOPOLİMERLERİN SENTEZİ VE KOLESTEROL OKSİDAZ EMZİMİ İÇİN TUTUKLAMA MATRİSİ OLARAK KULLANILMASI

Çırpan, Ali

Doktora, Kimya Bölümü

Tez Yöneticisi: Prof. Dr. Levent Toppare

Şubat 2004, 115 sayfa

Tiyofen-3-asetik asitin kolesteril esteri (CM) ve poli(3-metiltiyenil metakrilat) (PMTM) kullanılarak iletken kopolimerlerin sentezleri ve karakterizasyonları gerçekleştirildi.  $\beta$  pozisyonunda kolesteril gurubu bulunan yeni bir politiyofen kimyasal olarak nitrometan/karbon tetraklorür solvent çifti içinde  $FeCl_3$  katalizörü kullanılarak polimerleştirildi. Ayrıca polimerleşme sabit akım elektroliz yöntemi kullanılarak diklorometan içerisinde de gerçekleştirildi. Daha sonra elde edilen bu polimerlerle PCM1 (kimyasal yöntemle elde edilen), PCM4 (sabit akım elektrolizden elde edilen) ve CM ile pirol kullanılarak iletken kopolimerler sentezlendi. Tiyofen fonksiyonlu metakrilat monomeri (MTM) 3-tiyofen metanol ve metakriloil kloritin esterleşme reaksiyonu ile sentezlendi. Bu

metakrilat monomeri azobis (izobutronitril) (AIBN) başlatıcısı kullanılarak serbest radical yöntemiyle polimerleştirildi. Poli (3-metiltienil metakrilat)/polipirol (PMTM)/PPy, poli(3-metiltienil metakrilat)/politiyofen (PMTM)/PTh aşı kopolimerleri sabit gerilim elektroliz yöntemi ile sentezlendi. Yalıtkan PMTM2 ile kaplanmış platin elektrotlar pirol ve tiyofenin polimerleşmesi sırasında anot olarak kullanıldı. Ayrıca PMTM1 polimerinin kendi kendine tiyofen ünitesinden tekrar polimerleştirilmesi galvanostatik ve kimyasal teknikler ile gerçekleştirildi. Elde edilen tüm ürünlerin karakterizasyonları CV, FTIR, NMR, DSC, TGA ve SEM teknikleri kullanılarak yapıldı. İletkenlik ölçümleri ise dört-nokta tekniği ile yapıldı.

Sodyumdodesil sulfat (SDS) katkılı poli (3-metiltienil metakrilat) ile pirol ve tiyofen kopolimer matrisinde invertazın tutuklanması gerçekleştirildi.. Politiyofen de tutuklama matrisi olarak kullanıldı. Kolesterol oksidaz enzimi tiyofen-3-il asetik asit kolesteril ester ile polipirol (CM/PPy) ve polipirol (PPy) iletken polimer matrislerinde elektrokimyasal metotla tutuklandı. Destek elektrolit olarak p-toluen sulfonik asit kullanıldı. Enzim elektrotlarının kinetik parametreleri (Kinetic parametreler;  $V_{max}$  ve Michealis-Menten sabiti;  $K_m$ ) ve kullanım ömürleri araştırıldı. Filimlerin yüzey morfolojileri incelendi.

Anahtar kelimeler: Elektrokimyasal polimerleşme, iletken kopolimerler, enzim tutuklama, kolesterol oksidaz, invertaz.

**To My Brother, İrfan Çırpan**

## ACKNOWLEDGMENTS

I would like to express my sincere appreciation to Prof. Dr. Levent Toppare for his continuous guidance and contributions to my enjoyment and interest in research. He made this document possible by helping and encouraging me in all stages of my PhD work. I am grateful to him not only being my advisor and counselor but also being my friend.

I would like to extend my thanks to Prof. Dr. Yusuf Yağcı and Prof. Dr. Ahmet Önal for their discussions and helps through out this study.

I would like to thank to Assoc. Prof. Dr. Ufuk Bakır for her valuable criticism and comments on enzyme immobilization studies.

Thanks also should go to Dr. Selmiye Alkan for her friendship, useful conversations and cooperation.

I would like to thank to my friends: Atilla Cihaner, Hasan Koyuncu, Yusuf Güner, Ümit Kanışkan and Ömer Reis for their friendship.

I would like to thank all the post and present members of Toppare's group for their helps, their friendships and for making lab life more fun.

Finally, I wish to express my eternal gratitude to my family, especially to my brother, İrfan Çırpan, for his continuous supports and attempts to understand and encourage me during this work.

I also wish to thank to my colleagues in Chemistry Department of METU.

## TABLE OF CONTENTS

ABSTRACT.....	iii
ÖZ .....	v
ACKNOWLEDGMENTS .....	viii
TABLE OF CONTENTS .....	ix
LIST OF FIGURES .....	xv
LIST OF TABLES .....	xviii
ABBREVIATIONS .....	xix
CHAPTERS	
I. INTRODUCTION .....	1
1.1 Conducting Polymers.....	1
1.1.1 History of Conducting Polymer .....	1
1.1.2 Band Theory and Doping-Induced Transitions in Conjugated Polymers .....	2
1.1.3 Synthesis of Conducting Polymers.....	6
1.1.3.1 Electrochemical Polymerization.....	7
1.1.3.2 Chemical Polymerization .....	9
1.1.4 Polymer Electrochemistry .....	11
1.1.4.1 Cyclic Voltammetry Background.....	11
1.1.5 Conducting Copolymers.....	13
1.1.5.1 Blends .....	13
1.1.5.2 Block Copolymers .....	14
1.1.5.3 Graft Copolymers .....	15

1.1.6 Application of Conducting Polymers .....	17
1.2 Enzymes .....	20
1.2.1 Enzyme Classification .....	20
1.2.2 Kinetics of Enzyme Reactions .....	21
1.2.3 Immobilization of Enzymes .....	25
1.2.3.1 Adsorption .....	26
1.2.3.2 Covalent Binding .....	27
1.2.3.3 Entrapment .....	28
1.2.3.4 Encapsulation .....	29
1.2.3.5 Crosslinking .....	30
1.2.4 Enzyme Immobilization by Electropolymerization .....	30
1.2.5 Industrial applications of Immobilized Enzymes .....	33
1.2.5.1 Application of Immobilized Enzymes in the Food Industry .....	33
1.2.5.2 Application of Immobilized Enzyme in the Pharmaceutical Industry .....	33
1.2.5.3 Affinity Chromatography .....	34
1.2.5.4 Application of Immobilized Enzymes for Analytical Uses .....	35
1.2.6 Immobilization of Invertase .....	36
1.2.7 Immobilization of Cholesterol Oxidase .....	36
1.3 Aim of the Study .....	39
II. EXPERIMENTAL .....	40
2.1 Materials .....	40
2.2 Polymer Electrochemistry .....	41
2.2.1 Cyclic Voltammetry .....	41
2.2.2 Constant Current (Galvanostatic) Methods .....	42
2.2.3 Constant Potential (Potentiostatic) Methods .....	42
2.3 Instrumentation .....	42
2.3.1 Nuclear Magnetic Resonance Spectrometer .....	44

2.3.2	Fourier Transform Infrared Spectrometry.....	44
2.3.3	Gel Permeation Chromotography.....	45
2.3.4	Thermal Analysis .....	45
2.3.5	UV-Vis Spectrophotometry.....	45
2.3.6	Scanning Electron Microscopy .....	45
2.3.7	Conductivity Measurement .....	46
2.4	Synthesis of Conducting Copolymers.....	47
2.4.1	Conducting Graft Copolymers of Poly (3-Methylthienyl Methacrylate) with Pyrrole and Thiophene.....	47
2.4.1.1	Synthesis of 3-Methylthienyl Methacrylate .....	47
2.4.1.2	Bulk Polymerization of 3- Methylthienyl Methacrylate .....	48
2.4.1.3	Cyclic Voltammetry .....	48
2.4.1.4	Synthesis of Copolymers with Pyrrole by Electrochemical Polymerization.....	48
2.4.1.5	Synthesis of Copolymers with Thiophene by Electrochemical Polymerization.....	49
2.4.1.6	Oxidative Polymerization of PMTM1 with FeCl <sub>3</sub> ..	49
2.4.1.7	Oxidative Polymerization of PMTM1 by Constant Current Electrolysis .....	49
2.4.2	Synthesis and Characterization of Conducting Copolymers of Thiophene-3-yl Acetic Acid Cholesteryl Ester with Pyrrole .....	50
2.4.2.1	Synthesis of Cholesteryl Containing Thiophene Monomer .....	50
2.4.2.2	Cyclic Voltammetry .....	51
2.4.2.3	Potentiostatic Polymerization of CM .....	51
2.4.2.3.1	Self Polymerisation of CM.....	51
2.4.2.3.2	Synthesis of Copolymers of CM with Pyrrole .....	51

2.4.2.3.3	Synthesis of Copolymers of CM with Thiophene .....	52
2.4.2.4	Chemical Polymerization of CM and Doping with Iodine .....	52
2.4.2.5	Galvanostatic Polymerization of CM .....	53
2.4.2.6	Synthesis of Block Copolymers of PCM1 with Pyrrole and Thiophene.....	53
2.4.2.7	Synthesis of Block Copolymers of PCM4 with Pyrrole and Thiophene.....	54
2.5	Immobilization of Enzymes.....	54
2.5.1	Immobilization of Invertase in Conducting Copolymers of 3-Methylthienyl Methacrylate .....	54
2.5.1.1	Preparation of Enzyme Electrodes .....	54
2.5.1.2	Activity determination of Invertase.....	55
2.5.1.2.1	Preparation of Nelson's Reagent.....	55
2.5.1.2.2	Preparation of Arsenomolibdate Reagent	55
2.5.1.2.3	Activity Assay .....	56
2.5.1.3	Determination of Kinetic Parameters .....	56
2.5.1.4	Determination of Temperature .....	56
2.5.1.5	Determination of Operational Stability .....	57
2.5.1.6	Morphologies of Films .....	57
2.5.2	Immobilization of Cholesterol Oxidase in Conducting Copolymer of Thiophene-3-yl Acetic Acid Cholesteryl Ester with Pyrrole.....	57
2.5.2.1	Synthesis of Copolymer.....	57
2.5.2.2	Preparation of Enzyme Electrodes .....	58
2.5.2.3	Preparation of Cholesterol Solution .....	58
2.5.2.4	Enzyme Activity Measurement .....	59
2.5.2.5	Kinetic Studies of Free and Immobilized COD.....	59
2.5.2.6	Operational Stability of Immobilized COD.....	60
2.5.2.7	Surface Morphologies of Enzyme-Entrapped Film	60

III. RESULTS AND DISCUSSION .....	61
3.1 Conducting Copolymers .....	61
3.1.1 Conducting Graft Copolymers of Poly (3-Methylthienyl Methacrylate) with Pyrrole and Thiophene.....	61
3.1.1.1 Bulk Polymerization of 3-Methylthienyl Methacrylate.....	61
3.1.1.2 Cyclic Voltammetry .....	62
3.1.1.3 Oxidative Polymerization of PMTM1 .....	63
3.1.1.4 Synthesis of Copolymers.....	66
3.1.1.5 Conductivities of PMTM2/PPy and PMTM2/PTh Films.....	68
3.1.1.6 Thermal Properties .....	68
3.1.1.7 Morphologies of the Films .....	74
3.1.2 Synthesis and Characterization of Conducting Copolymers of Thiophene-3-yl Acetic Acid Cholesteryl Ester with Pyrrole.....	76
3.1.2.1 Cyclic Voltammetry .....	76
3.1.2.2 Characterization.....	78
3.1.2.3 <sup>1</sup> H NMR and FT-IR Characterization.....	79
3.1.2.4 Thermal Analysis.....	83
3.1.2.5 Conductivity Measurement.....	89
3.1.2.6 Scanning Electron Microscopy.....	89
3.2 Immobilization of Enzyme .....	91
3.2.1 Immobilization of Invertase in Conducting Copolymers of 3- Methylthienyl Methacrylate .....	91
3.2.1.1 Morphologies of the Films .....	92
3.2.1.2 Kinetic Studies of Immobilized Invertase .....	94
3.2.1.3 Operational Stability of the Enzyme Electrodes.....	94
3.2.1.4 Effect of Temperature on the Enzyme Electrode Response.....	96

3.2.2 Immobilization of Cholesterol Oxidase in Conducting Copolymer of Thiophene-3-yl Acetic Acid Cholesteryl Ester with Pyrrole .....	96
3.2.2.1 Kinetic Studies of Free and Immobilized COD.....	97
3.2.2.2 Operational Stability of Immobilized COD.....	98
3.2.2.3 Surface Morphologies of Enzyme-entrapped Film	100
 IV. CONCLUSION.....	 102
REFERENCES.....	103
VITA .....	113

## LIST OF FIGURES

1.1 Molecular structure, doping materials and conductivity of common organic conducting polymers.....	3
1.2 Band diagrams for neutral and positive solitons. (a) Schematic representation of neutral (left) and positive (right) solitons in degenerate PA, where D represents a dopant ion; (b) band diagrams for neutral (left) and positive (right) solitons with associated electronic transitions .....	5
1.3 Band theory and doping-induced structural transitions of polypyrrole. (a) Band theory of conjugated polymers. (b) Structural changes associated with polaron and bipolaron formation as a result of oxidative doping in polypyrrole.....	6
1.4 Resonance stabilization and electropolymerization mechanism of pyrrole. (a) Resonance stabilization of radical cation of pyrrole. (b) Proposed mechanism for the electrochemical polymerization of pyrrole .....	8
1.5 Lewis acid oxidative polymerization of an alkyl substituted thiophene .....	9
1.6 Potential coupling reactions for pyrrole during oxidative polymerization.	11
1.7 Schematic representation of transmissive electrochromic devices.....	18
1.8 Schematic representation of LEDs .....	19
1.9 Plot of initial velocity against substrate concentration for enzyme catalyzed reaction .....	24
1.10 Lineweaver- Burk plot.....	25
1.11 Principal methods of immobilization .....	26
1.12 The reaction catalyzed by invertase.....	36
1.13 The reaction catalyzed by cholesterol oxidase .....	37
2.1 H-shaped electrolysis cell .....	43

2.2 Cyclic voltammetry cell .....	44
2.3 Four-probe conductivity measurement .....	47
2.4 Electrochemical synthesis route for copolymerization.....	58
3.1 PMTM synthesis route.....	61
3.2 Cyclic voltammograms of (a) PMTM2 in the presence of thiophene (b) thiophene on a bare Pt electrode (c) PMTM2 in the presence of pyrrole (d) pyrrole on a bare Pt electrode.....	63
3.3 Galvanostatic polymerization route.....	64
3.4 FTIR spectra of PMTM .....	64
3.5 FTIR spectra of CPMTM .....	65
3.6 FTIR spectra of GPMTM .....	65
3.7 Electrochemical synthesis route for copolymerization.....	66
3.8 FTIR spectra of PMTM/PPy doped with $\text{BF}_4^-$ .....	67
3.9 FTIR spectra of PMTM/PTh doped with $\text{BF}_4^-$ .....	67
3.10 DSC thermograms of (a) PMTM2 (b) GPMTM1P (c) GPMTM1D (d) PMTM2/PTh ( $\text{BF}_4^-$ doped). .....	70
3.11 TGA curves for (a) PMTM2 (b) GPMTM1D (c) GPMTM1P (d) PMTM2/PTh ( $\text{BF}_4^-$ doped) .....	72
3.12 SEM micrographs of (a) Electrode side of washed PMTM2/PPy film ( $\text{PTS}^-$ doped) (b) Electrode side of washed PMTM2/PPy film ( $\text{DS}^-$ doped) (a) Solution side of unwashed PMTM2/PPy film ( $\text{BF}_4^-$ doped) (b) Solution side of washed PMTM2/PPy film ( $\text{BF}_4^-$ doped).....	75
3.13 Synthesis scheme of CM .....	76
3.14 Cyclic voltammograms of (a) monomer (CM), (b) CM in the presence of pyrrole, (c) pyrrole on a bare Pt electrode, (d) CM in the presence of thiophene and (e) thiophene on a bare Pt electrode.....	77
3.15 Reactions with CM .....	78
3.16 H-NMR spectra of CM .....	80
3.17 H-NMR spectra of PCM.....	80
3.18 FTIR spectra of CM.....	81

3.19 FTIR spectra of PCM .....	81
3.20 FTIR spectra of PCM4 .....	82
3.21 FTIR Spectra of PCM/PPy copolymer doped with PTS-.....	82
3.22 FTIR spectra of PCM/Py copolymer doped with DS-.....	83
3.23 TGA thermograms of (a) CM and (b) PCM1 .....	85
3.24 TGA thermograms of (a) PPy/CM (PTSA doped) and (b) PPy/CM (SDS doped) .....	86
3.25 DSC thermograms of (a) CM and (b) PCM1 .....	87
3.26 DSC thermograms of (a) PPy/CM (PTSA doped) and (b) PPy/CM (SDS doped) .....	88
3.27 SEM micrographs of (a) electrode side of washed PPy/CM (PTSA doped), (b) electrode side of washed PPy/CM (DS <sup>-</sup> doped), (c) electrode side of unwashed PPy/PCM4 (DS <sup>-</sup> doped) and (d) electrode side of washed PPy/PCM4 (DS <sup>-</sup> doped).....	90
3.28 Scanning electron micrographs of (a) solution side of EE2 (b) solution side of EE4 (c) solution side of EE3.....	93
3.29 Operational stability of (a) EE2, (b) EE3, (c) EE4 and (d) EE5.....	95
3.30 Optimum temperature of enzyme electrodes.....	96
3.31 Reaction scheme for the enzymatic measurement of cholesterol.....	97
3.32 Operational stability of the PPy/PTSA/COD electrode.....	99
3.33 Operational stability of the CM/PPy/PTSA/COD electrode .....	99
3.34 Scanning electron micrographs of (a) solution side of PPy/PTSA/COD electrode (b) electrode side of PPy/PTSA/COD electrode (c) solution side of CM/PPy/PTSA/COD electrode (d) electrode side of CM/PPy/PTSA/COD electrode .....	101

## LIST OF TABLES

3.1 Synthesis of poly (3- methylthienyl methacrylate) .....	62
3.2 Conductivities of the films (PMTM) .....	68
3.3 Conductivities of the films (CM) .....	89
3.4 Invertase activities in PMTM/PPy/SDS and (PMTM/PPy)/SDS polymer matrices .....	91
3.5 Kinetic parameters for hydrolytic breakdown of sucrose to glucose and fructose .....	94
3.6 Kinetic parameters of free and immobilized enzyme .....	98

## ABBREVIATION

AIBN	Azobisisobutyronitrile
AN	Acetonitrile
CB	Conduction band
CM	Thiophene-3-yl acetic acid cholesteryl ester
COD	Cholesterol oxidase
CPs	Conducting polymers
CPMTM	Chemically polymerized poly (3-methylthienyl methacrylate)
CV	Cyclic voltammetry
DSC	Differential scanning calorimetry
ECDs	Electrochromic devices
EPR	Electron paramagnetic resonance
FTIR	Fourier transform infrared spectrophotometer
GPMTM	Galvanostatically polymerized poly (3-methylthienyl methacrylate)
HOMO	highest occupied molecular orbital
LEDs	Light-emitting diodes
LUMO	lowest unoccupied molecular orbital
MTM	3-Methylthienyl methacrylate
NMR	Nuclear magnetic resonance
NM	Nitromethane
PA	Polyacetylene
PAn	Polyaniline
PEMA	Poly (ethyl methacrylate)
PMMA	Poly (methyl methacrylate)
PMTM	Poly (3-methylthienyl methacrylate)

PPP	poly(p-phenylene)
PPV	poly(p-phenylene vinylene)
PPy	Polypyrrole
Py	Pyrrole
PS	Polystyrene
PTh	Polythiophene
PTSA	p-toluene sulfonic acid
PVC	Polyvinylchloride
SEM	Scanning electron microscope
TBAFB	Tetrabutylammonium tetrafluoroborate
TGA	Thermal gravimetry analysis
VB	Valance band

## CHAPTER I

### INTRODUCTION

#### 1.1 Conducting Polymers

##### 1.1.1 History of Conducting Polymers

The chemistry Nobel Prize in year 2000 went to Alan Heeger, Alan MacDiarmid, and Hideki Shirakawa "for the discovery and development of electrically conductive polymers." The three winners established that polymer plastics can be made to conduct electricity if alternating single and double bonds link their carbon atoms, and electrons are either removed through oxidation or introduced through reduction. Normally the electrons in the bonds remain localized and cannot carry an electric current, but when the team "doped" the material with strong electron acceptors such as iodine, the polymer began to conduct nearly as well as a metal, with conductivity  $10^{11}$  times higher than pure polyacetylene (PA) [1,2]. Although polyacetylene exhibits a very high conductivity in the doped form, the material is not stable against oxygen or humidity and is intractable. For these reasons, much work has been devoted to synthesizing soluble and stable polyacetylenes [3,4]. Unfortunately, these substituted derivatives exhibit electrical conductivities that are much lower than the parent polymer. The discovery of polyacetylene led to the search for new structures that could lead to new and improved polymer properties.

New conducting polymer structures (Figure 1.1) have been developed over the past two decades with the hope of obtaining better properties than polyacetylene. New classes of conducting polymers include polythiophene [5,6] (PTh), polyfuran [6], polypyrrole [7] (PPy), poly(p-phenylene) [8] (PPP), poly(p-phenylene vinylene) [9] (PPV), polyfluorene, [10] and polyaniline [11] (PAn). Although none have exhibited higher conductivity than PA, these polymers have been useful in designing new structures that are soluble and stable. Electron-rich heterocycle based polymers such as polythiophene and polypyrrole are very stable in the p-doped form and this has made these systems two of the most studied conducting polymers. Their stability is due to their lower polymer oxidation potentials which follow the order of PA>PTh>PPy. Also, these structures are more easily modified than PA, allowing for more diversity of structures.

### **1.1.2 Band Theory and Doping-Induced Transitions in Conjugated Polymers**

The excitation and/or removal/insertion of electrons in conjugated polymers as a result of electrochemical or photochemical doping processes necessitates discussion of band theory. In its most simple form for conjugated polymers, the high extent of conjugation gives rise to two discrete energy bands, the lowest energy containing the highest occupied molecular orbital (HOMO), also known as the valence band (VB); and that containing the lowest unoccupied molecular orbital (LUMO), known as the conduction band (CB). The energy distance between these two bands is defined as the band gap ( $E_g$ ), and in neutral conjugated polymers refers to the onset energy of the  $\pi$ - $\pi^*$  transition. The  $E_g$  of conjugated polymers can be approximated from the onset of the  $\pi$ - $\pi^*$  transition in the UV-Vis spectrum. In their neutral form, conjugated polymers are semiconducting, but on oxidation (p-doping) or reduction (n-doping), interband transitions form between the VB and CB, lowering the effective band gap, and resulting in the formation of charge carriers along the polymer backbone.

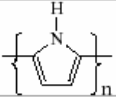
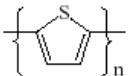
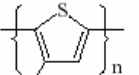
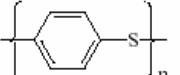
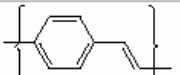
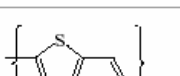
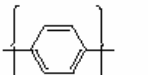
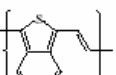
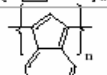
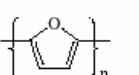
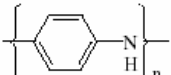
Polymer	Structure	Doping materials	$\Omega^{-1}\text{cm}^{-1}$
Polyacetylene	(CH) <sub>n</sub>	I <sub>2</sub> , Br <sub>2</sub> , Li, Na, AsF <sub>5</sub>	10000
Polypyrrole		BF <sub>4</sub> <sup>-</sup> , ClO <sub>4</sub> <sup>-</sup>	500-7500
Polythiophene		BF <sub>4</sub> <sup>-</sup> , ClO <sub>4</sub> <sup>-</sup>	1000
Poly(3-alkylthiophene)		BF <sub>4</sub> <sup>-</sup> , ClO <sub>4</sub> <sup>-</sup>	1000-10000
Polyphenylene sulfide		AsF <sub>5</sub>	500
Polyphenylenevinylene		AsF <sub>5</sub>	10000
Polythienylenevinylene		AsF <sub>5</sub>	2700
Polyphenylene		AsF <sub>5</sub> , Li, Na	1000
Polyisothianaphthene		BF <sub>4</sub> <sup>-</sup> , ClO <sub>4</sub> <sup>-</sup>	50
Polyazulene		BF <sub>4</sub> <sup>-</sup> , ClO <sub>4</sub> <sup>-</sup>	1
Polyfuran		BF <sub>4</sub> <sup>-</sup> , ClO <sub>4</sub> <sup>-</sup>	100
Polyaniline		HCl	200

Figure 1.1 Molecular structure, doping materials and conductivity of common organic conducting polymers.

Initial studies of band theory as applied to conjugated polymers focused on poly(acetylene). PA is unique in that both resonance forms of the neutral polymer are degenerate, leading to the formation of solitons on oxidation. The localized electronic state associated with the soliton is a nonbonding state at an energy lying at the middle of the  $\pi$ - $\pi^*$  gap, between the bonding and antibonding levels of the perfect chain. The soliton is a defect both topological and mobile because of the translational symmetry of the chain [12]. Soliton model was first proposed for degenerated conducting polymers (PA in particular) and it was noted for its extremely one dimensional character, each soliton being confined to one polymer chain (see Figure 1.2). Thus, there was no conduction via interchain hopping. Furthermore, solitons are very susceptible to disorder, and any defect such as impurities, twists, chain ends or crosslinks will localize them [13,14].

A different scenario exists for aromatic polymers because of their nondegenerate ground states. As an example, the oxidative doping of PPy is shown in Figure 1.3(a). Application of an oxidizing potential destabilizes the VB, raising the energy of the orbital to a region between the VB and CB. Removal of an electron from the destabilized orbital results in a radical cation or polaron. Further oxidation results in the formation of dication or bipolarons, dispersed over a number of rings. These radical cations and dications are the charge carriers responsible for conductivity in conjugated polymers. Because of the nondegenerate energy transitions of conjugated polymers (excluding PA), structural changes result and are based on the most widely accepted mechanism as shown for PPy in Figure 1.3(b) [15]. Electron paramagnetic resonance (EPR) spectroscopy results support this mechanism, showing that neutral and heavily doped polymers possess no unpaired electrons, while lightly doped polymers do display an EPR signal [16,17]. The theory presented above is based on the seminal work of Fesser, Bishop, and Campbell, whose FBC theory is one of the most widely cited by scientists attempting to interpret optical transitions in their conjugated polymers [18].

Another increasingly accepted model for oxidative doping in conjugated polymers is the formation of p-dimers instead of bipolarons. In the p-dimer theory, polarons from separate polymer chains interact, forming a diamagnetic species with no EPR signal [19-21]. Apperloo et al. performed studies on thiophene-based oligomers building a persuasive case for p-dimer formation [22,23]. However, it is not yet clear which mode of oxidative doping is responsible for the observed properties in conjugated polymers, leaving the door open for continued study. Through both of these theories, organic chemists have been able to interpret and modify the band structure of conjugated polymers to tune their optical and electrical properties. Much of the work performed on these materials was inspired by the color changes observed in inorganic and organic small molecules. The ability to control the electronics and structure of polymers set them apart from the traditional materials and opened up a huge area of research that has seen tremendous success over the past several decades.

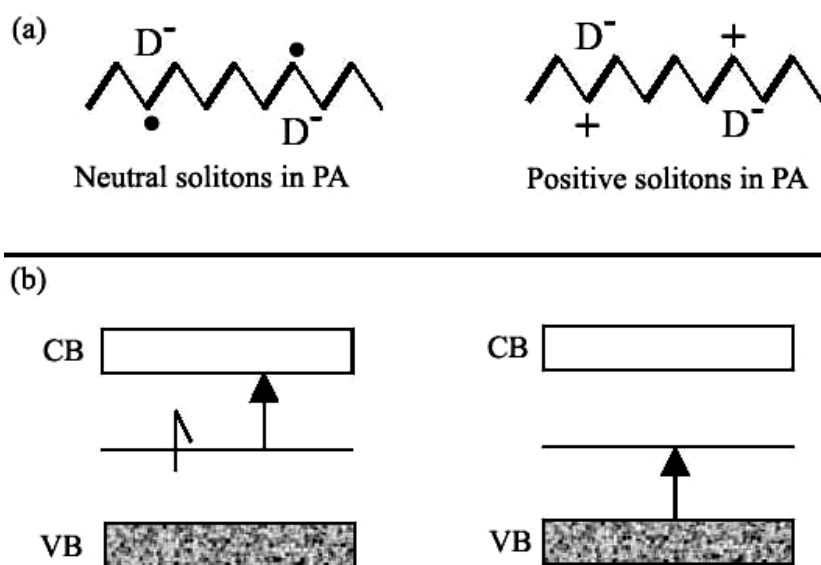


Figure 1.2 Band diagrams for neutral and positive solitons. (a) Schematic representation of neutral (left) and positive (right) solitons in degenerate PA, where D represents a dopant ion; (b) band diagrams for neutral (left) and positive (right) solitons with associated electronic transitions.

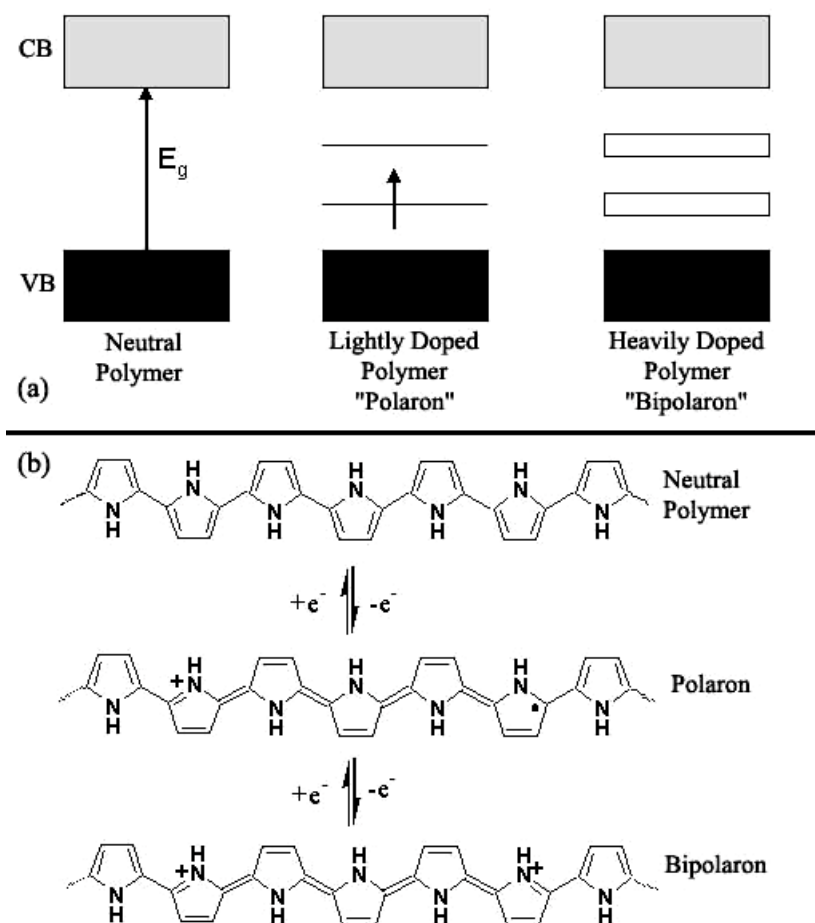


Figure 1.3 Band theory and doping-induced structural transitions of polypyrrole. (a) Band theory of conjugated polymers. (b) Structural changes associated with polaron and bipolaron formation as a result of oxidative doping in polypyrrole.

### 1.1.3 Synthesis of Conducting Polymers

Conductive polymers may be synthesized by any one of the following techniques [24]:

- Electrochemical polymerization
- Chemical polymerization
- Photochemical polymerization
- Methathesis polymerization

- Concentrated emulsion polymerization
- Inclusion polymerization
- Solid-state polymerization
- Plasma polymerization
- Pyrolysis
- Soluble precursor polymer preparation
- Microwave initiation

### 1.1.3.1 Electrochemical Polymerization

Electropolymerization is a standard oxidative method for preparing electrically conducting conjugated polymers. Smooth, polymeric films can be efficiently electrosynthesized onto conducting substrates where their resultant electrical and optical properties can be probed easily by several electrochemical and coupled in situ techniques. Electropolymerization involves the oxidation of a monomer dissolved in a supporting electrolyte solution by applying an external potential to form reactive radical cations (also known as the monomer oxidation potential) (Figure 1.4(b)). After the initial oxidation, two routes for polymer formation are possible. In the first pathway, a monomer radical cation can couple with neutral monomer, and after a second oxidation and loss of two protons, forms a neutral dimer [25]. The second route involves the coupling of two radical cations followed by the loss of two protons to yield neutral dimer [26-28]. Then the neutral dimer is oxidized and the process is repeated until an electroactive polymer film is deposited onto the conducting substrate. Because of the oxidative nature of electropolymerizations, the deposited polymer is typically in its oxidized state, thus necessitating the presence of a supporting electrolyte to compensate the positive charges along the polymer backbone. The efficiency of the polymerization is dictated by the ease with which electrons can be removed from the monomer and by the stability of the resultant radical cation as shown in Figure 1.4(a) for the resonance stabilization of pyrrole. Electron-rich monomers, such as thiophene and pyrrole, are able to lose an electron more easily, and are also able to

stabilize the resultant radical cation through resonance across the p-electron system better than relatively electron-poor compounds such as benzene. Upon electropolymerization, stable, electroactive polymers derived from electron-rich heterocycles can be formed. Despite the facile nature of electrochemical polymerization, this method possesses the major limitation of yielding insoluble materials, precluding the analysis of primary structure by traditional analytical techniques. Because of this limitation, chemical polymerization methods have gained popularity for synthesizing novel soluble conjugated polymers.

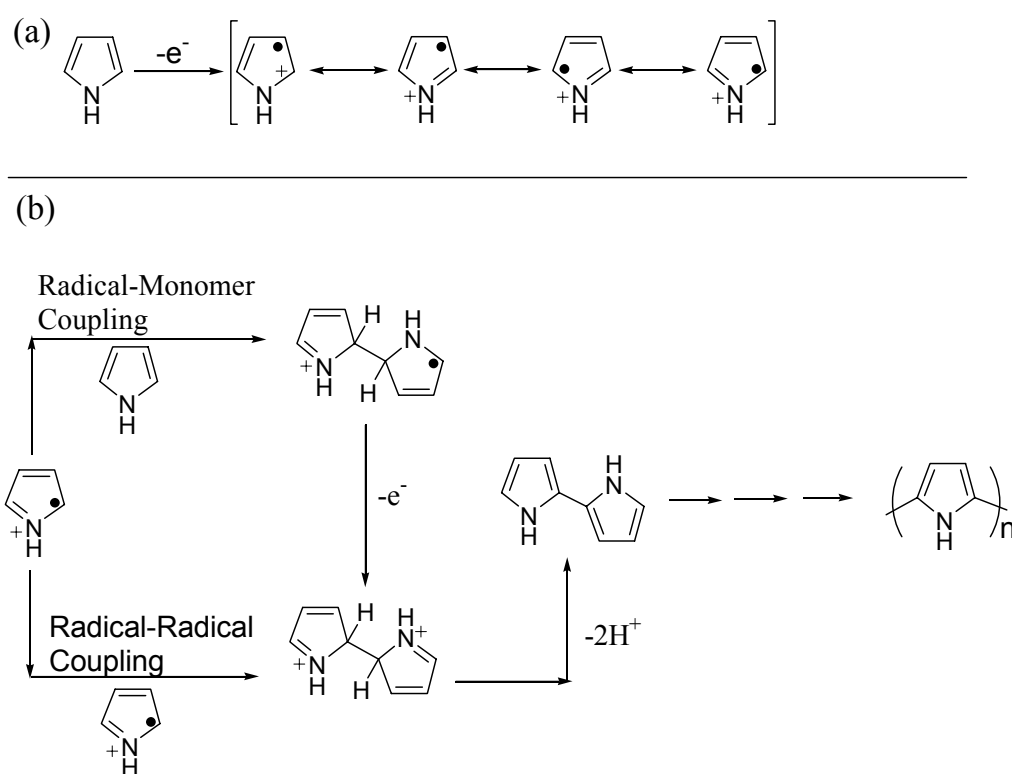


Figure 1.4 Resonance stabilization and electropolymerization mechanism of pyrrole. (a) Resonance stabilization of radical cation of pyrrole. (b) Proposed mechanism for the electrochemical polymerization of pyrrole.

### 1.1.3.2 Chemical Polymerization

Among the chemical polymerization techniques, oxidative methods represent the least expensive and most widely exploited means by which conjugated polymers can be prepared [29]. Oxidative chemical polymerizations are accomplished by exposing the monomer to a two-electron stoichiometric amount of oxidizing agent, resulting in the formation of the polymer in its doped and conducting state. Isolation of the neutral polymer is achieved by exposing the material to a strong reducing agent such as ammonia or hydrazine as shown in Figure 1.5. The mechanism of oxidative chemical polymerizations is thought to be very similar to that of electrochemical polymerizations. Heterocyclic monomers, such as thiophene and its derivatives, are typically polymerized in the presence of anhydrous  $\text{FeCl}_3$  [30] although other Lewis acids can also be used [31]. Furthermore, benzene can be polymerized to form PPP by adding  $\text{AlCl}_3/\text{CuCl}_2$  [32].

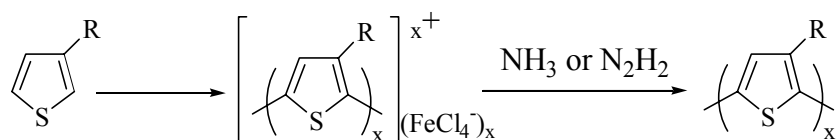


Figure 1.5 Lewis acid oxidative polymerization of an alkyl substituted thiophene.

A tremendous advantage of chemical oxidative polymerizations is that, unlike unsubstituted heterocycles that form insoluble powders, properly substituted heterocyclic and other aromatic monomers form highly soluble polymers. These polymers can be analyzed by traditional analytical techniques to determine their primary structure. The nature of the polymerization conditions also allows for easy scale-up and production of large quantities of polymer. Unfortunately, chemical oxidative polymerizations suffer from several disadvantages that often result in poor quality polymers. As stated earlier, Lewis acid catalyzed polymerizations yield the oxidized polymer, which is thought to be

more rigid [33], resulting in its precipitation from the polymerization medium, limiting the degree of polymerization. Also, the use of strong oxidizing agents can result in the overoxidation and eventual decomposition of the polymer, a disadvantage averted by the use of finely controlled electrochemical methods [34]. Unsubstituted heterocycles, like thiophene and pyrrole, present a unique problem for both oxidative polymerization techniques in that several side reactions can occur leading to “coupling defects” along the polymer backbone. It is generally believed that oxidative coupling occurs at sites on the heterocyclic ring where a high spin density resides for the radical cation. For thiophene, pyrrole, and furan, the highest spin densities have been measured at the 2- and 5-positions, also referred to as the  $\alpha$  positions [35,36]. Still, the 3- and 4-positions (referred to as the  $\beta$  positions) have a measurable spin density, meaning that some coupling reactions will occur at these positions. Various coupling events for the electrochemical polymerization of pyrrole are shown in Figure 1.6. Specific to this discussion,  $\alpha$ - $\beta$  and  $\beta$ - $\beta$  coupling events are shown that result in polymers with irregular backbones and poor electronic properties. Main chain imperfections such as these can be eliminated by “blocking” the 3- and 4-positions of the monomer by the attachment of various alkyl and alkoxy groups. In addition, several other electronic properties are dramatically affected by the structural modifications including monomer oxidation potential, electronic band gap, and electrochromic properties of the resultant polymers.

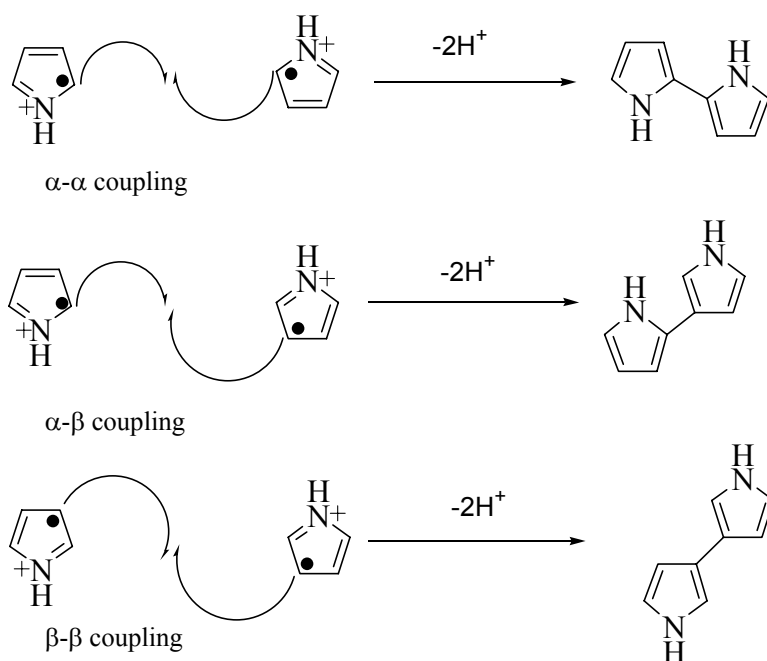


Figure 1.6 Potential coupling reactions for pyrrole during oxidative polymerization.

## 1.1.4 Polymer Electrochemistry

### 1.1.4.1 Cyclic Voltammetry Background

The arsenal of electrochemical methods that can be applied to the study of conducting polymer films deposited on a conducting surface is fairly broad and it has been thoroughly reviewed by Doblhofer et al [37]. Among these methods, cyclic voltammetry (CV) has become increasingly popular as a mean to study redox states, due to its simplicity and versatility. The electrode potential at which a polymer undergoes reduction or oxidation can be rapidly located by CV. Furthermore, CV reveals information regarding the stability of the product during multiple redox cycles. Since the rate of potential scan is variable, both fast and slow reactions can be followed. A very important aspect of this method is its ability to generate a new redox species during the first potential scan and then

probe the fate of species on the second and subsequent scans. Therefore, CV allows the growth of a polymer film along with its further characterization during a single experiment.

In cyclic voltammetry (CV), the potential is increased linearly from an initial potential to a peak potential and back to the initial potential again, while the current response is measured. For freely diffusing species, as the potential is increased, easily oxidized species near the electrode surface react, and a current response is measured. When the direction of the scan is reversed, the oxidized species near the electrode surface are reduced, and again a current response is measured. The Randles-Sevcik equation [38] states that the peak current is given by:

$$i_p = (2.69 \times 10^5) n^{3/2} A D^{1/2} C^b V^{1/2}$$

where  $n$  is the number of electrons,  $A$  is the surface area of the electrode ( $\text{cm}^2$ ),  $D$  is the diffusion constant ( $\text{cm}^2/\text{s}$ ),  $C^b$  is the bulk concentration of electroactive species ( $\text{mol}/\text{cm}^3$ ), and  $V$  is the scan rate ( $\text{V}/\text{s}$ ). Therefore, for a diffusion-controlled system, the peak current is proportional to the square root of the scan rate. Of course the rules change in electroactive polymer electrochemistry, because the polymer is adhered to the electrode surface. Therefore, the process is not diffusion controlled, and cannot be described by the Randles-Sevcik equation discussed above. Instead, the peak current for a surface bound species is given by the following equation [39,40]:

$$i_p = n^2 F^2 \Gamma V / 4RT$$

where  $\Gamma$  is the concentration of surface bound electroactive centers ( $\text{mol}/\text{cm}^2$ ) and  $F$  is Faradays constant ( $96,485 \text{ C}/\text{mol}$ ). Thus, if a species is surface bound, both the anodic and cathodic peak current will scale linearly with scan rate. In a scan rate dependence experiment, the electroactive polymer is washed and placed in

monomer- free electrolyte solution, and the polymer is then cycled between its oxidized and reduced forms at various scan rates while the  $i_p$  of both oxidation and reduction is monitored. If the  $i_p$  scales linearly with scan rate, then the process is said to be non-diffusion controlled, and the electroactive centers of the polymer are adhered to the electrode surface.

### **1.1.5 Conducting Copolymers**

A method to impart processability into a conducting polymer is to copolymerize it with other polymers to form a block or graft copolymer. The block or graft copolymer approach allows for the physical and chemical properties of individual polymeric components to be tailored. A blend of a conducting polymer with an insulating polymer also has considerable utility for improving the processing of the conducting polymer. To the extent that the conducting polymer is incorporated as inert filler, the physical properties of the matrix and its processability, for example in the melt determine the properties of the blend. Publication in the field of blends of conducting polymers with insulating polymers is voluminous, in the order of about a dozen papers per month published across the chemical journal spectrum.

#### **1.1.5.1 Blends**

Processability of a conducting polymer is still a problem because of their poor mechanical and physical properties. One method to solve this problem is blending conducting polymers with ordinary thermoplastic polymers. Several attempts have been described to produce conducting polymer composites with better physical properties by either chemically or electrochemically [41-44]. Heeger et. al. have extensively studied camphorsulfonic acid-doped polyaniline blended into a PMMA matrix [45]. After incrementally blending the doped polyaniline into the matrix and measuring the conductivity, the conductivity increased at a rapid rate until a volume fraction of 0.3% when a plateau of the

conductivity was reached. From a conductivity of  $10^{-3}$  S/cm at 0.3 % volume fraction the conductivity very slowly increased to a maximum of  $10^2$  S/cm for the unblended camphorsulfonic acid doped polyaniline. Sulfonic acid substituted polyaniline was blended into polyvinylalcohol [46]. Laska and coworkers studied the effect of blending polyaniline doped with a variety of phosphoric acid diesters into PMMA, PVC, PS and cellulose derivatives on the thermal processing and mechanical properties of the matrix [47]. Roncali and Garnier electrochemically polymerized poly (3-methylthiophene) in the presence of PMMA in the electrochemical cell to yield a composite in one step in the form of a 5 mm flexible film [48]. The conductivity reached values of up to 30 S/cm, however the homogeneity through the thickness of the film was not very good: the electrode-side of the film produced the high conductivities reproducibly while the electrolyte-side conductivity was inconsistent from sample to sample. The interaction of undoped poly(3-dodecylthiophene) with poly(octadecylacrylate) was studied from a structural and conformational perspective [49,50]. They determined that the polythiophene was induced into a more ordered conformation of the rigid rod backbone because of the hydrophobic interactions and cocrystallizations of the long alkyl substituents on both polymers.

#### **1.1.5.2 Block Copolymers**

Preparation of block copolymers of an insulating polymer with a conducting polymer is only possible for a few of the conducting polymers. Most of the syntheses of conducting polymers can be characterized as polycondensation in type, which is incompatible with the living techniques usually employed to synthesize block copolymers. Usually an anionic technique is utilized to synthesize the insulating block. The living end is quenched with a reactive group that can then be used to either initiate or attach the conducting polymer to the first block. The first diblock copolymers of a conducting polymer with an insulating polymer prepared contained polyacetylene copolymerized with either polystyrene [51,52] or polyisoprene [53,54]. The copolymers are prepared by first

polymerizing the styrene or isoprene under conventional anionic conditions with n-butyl lithium as initiator. The living end is then converted into either a transition metal alkyl with titanium tetrabutoxide/triethylaluminum (Shirakawa catalyst) or to a cobalt intermediate with cobalt dichloride (Luttinger catalyst). The acetylene is introduced into polymerization flask to yield diblock copolymer. The most extensively studied diblock copolymer is polystyrene-b-polyparaphenylene [55,56]. Styrene is first polymerized via anionic polymerization, followed by 1,3-cyclohexadiene. The polymerized cyclohexene backbone units are converted by dehydrogenation into phenylene units to yield the final block copolymer. Diblock copolymers of PMMA and polyparaphenylene using anionic polymerization followed by dehydrogenation [57]. Block copolymers in this field is polythiophene copolymerized with methylmethacrylate [58] or styrene [59]. The synthesis of poly(3-methylthiophene-b-methylmethacrylate) first requires the thiophene segment to be built by the Grignard coupling of 2,5-diiodo-3-methylthiophene. The methylmethacrylate polymerization is then initiated by the Grignard reagent to yield the block copolymer. Upon doping with iodine the copolymer exhibits a conductivity of 6.5 S/cm.

Block polymerization of pyrrole on polytetrahydrofuran with short and long chain lengths, prepared by taking advantage of living polymerization, were performed [60]. The growth of PPy through the pyrrole moiety of the insulating polymer chain was indicated. Another indication was that the chain length of the insulating polymer did not influence thermal or electrochemical behaviors, surface morphologies, or conductivities of the copolymers significantly. However, the presence of different electrolytes during electrochemical preparation strongly affects the properties of the polymer films.

### **1.1.5.3 Graft Copolymers**

Graft copolymers consisting of an insulating polymer backbone and conducting polymer side chains or grafts are usually formed by first synthesizing

the backbone and then grafting the conducting polymer on the backbone. A wide distribution of chain lengths, crosslinks, other defects and ungrafted homopolymer in the matrix is a topic that is rarely discussed. In a similar way that the diblock copolymers are produced, graft copolymers of polyisoprene and polyacetylene can be synthesized [61]. The polyisoprene is first synthesized and isolated. A fraction of the isoprene double bonds are epoxidized with m-chloroperbenzoic acid and then reacted with the Shirakawa catalyst titanium tetrabutoxide/triethylaluminum and acetylene monomer to yield the graft copolymer.

Hallensleben et. al. [62] started with poly(2-(2-thienyl)ethylmethacrylate-co-methylmethacrylate) and poly(2-(3-thienyl)ethylmethacrylate-co-methylmethacrylate) to oxidatively graft thiophene onto the backbone. In this work, they studied the effect of the density of the thienylmethacrylate in the backbone, the concentration of thiophene monomer, and the time of the reaction on the incorporation of polythiophene and the solubility of the copolymers. They also found that the aggregated solutions could be cast into films which, upon doping with iodine, showed conductivities of  $10^{-1}$  S/cm. In addition to these examples, graft copolymers of poly(styrene-g-pyrrole) [63], poly(methylmethacrylate-g-pyrrole) [64,65], and poly(styrene-g-aniline) [20] have been produced.

Graft copolymers of polystyrene with polythiophene were synthesized [66]. Styrene and 2-vinylthiophene or 3-vinylthiophene was polymerized via free-radical polymerization to yield the backbone. Thiophene was then oxidatively polymerized in the presence of the backbone to yield the graft copolymer.

Recently [67-70], the formation of electrochemical block copolymers of PPy and poly[(methylmethacrylate)-co-(2-N-pyrrolyl)ethyl methacrylate] (PMMA-co-PEMA) was pointed out. The block copolymer synthesized had the same conductivity as that of the pure PPy; in addition, an increase in the thermal stability of the copolymer was observed [68].

### 1.1.6 Application of Conducting Polymers

Traditionally polymers have been associated with insulating properties in the electronic industry and are applied as insulators of metallic conductors or photoresists. Since the remarkable discovery in 1977 of the doping of polyacetylene, which resulted in increasing the conductivity of polyacetylene by eleven orders of magnitude [1,2] many academic and industrial research laboratories initiated projects in the field of conducting polymers. Although the initial emphasis was on the conduction properties obtained by doping of conjugated polymers, since over a decade the research has focused on soluble and intrinsically (semi)conducting polymers. In the 25 years that have elapsed, many novel materials were designed, synthesized and developed for their specific physical or chemical properties and implemented in a variety of applications.

In the recent years, CPs have gained a lot of attention for electrochromic devices (ECDs) [71-79]. This is due to the fact that all electroactive and CPs are potentially electrochromic materials, and are more processable than inorganic electrochromic materials and offer the advantage of a high degree of color tailorability. Electrochromism can be exploited in a series of optical devices with potential use in various applications, such as in information display and storage, in the automotive industry (as rear-view mirrors and visors), and in architecture (as smart windows to control luminosity and save energy through the control of sunlight transmission) [79]. Basically, an electrochromic device is a two-electrode electrochemical cell in a sandwich configuration of thin layers. The arrangement of these layers depend on the operation mode, which can be reflective or transmissive [74,75]. The reflective mode is used to display or to decrease the reflected light, for example, in a car rear-view mirror. In these devices, one of the electrical contacts should be covered with a reflective layer, as a mirror. Transmissive mode operation is very similar, but all layers must become fully transparent when desired. The schematic representations of the transmissive ECDs are shown in Figure 1.7. The requirements for high performance electrochromic

devices are: a) high electrochromic efficiency, expressed in  $\text{cm}^2/\text{C}$  and related to the injected charge in the material to change its color; b) short response time; c) good stability; d) optical memory, defined as the color stability under open circuit potential conditions; e) optical contrast, also called write-erase efficiency, and f) color uniformity.

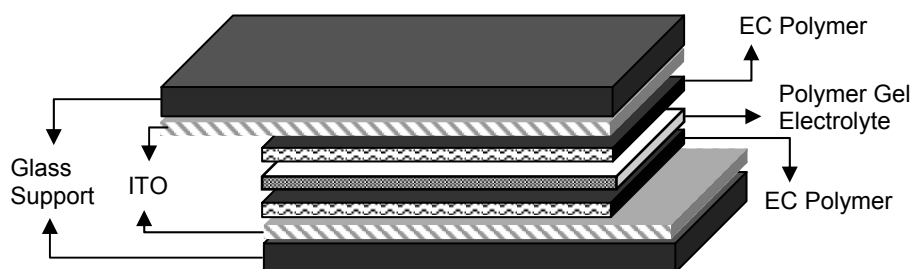


Figure 1.7 Schematic representation of transmissive electrochromic devices

In 1990 the Cambridge group reported emission of light from a plastic sandwich that was connected to a battery [9]. The discovery of electroluminescence (EL), i.e., the emission of light upon excitation by the flow of electric current, in conjugated polymers has provided a new impetus to the development of light-emitting diodes (LEDs) for display and other applications [80]. In LEDs, the injected holes and electrons recombine and produce luminescence with a wavelength (color) that depends on the energy difference between the excited state and the molecular ground state. For the majority of conjugated polymers, electron injection is more difficult than hole injection, since the majority of conjugated polymers are more easily oxidized than reduced. Using metals with a low work function (e.g. calcium) as the cathode material has remedied this. However, calcium is highly susceptible to atmospheric degradation and should therefore be encapsulated by a metal that is not sensitive towards oxygen and moisture, like aluminum (Figure 1.8). With the appropriate choice of polymer and device design, external efficiencies of up to 4 % can be obtained, which is comparable with the best EL devices based on inorganic materials. Turn-on voltages of 5 V or below have also been achieved by the use of charge-

transporting layers, enabling devices to be run from low-power sources like batteries.

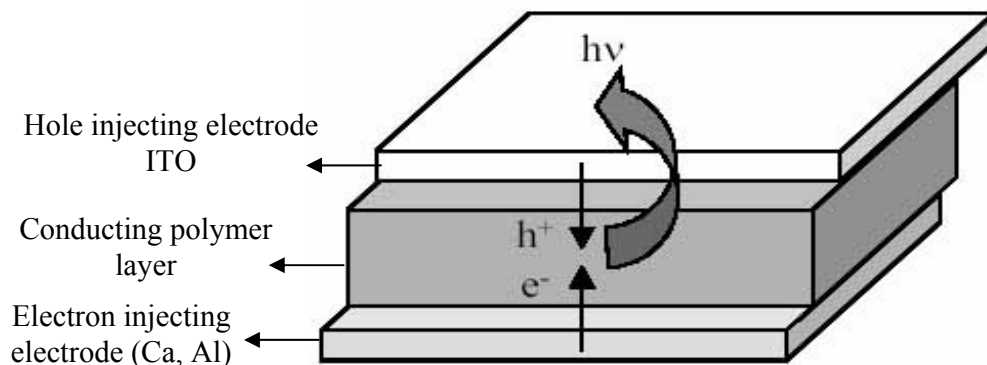


Figure 1.8 Schematic representation of LEDs

Polymer-based electroluminescent displays provide a good alternative to the well established display technologies based on cathode-ray tubes and liquid-crystal displays with respect to processability and viewing-angle. Especially for the application in large-area displays and flexible displays, for which the conventional methods are not well suited, polymer light-emitting diodes offer great advantages. Two years after the breakthrough in Cambridge, the Santa Barbara group reported the first results on polymer-based photovoltaic cells, [81,82] the principles of which can be regarded as the inverse of the EL process. In photovoltaic devices a bound electron-hole pair (exciton) is created upon illumination, which needs to be dissociated into separate charges that must be driven out by the built-in potential field between two electrodes with different work functions. To dissociate the exciton, the concept of electron donor and acceptor is frequently used, in which the electron affinity of the electron acceptor should be larger than the ionization potential of the donor.

The importance of the field of semiconducting polymers was recently stressed by awarding the 2000 Nobel Prize in chemistry to the discoverers Heeger, Shirakawa and MacDiarmid. Since the last decade the research has focused on the

applications of soluble and intrinsically semiconducting polymers as active material in field-effect transistors [83,84], light-emitting diodes [9,85-87], photodetectors [88], photovoltaic cells [89,90], sensors [91] and lasers (solution [92] and solid-state [93,94]). In addition to the good performance of the material in these devices, they also provide a way towards patterned structures by inexpensive techniques such as spin casting, photolithography [95], ink jet printing [96,97], soft lithography [98], screen printing [99] and micromolding [100] onto almost any type of substrate, including flexible ones [101].

## **1.2 Enzymes**

Enzymes are biological catalysts responsible for supporting almost all of the chemical reactions that maintain animal homeostasis. Because of their role in maintaining life processes, the assay and pharmacological regulation of enzymes have become key elements in clinical diagnosis and therapeutics. The macromolecular components of almost all enzymes are composed of protein, except for a class of RNA modifying catalysts known as ribozymes. Ribozymes are molecules of ribonucleic acid that catalyze reactions on the phosphodiester bond of other RNAs. Enzymes are found in all tissues and fluids of the body. Intracellular enzymes catalyze the reactions of metabolic pathways. Plasma membrane enzymes regulate catalysis within cells in response to extracellular signals, and enzymes of the circulatory system are responsible for regulating the clotting of blood. Almost every significant life process is dependent on enzyme activity.

### **1.2.1 Enzyme Classification**

Presently more than 2000 different enzyme activities have been isolated and characterized. The sequence information of a growing number of organisms opens the possibility to characterize all the enzymes of an organism on a genomic level. The smallest known organism, *Mycoplasma genitalium*, contains 470 genes

of which 145 are related to gene replication and transcription. Baker's yeast has 7000 genes coding for about 3000 enzymes. Thousands of different variants of the natural enzymes are known. The number of reported 3-dimensional enzyme structures is rapidly increasing. In the year 2000 the structure of about 1300 different proteins were known. The enzymes are classified into six major categories based on the nature of the chemical reaction they catalyze:

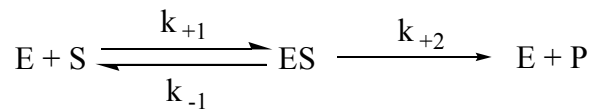
1. Oxidoreductases catalyze oxidation or reduction of their substrates
2. Transferases catalyze group transfer
3. Hydrolases catalyze bond breakage with the addition of water
4. Lyases remove groups from their substrates
5. Isomerases catalyze intramolecular rearrangements
6. Ligases catalyze the joining of two molecules at the expense of chemical energy

Only a limited number of all the known enzymes are commercially available and even smaller amount is used in large quantities. More than 75% of industrial enzymes are hydrolases. Protein-degrading enzymes constitute about 40% of all enzyme sales. Proteinases have found new applications but their use in detergents is the major market. More than fifty commercial industrial enzymes are available and their number increases steadily.

### **1.2.2 Kinetics of Enzyme Reactions**

Enzymes possess unique catalytic function, so their efficiency is usually determined by measuring their effect on the rate of chemical reaction. The rates of enzyme catalyzed reactions were first studied in the latter part of nineteenth century, when no enzyme was available in pure form and the methods of assay were primitive. Furthermore, instead of measuring initial rates of reaction at various initial substrate concentrations, the commonly used method was to follow the course of reaction over a period of time [102]. In 1913, Michaelis and Menten

[103] measured initial rates of the breakdown of sucrose into glucose and fructose catalyzed by invertase at different substrate concentrations and controlled pH by allowing the autorotation of the product. It was postulated that the enzyme and its substrate form an enzyme-substrate complex to account for rectangular hyperbolic relationship between the substrate concentration and the reaction velocity. They proposed a mechanistic scheme for the enzyme-catalyzed reaction involving single substrate and single intermediate and equilibrium between the free enzyme and the enzyme-substrate and enzyme-product complexes, where E is the free enzyme, S is the substrate, ES is the enzyme-substrate complex and P is the reaction product.



Michaelis and Menten derived the rate equation based on the assumption that the rate of breakdown of the ES to product was much slower than the dissociation of ES into enzyme and substrate therefore,

$$k_{+2} \ll k_{-1}$$

However, the formulation of Michaelis and Menten, which treats the first step of enzyme catalysis as an equilibrium, makes unnecessary and unwarranted assumptions about the rate constants. Thus, a more valid derivation was proposed by Briggs and Haldane [104] based on the initial rate of reaction. It was assumed that almost immediately after the reaction starts a steady state is achieved in which the concentration of the intermediate (enzyme-substrate complex) is constant.

$$d[ES]/dt = k_{+1} [E][S] - k_{-1} [ES] - k_{+2} [ES] = 0 \quad (1)$$

Since the total enzyme concentration,  $[E]_0$  can be written as the sum of  $[E]$  and  $[ES]$ ,

$$d[ES]/dt = k_{+1}[E]_0[S] - (k_{-1}[S] + k_{+2})[ES] = 0 \quad (2)$$

dividing (2) by  $k_{+1}$  and solving for  $[ES]$

$$[ES] = \frac{[E]_0 [S]}{(k_{-1} + k_{+2}) / k_{+1} + [S]}$$

the rate equation is

$$v = k_{+2} [ES] = \frac{k_{+2}[E]_0 [S]}{(k_{-1} + k_{+2}) / k_{+1} + [S]}$$

$$v = \frac{v_{\max} [S]}{K_m + [S]}$$

$K_m$  is known as *Michaelis constant*, is the equilibrium constant for dissociation of enzyme-substrate complex and inversely related to the affinity of the enzyme for its substrate. The  $v_{\max}$  is the *maximum velocity of reaction* which is attained when the entire enzyme is in the form of enzyme substrate complex. It was shown that this theory and equation could account accurately for their results with invertase, and because of the definitive nature of their experiments, which have served as a standard for almost all subsequent enzyme kinetic measurements. Today, Michaelis and Menten are regarded as the founders of modern enzymology and equation 1 is generally known as the *Michaelis-Menten equation*. The initial rate of reaction obeying Michaelis-Menten equation as a function of the substrate concentration at constant enzyme concentration is given in Figure 1.9.

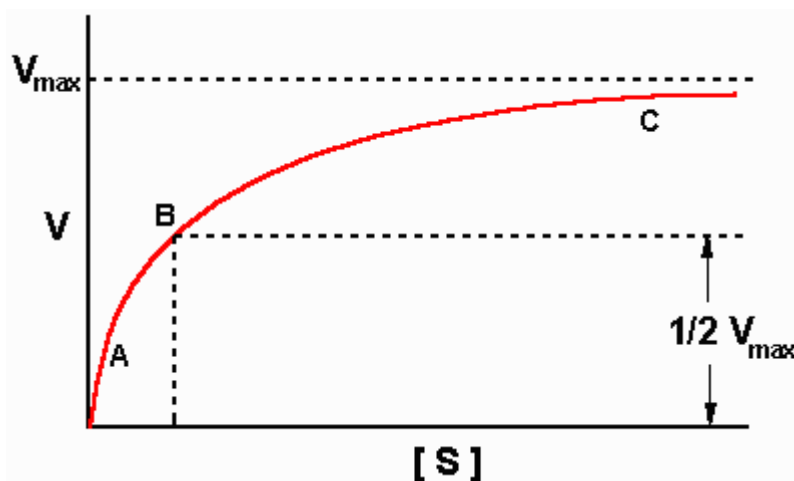


Figure 1.9 Plot of initial velocity against substrate concentration for enzyme catalyzed reaction.

At very low substrate concentrations, velocity is directly proportional to  $[S]$  so that reaction is apparently first order in  $S$ . At very high substrate concentrations, velocity will approach to  $v_{\max}$  and the reaction is apparently zero order in  $S$ . Under these conditions, the enzyme is said to be saturated with substrate. Graphical representation of Michaelis and Menten equation is desirable if a series of initial velocities at different substrate concentrations is measured, so that the kinetic parameters,  $K_m$  and  $v_{\max}$  can be determined. However, the plot of  $v$  against  $S$ , generating a rectangular hyperbola which is unsatisfactory in practice due to difficulty in drawing hyperbolas accurately and then estimating asymptotes. Therefore, in order to determine these kinetic parameters, for an enzyme catalyzed reaction, a linear relation would be more useful. Lineweaver and Burk [105] have preferred to rewrite the Michaelis and Menten equation in a form that permits the results to be plotted as a straight line,

$$\frac{1}{v} = \frac{K_m}{v_{\max}} \frac{1}{[S]} + \frac{1}{v_{\max}}$$

The plot of  $1/v$  versus  $1/[S]$  will give a straight line of slope  $K_m/v_{max}$  and y intercept of  $1/v_{max}$  (Figure 1.10)

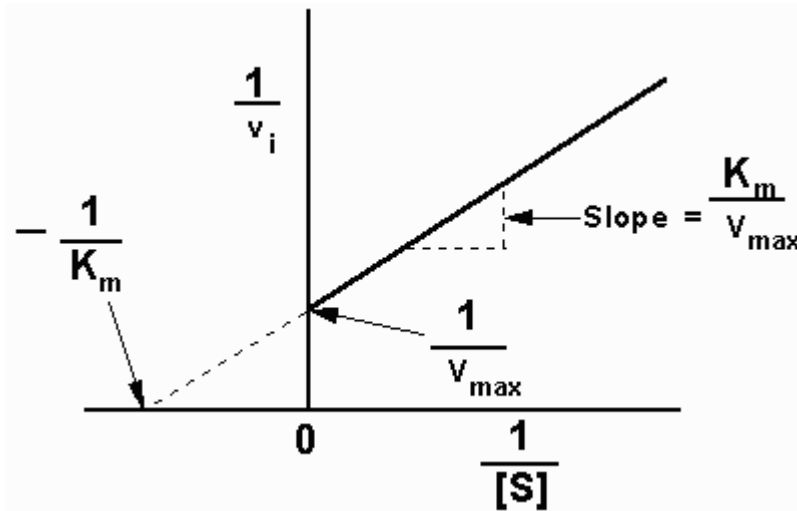


Figure 1.10 Lineweaver- Burk plot

### 1.2.3 Immobilization of Enzymes

The technology for immobilization of cells and enzymes evolved steadily for the first 25 years of its existence [106], but in recent years it has reached a plateau, if not a slight decline. However, the expansion of biotechnology, and the expected developments that will grow from advances in genetic technology, has revitalized enthusiasm for immobilization of enzymes and cells [107]. Research and development work has provided a bewildering array of support materials and methods for immobilization. Much of the expansion may be attributed to developments to provide specific improvements for a given application [108]. Surprisingly, there have been few detailed and comprehensive comparative studies on immobilization methods and supports. Therefore, no ideal support material or method of immobilization has emerged to provide a standard for each type of immobilization. Selection of support material and method of immobilization is made by weighing the various characteristics and required

features of the enzyme/cell application against the properties, limitations, characteristics of the combined immobilization/support.

In solution, soluble enzyme molecules behave as any other solute in that they are readily dispersed in the solution and have complete freedom of movement. Enzyme immobilization is a technique specifically designed to greatly restrict the freedom of movement of an enzyme. Most cells are naturally immobilized one way or another, so immobilization provides a physical support for cells. There are five principal methods for immobilization of enzymes/cells: adsorption, covalent binding, entrapment, encapsulation, and crosslinking (Figure 1.11). The relative merits of each are discussed briefly below.

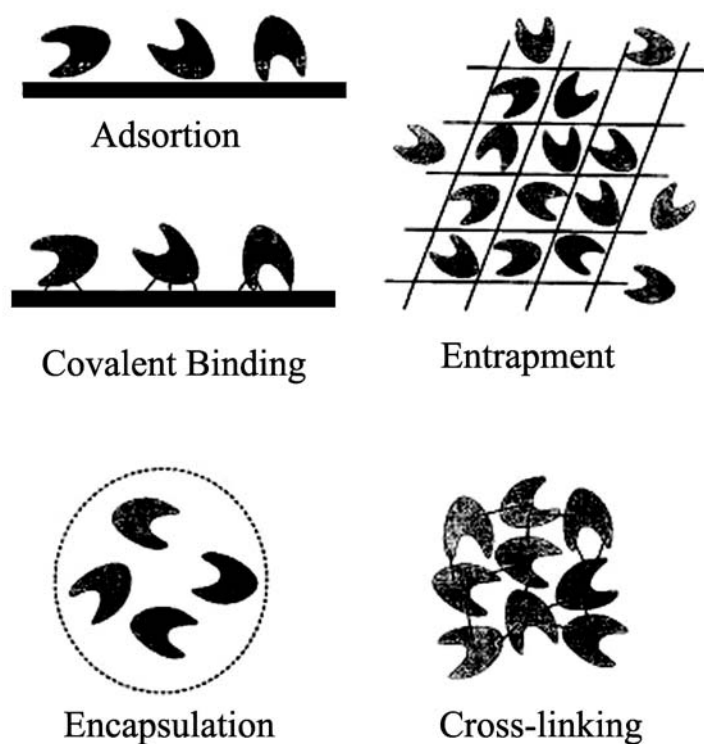


Figure 1.11 Principal methods of immobilization

### 1.2.3.1 Adsorption

Immobilization by adsorption (Figure 1.11) is the simplest method and involves reversible surface interactions between enzyme/cell and support material [109,110]. The forces involved are mostly electrostatic, such as Van der Waals

forces, ionic and hydrogen bonding interactions, although hydrophobic bonding can be significant. These forces are very weak, but sufficiently large in number to enable reasonable binding. For example, it is known that yeast cells have a surface chemistry that is substantially negatively charged so that use of a positively charged support will enable immobilization. Existing surface chemistry between the enzyme/cells and support is utilized so no chemical activation/modification is required and little damage is normally done to enzymes or cells in this method of immobilization. The procedure consists of mixing together the biological component(s) and a support with adsorption properties, under suitable conditions of pH, ionic strength, and so on, for a period of incubation, followed by collection of the immobilized material and extensive washing to remove nonbound biological components.

### **1.2.3.2 Covalent Binding**

This method of immobilization (Figure 1.11) involves the formation of a covalent bond between the enzyme/cell and a support material [110-112]. The bond is normally formed between functional groups present on the surface of the support and functional groups belonging to amino acid residues on the surface of the enzyme. A number of amino acid functional groups are suitable for participation in covalent bond formation. Those that are most often involved are the amino group (NH<sub>2</sub>) of lysine or arginine, the carboxyl group (CO<sub>2</sub>H) of aspartic acid or glutamic acid, the hydroxyl group (OH) of serine or threonine, and the sulfhydryl group (SH) of cysteine [113].

Many varied support materials are available for covalent binding, and the extensive range of supports available reflects the fact that no ideal support exists. Therefore, the advantages and disadvantages of a support must be taken into account when considering possible procedures for a given enzyme immobilization [114]. Many factors may influence the selection of a particular support, and research work has shown that hydrophilicity is the most important factor for

maintaining enzyme activity in a support environment [115]. Consequently, polysaccharide polymers, which are very hydrophilic, are popular support materials for enzyme immobilization. For example, cellulose, dextran, starch, and agarose are used for enzyme immobilization. The sugar residues in these polymers contain hydroxyl groups, which are ideal functional groups for chemical activation to provide covalent bond formation. Also, hydroxyl groups form hydrogen bonds with water molecules and thereby create an aqueous (hydrophilic) environment in the support. The polysaccharide supports are susceptible to microbial/fungal disintegration, and organic solvents can cause shrinkage of the gels.

### **1.2.3.3 Entrapment**

Immobilization by entrapment (Figure 1.11) differs from adsorption and covalent binding in that enzyme molecules are free in solution, but restricted in movement by the lattice structure of a gel [106]. The porosity of the gel lattice, controlled to ensure that the structure is tight enough to prevent leakage of enzyme or cells, yet at the same time allow free movement of substrate and product. Inevitably, the support will act as a barrier to mass transfer, and although this can have serious implications for reaction kinetics, it can have useful advantages since harmful cells, proteins, and enzymes are prevented from interaction with the immobilized biocatalyst [116].

Entrapment can be achieved by mixing an enzyme with a polyionic polymer material and then crosslinking the polymer with multivalent cations in ion-exchange reaction to form a lattice structure that traps the enzymes. Alternatively, it is possible to mix the enzyme with chemical monomers which can be polymerized to form a crosslinked polymeric network, trapping the enzyme in the interstitial spaces of the lattice. The latter method is more widely used, and a number of acrylic monomers are available for the formation of hydrophilic copolymers. For example, acrylamide monomer is polymerized to form

polyacrylamide and methylacrylate is polymerized to form polymethacrylate. In addition to the monomer, a crosslinking agent is added during polymerization to form crosslinkages between the polymer chains and help to create a three-dimensional network lattice. The pore size of the gel and its mechanical properties are determined by the relative amounts of monomer and crosslinking agent.

#### **1.2.3.4 Encapsulation**

Encapsulation (Figure 1.11) of enzymes and or cells can be achieved by enveloping the biological components within various forms of semipermeable membranes [117,118]. It is similar to entrapment in that the enzymes/cells are free in solution, but restricted in space. Large proteins or enzymes cannot pass out of or into the capsule, but small substrates and products can pass freely across the semipermeable membrane. Many materials have been used to construct microcapsules varying from 10—100  $\mu\text{m}$  in diameter; for example, nylon and cellulose nitrate have proven popular. The problems associated with diffusion are more acute and may result in rupture of the membrane if products from a reaction accumulate rapidly. A further problem is that the immobilized cell or enzyme particle may have a density fairly similar to that of the bulk solution with consequent problems in reactor configuration, flow dynamics, and so on. It is also possible to use biological cells as capsules, and a notable example of this is the use of erythrocytes (red blood cells). The membrane of the erythrocyte is normally only permeable to small molecules. However, when erythrocytes are placed in a hypotonic solution, they swell, stretching the cell membrane and substantially increasing the permeability. In this condition, erythrocyte proteins diffuse out of the cell and enzymes can diffuse into the cell. Returning the swollen erythrocytes to an isotonic solution enables the cell membrane to return to its normal state, and the enzymes trapped inside the cell do not leak out. A distinct advantage of this method is coimmobilization. Cells and/or enzymes may be immobilized in any desired combination to suit particular applications.

### **1.2.3.5 Crosslinking**

This type of immobilization (Figure 1.11) is support-free and involves joining the cells (or the enzymes) to each other to form a large, three-dimensional complex structure, and can be achieved by chemical or physical methods [119]. Chemical methods of crosslinking normally involve covalent bond formation between the cells by means of a bi- or multifunctional reagent, such as glutaraldehyde and toluene diisocyanate. However, the toxicity of such reagents is a limiting factor in applying this method to living cells and many enzymes. Both albumin and gelatin have been used to provide additional protein molecules as spacers to minimize the close proximity problems that can be caused by crosslinking a single enzyme. Physical crosslinking of cells by flocculation is well known in the biotechnology industry and does lead to high cell densities. Flocculating agents, such as polyamines, polyethyleneimine, polystyrene sulfonates, and various phosphates, have been used extensively and are well characterized. Crosslinking is rarely used as the only means of immobilization because the absence of mechanical properties and poor stability are severe limitations. Crosslinking is most often used to enhance other methods of immobilization, normally by reducing cell leakage in other systems.

### **1.2.4 Enzyme Immobilization by Electropolymerization**

Electropolymerization is an efficient enzyme immobilization method used in biosensor development. Conducting polymers such as, polythiophene, polyaniline, polyindole polypyrrole [120], can be grown electrochemically on an electrode surface, and it could be demonstrated that electrochemical polymerization is an easy and attractive approach for the immobilization of enzymes at electrode surface. However, conducting polymers have additionally been used in amperometric enzyme electrodes with the intention of coupling the electron-transfer reaction between enzyme and electrode via the ramified conducting network of the polymer. Some of these electropolymers can also serve

as mediator, decreasing the work potential and thereby avoiding interference from other species.

In recent years, there has been a growing interest in electrochemical microdevices owing to their potential application in monitoring and diagnostic tests in clinical laboratories. In particular, the development of microfabricated biosensors constitutes an attractive avenue for the *ex vivo* and *in vivo* measurements of metabolites, for example glucose, hormones, neurotransmitters, antibodies and antigens. However, the stable immobilization of macromolecular enzymes on conductive microspheres with complete retention of their biological recognition properties is a crucial problem for the commercial development of miniaturized biosensors. Effectively, most of the conventional procedures of enzyme immobilization such as cross-linking, covalent binding and entrapment in gels or membranes suffer from a low reproducibility and a poor spatially controlled deposition. Apart from these conventional methods, the immobilization of enzymes in electropolymerized films is gaining importance [120-122]. Effectively, the electrochemical formation of polymer layers of controlled thickness constitutes a reproducible and nonmanual procedure of biosensor fabrication. This approach has received considerable attention due to increase demand for miniaturized biosensors [123].

The electrochemical method involves the entrapment of enzymes in organic polymers during their electrogeneration on an electrode surface. The polymer formation is carried out by controlled potential electrolysis of an aqueous solution containing monomers and enzymes. Recently, a more sophisticated approach involving the adsorption of amphiphilic monomers and enzymes before the electropolymerization step has been described [122]. Another electrochemical method involves, initially, the electropolymerization of functionalized conducting polymers. Then the attachment of enzymes to the polymer surfaces can be obtained by chemical grafting or by affinity of the enzyme at the functional group [124,125]. In comparison to the physical entrapment of enzymes within polymer

films such as polypyrrole, polythiophene, polyacetylene or polyaniline, this approach preserves a better access of substrate to the immobilized enzymes and facilitates macromolecular interactions. However, the amount of immobilized enzymes is restricted to a monolayer at the interface polymer-solution. Ten years ago, an elegant strategy of biosensor construction based on the entrapment of enzymes in polymer films during their electrogeneration on electrode surface appeared [126,127]. This method involves the application of an appropriate potential to the working electrode soaked in aqueous solution containing both enzyme and monomer molecules. Enzymes present in the immediate vicinity of the electrode surface are thus incorporated in the growing polymer. In addition, the entrapment of enzymes occurs without chemical reaction that could affect their activity. The advantage of electrochemical polymerization is that films can be prepared easily in a rapid one-step procedure. Furthermore, this method enables exact control of the thickness of the polymer layer based on the measurement of the electrical charge passed during the electrochemical polymerization. One major advantage of electrochemical deposition procedures over more conventional methods is the possibility to precisely electrogenerate a polymer coating over small electrode surfaces of complex geometry. Moreover, the recent design of electrochemical micro cell allows the electrogeneration of polymer films from small volumes of electrolyte. The amount of enzyme required for its entrapment within the polymeric film is thus markedly reduced. Most of the electrochemically deposited polymer films used for the enzyme immobilization are conducting polymers for example, polyacetylene, polythiophene, polyaniline, polyindole and polypyrrole.

Often, the thickness of the growing polymer film is controlled by measuring the charge transferred during the electrochemical polymerization process. However, most authors have their individual way of electrode surface pretreatment, choose specific concentrations for the enzyme and the monomer, and use different electrolyte salts and hence counter anions incorporated in the growing polymer film.

## **1.2.5 Industrial Applications of Immobilized Enzymes.**

### **1.2.5.1 Application of Immobilized Enzymes in the Food Industry:**

Since foods are biological materials whose nutrition, aroma, flavor etc must be carefully preserved during processing, it is more prudent to manipulate the process by biological means rather than harsh chemical treatments, which might affect the properties of foods adversely. Immobilized enzymes have been long used in the food industry. Some of the applications of immobilized enzymes in the food industry are described below.

Enzymes such as glucose isomerase have been widely used in the preparation of high fructose syrups from glucose. Soluble glucose isomerase was employed for the purpose, but considering the high cost that was involved in the process, glucose isomerase immobilized on cellulose ion-exchange polymer was used for the above reaction which made the process more economically favorable. Glucose can be used as a substrate for high fructose syrups. High amounts of glucose can be obtained by conversion of starch to glucose. This has become an industrially viable process by using immobilized aminoglucosidase to convert starch to glucose. Enzyme immobilization has proved to be a boon to the cheese industry. Immobilized enzymes have been used for continuous coagulation of milk for cheese production, turning waste whey into an economically valuable product and for rendering of milk [128].

### **1.2.5.2 Application of Immobilized Enzyme in the Pharmaceutical Industry:**

Immobilized enzymes find their application in therapy, clinical analysis, preventive medicines etc. They could be used in the form of suspensions and could be injected intramuscularly or elsewhere. Total amount of immobilized enzymes injected and the substrate availability for the enzyme dictates the decisions for the sites of injection. Diseases that are caused because of enzyme

deficiency in the body for e.g., lysosomal storage diseases can be cured in theory by injecting the soluble enzyme from an extraneous source. However, soluble enzyme injection may cause problems such as allergy due to the presence of foreign enzyme protein, which could be fatal, instability of the soluble enzyme etc. Immobilization offsets both of these problems by preventing interaction between the enzyme and the body's immune response system and by stabilizing the enzyme. Encapsulation within a non-antigenic polymer such as nylon is the best form of immobilization for the above application. Another application of immobilized enzymes is in enzyme therapy. Enzyme therapy differs from enzyme replacement in that the enzyme to be added to the body is not the one that is normally found in the body. Due to this normal environmental condition are altered in order to control a diseased state. An example of this is the use of asparaginase in the treatment of certain leukemic cells. Certain leukemia cells cannot synthesize asparagine, while normal cells can do so. Using immobilized asparaginase in the blood reduces the blood asparagine concentration to a minimal level and the leukaemia cells die of asparagine starvation [128].

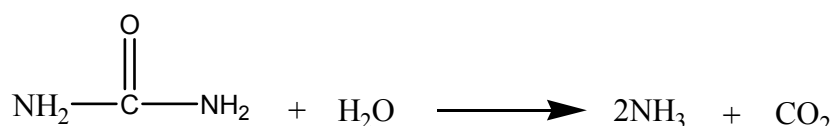
### **1.2.5.3 Affinity Chromatography:**

Many biochemical studies involve elucidation of the structure and function of biologically active substances such as enzymes, nucleic acids, antibodies and hormones. Precipitation with organic solvents, electrophoresis, ion exchange chromatography, gel filtration chromatography are some of the methods that are widely used for the isolation and purification of biologically active substances. However, the specificity of separation by these methods are low. Affinity chromatography is therefore used as a purification procedure based on the biological specificity exhibited by biological substances. In this *case*, a substance that is biologically related to the substance to be purified is selected as a ligand, then immobilized and then used as the adsorbent for affinity chromatography. The sample containing the substance that needs to be purified is passed through the column containing the immobilized enzyme (adsorbent). Only substances that

have specific affinity toward the immobilized ligand is adsorbed on the immobilized ligand, while the remaining substances in the sample pass through the column without any interaction. The high specificity of this method helps to remove many impurities that cannot be removed by conventional methods [128].

#### 1.2.5.4 Application of Immobilized Enzymes for Analytical Uses:

The first enzyme electrode to be prepared was a glucose-sensitive electrode made by immobilizing glucose oxidase on polyacrylamide gel and held in place around the electrode using cellulose acetate. The concentration of glucose in biological solutions and tissues can be measured by using this electrode. The enzyme catalyzes the removal of oxygen from the solution at a rate dependent upon the concentration of glucose present [129,130]. The immobilization of the enzyme can be done by chemical modification of the molecules by introduction of insolubilizing groups or by physical entrapment, using polyacrylamide gels as described in the case of glucose oxidase electrode above. Another example of the enzyme electrode is the Urea Electrode. Urease was immobilized by physical entrapment in polyacrylamide gel and held over the surface of a monovalent cation electrode.



The sensing mechanism is rather simple. The urea diffuses into the urease layer, where it is converted into the ammonium ions, which are sensed by the cation electrode. Amino acid electrodes and uric acid electrodes are some of the other kinds of electrodes, which are used widely today and are prepared from immobilized enzymes. Thus immobilized enzymes are used widely for analytical purposes.

### 1.2.6 Immobilization of Invertase

$\beta$ -fructofuranosidase (EC No.3.2.1.26) catalyses the hydrolysis of sucrose to glucose and fructose which is known as invert sugar (Figure 1.12). Sucrose crystallizes more readily than invert sugar, so the latter is widely used in the production of noncrystallizing creams, in making jam and artificial honey. Invertase occurs in the small intestine of mammals and in the tissues of certain animals and plants. It may be obtained in a relatively pure state from yeast, which is a very good source. Although, invertase has rather lower probability of achieving commercial use in immobilized form, it is one of the most studied of all enzymes because of being a model enzyme for experimental purposes.

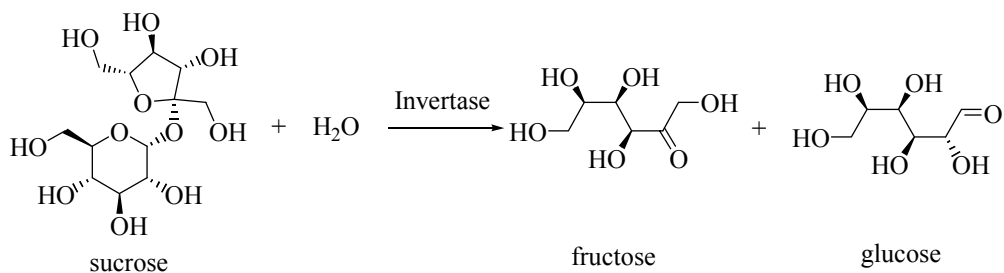


Figure 1.12 The reaction catalyzed by invertase

The immobilization of invertase on polyethylene [131], polyaniline [132] corn grifts [133], gelatin [134], carbohydrate moieties [135], polyelectrolytes [136], porous cellulose beads [137], diazonium salt of 4-aminobenzoylcellulose [138] and poly (ethylene-vinylalcohol) [137] has been studied. The invertase enzyme has been immobilized into conducting copolymers by electropolymerization [140,141].

### 1.2.7 Immobilization of Cholesterol Oxidase

Cholesterol oxidase is one of the industrially important enzyme. It catalyzes the oxidation of cholesterol and forms equimolar amounts of cholest-4-

en-3-one and hydrogen peroxide (Figure 1.13). Bacterial cholesterol oxidase catalyzes the first step in the primary metabolism of prokaryotes that can use cholesterol as their sole carbon source [143]. They are produced by and have been isolated from several microorganisms [144].

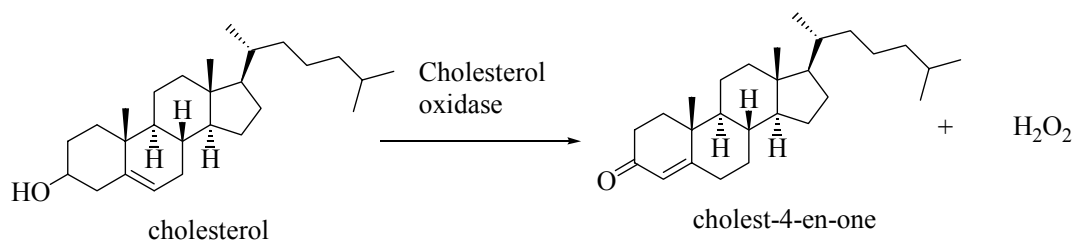


Figure 1.13 The reaction catalyzed by cholesterol oxidase.

Cholesterol oxidases have been exploited for their ability as hydrophilic enzymes to catalyze the reactions of hydrophobic steroid substrates. Cholesterol itself is an important component of eukaryotic cell membranes and its interactions with various phospholipids have been studied for decades. The melting temperature and order of liquid-crystalline phases of phospholipid bilayers have been shown to be dependent upon the mole fraction of cholesterol in the bilayer, by various spectroscopic techniques. Cholesterol oxidase has been employed in studies as a probe of membrane structure and the localization of cellular cholesterol [145]. The link between coronary artery disease and atherosclerosis and cholesterol has focused attention on lipoproteins and their lipid constituents.

Cholesterol is an extremely important biological molecule that is a precursor for the synthesis of the steroid hormones and bile salts [146]. It can be found in all body tissues, especially in the brain, spinal cord and in animal fats. Besides being present in human tissues, cholesterol is also found in the blood stream. Since its discovery in 1773, cholesterol has received much attention regarding its chemistry and biochemistry, its role in membrane integrity and function, and its association with human diseases such as hyperlipidemia, atherosclerosis, and cancer [147]. Cholesterol can be obtained from the diet in

foods of animal origin. Egg yolks and meats, particularly red meat and liver, are the major sources of dietary cholesterol. A high content of saturated fat in the diet tends to increase circulatory levels of LDL cholesterol and contributes to the development of atherosclerosis [148]. When there is too much cholesterol in your blood, the excess can become trapped in the walls of your arteries. By building up there, the cholesterol helps to cause hardening of the arteries or atherosclerosis. And atherosclerosis causes most heart attacks. The cholesterol buildup narrows the arteries that supply blood to the heart, slowing or even blocking the flow of blood to the heart. So, the heart gets less oxygen than it needs. This weakens the heart muscle, and chest pain (angina) may occur. If a blood clot forms in the narrowed artery, a heart attack (myocardial infarction) or even death can result.

It has been shown that cholesterol oxidase and horseradish peroxidase can be immobilized in a tetraethyl orthosilicate sol-gel film by physical adsorption, physically entrapped sandwich and microencapsulation techniques [149]. Photometric and amperometric techniques have been used for the detection of cholesterol. Cholesterol oxidase has been immobilized in the polyaniline film by electrochemical doping [150]. The enzyme electrode prepared in this manner needs only a very small amount of cholesterol oxidase and has a good bioelectrochemical response to cholesterol with a characteristic of a typical enzyme-catalyzed reaction. The characteristics of the enzyme electrode were affected by the concentration of Triton X-100.

Polypyrrole, overoxidized polypyrrole poly (o-phenylenediamine) bilayer biosensors have been developed with the enzyme cholesterol oxidase entrapped within an inner PPy layer onto which a non-conducting poly(o-phenylenediamine) film was then electrodeposited by Vidal et. al. [151-154]. They also showed that platinization of the electrode surface is of great interest for the development of cholesterol biosensors based on cholesterol oxidase enzyme entrapment in PPy films, leading to a significant improvement in the efficiency of the biosensor response [153].

Cholesterol oxidase was also immobilized in a octyl-agarose gel [155], and nylon membrane [156], copolymer of methyl and glycidal methacrylates [157], alkylamine glass beads [158] and polyacrylonitrile hollow fiber [159].

### **1.3 Aim of the Study**

- To achieve the synthesis of thiophene functionalized monomers and polymers and their characterization.
- To explore the electrochemical synthesis of conducting polymers, copolymers of thiophene functionalized monomer and polymer with pyrrole and thiophene.
- To investigate the electrochemical, thermal, morphological and conducting properties of resultant polymers and copolymers.
- To check the possibility of enzyme immobilization, invertase and cholesterol oxidase in both pristine polypyrrole and its copolymers via electrochemical polymerization and to compare the efficiency of immobilization between these two matrices.

## CHAPTER II

### EXPERIMENTAL

#### 2.1 Materials

Pyrrole (Py) (Aldrich) and thiophene (Sigma) were freshly distilled under reduced pressure. Pyrrole was kept at 0°C, in the dark, until it was used. Acetonitrile (AN) (Merck), methanol (Merck) nitromethane (NM) (Sigma), tetrabutylammonium tetrafluoroborate (TBAFB), *p*-toluene sulfonic acid (PTSA) (Sigma) and sodium dodecylsulfate (SDS) (Aldrich) were used without further purification. Dichloromethane and benzene were purified by usual methods and dried over CaH<sub>2</sub> and Na wire, respectively. Thiophene-3-acetic acid (Fluka), CuCl (Aldrich), NaOH (Aldrich), CaCl<sub>2</sub> (Aldrich), azobisisobutyronitrile (AIBN) (Aldrich), FeCl<sub>3</sub> (Merck), diethyl ether (Aldrich), propylene carbonate (Aldrich), triethylamine (TEA) (Baker) and cholesterol (Fluka) were used as received. Thionyl chloride (Fluka), methacryloyl chloride (Aldrich) and 3-thiophene methanol (Aldrich) were distilled under reduced pressure just before use.

Invertase ( $\beta$ -fructofuranosidase) type V (EC No.3.2.1.26) was purchased from Sigma and used as received without further purification. For the preparation of Nelson reagent, sodium carbonate, sodium potassium tartarate, sodium bicarbonate, sodium sulfate, copper sulfate and for the preparation of arsenomolibdate reagent, ammonium heptamolibdate, sodium hydrogen arsenate were used without any purification.

Cholesterol oxidase (COD) (E.C. 1.1.3.6) with a specific activity of 4.2 U/mg solid, horseradish peroxidase (HRP) (E.C. 1.11.1.7) with a specific activity of 157 U/mg solid were obtained from Sigma. Cholesterol and Triton X-100 were purchased from Sigma and used as received. All the reagents used were of analytical grade.

## **2.2 Polymer Electrochemistry**

Several different methods can be utilized to carry out the electropolymerization of thiophene and pyrrole-based monomers and include, cyclic voltammetry, constant current, and constant potential methods. In each case solution of monomer in a high dielectric constant solvent (such as acetonitrile or propylene carbonate) suitable for electrochemistry is prepared. It is necessary that the solvent be electrochemically inert (meaning that it will not undergo electrochemical reactions itself within the potential range being used for the experiment) and non-nucleophilic. In addition to solvent, a supporting electrolyte (such as the tetrabutylammonium perchlorate, tetrabutylammonium tetrafluoroborate, and tetrabutylammonium hexafluorophosphate) is also required to help current pass through the solution and to compensate charges that form on the polymer during oxidation and reduction.

### **2.2.1 Cyclic Voltammetry**

The most convenient method for initial studies on electrochemically polymerizable compounds is cyclic voltammetry (CV). This method consists of cycling the potential of an electrode, which is immersed in an unstirred solution, and measuring the resulting current at the working electrode. The background of cyclic voltammetry was presented in Chapter 1.

### **2.2.2 Constant Current (Galvanostatic) Methods**

In this technique, the current is controlled by a galvanostat and remains constant throughout the experiment while the potential is monitored as a function of time (chronopotentiometry). When a conducting polymer is deposited on the electrode surface, the potential of the monomer oxidation starts to decrease due to the reduction in monomer oxidation potential on the polymer, compared to the bare electrode. The thickness of conducting polymer films can be controlled by monitoring the charge which is obtained by multiplying the time of experiment by the constant current. Although simple in application, this method has drawback of the unknown nature of generated species since the potential is variable parameter.

### **2.2.3 Constant Potential (Potentiostatic) Methods**

Potentiostatic method is also an effective means of polymer deposition and is mainly used when a specific amount of charge must be passed while the potential is maintained below a certain value. With this approach the potential is stepped from a potential where there is no reaction, to a set potential where the reaction occurs. This is often the onset potential recorded by during potentiostatic growth and current response is monitored with respect to time (chronoamperometry). By keeping the potential constant, the creation of undesired species is prevented, hence the limitation becomes selective.

## **2.3 Instrumentation**

In this work, the synthesis of copolymers and enzyme immobilization processes were performed in a typical H-shaped electrolysis cell which is divided into anode and cathode compartments by a medium porosity sintered glass disc of 2.0 cm diameter. A Luggin capillary of reference electrode was inserted the anode side of the cell (Figure 2.1). Films were electrochemically polymerized by potentiostatic methods by using Wenking Model POS 73 and ST 88 potentiostats.

Platinum (Pt) flag electrodes as the working and counter and silver (Ag) wire (pseudo reference) reference electrodes were used during electrolyses, and all potentials were reported with respect to the Ag wire.

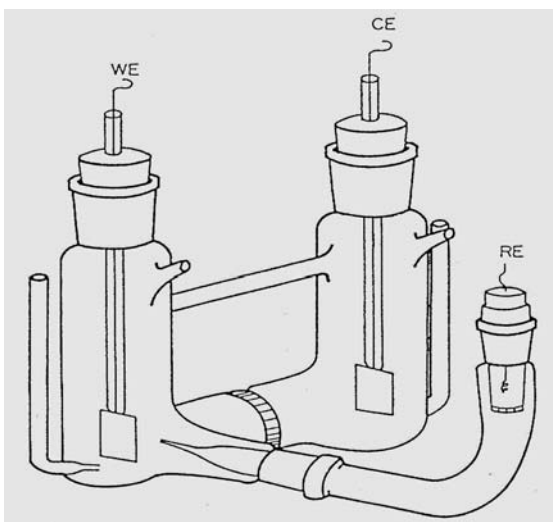


Figure 2.1 H-shaped electrolysis cell.

Cyclic voltammetry system is a convenient way of obtaining the oxidation-reduction peak potentials of the substrates such as monomers and to analyze the electroactivity of polymers. The cell (Figure 2.2) consists of a platinum bead working electrode of 1 cm wire in length, a platinum spiral counter electrode (3 cm coil), and a Ag/Ag<sup>+</sup> reference electrode. The volume of the cell was about 15 mL. CV experiments were carried out by a Bank Wenking POS 2 potentiostat/galvanostat. XY recorder was used to obtain the voltammograms

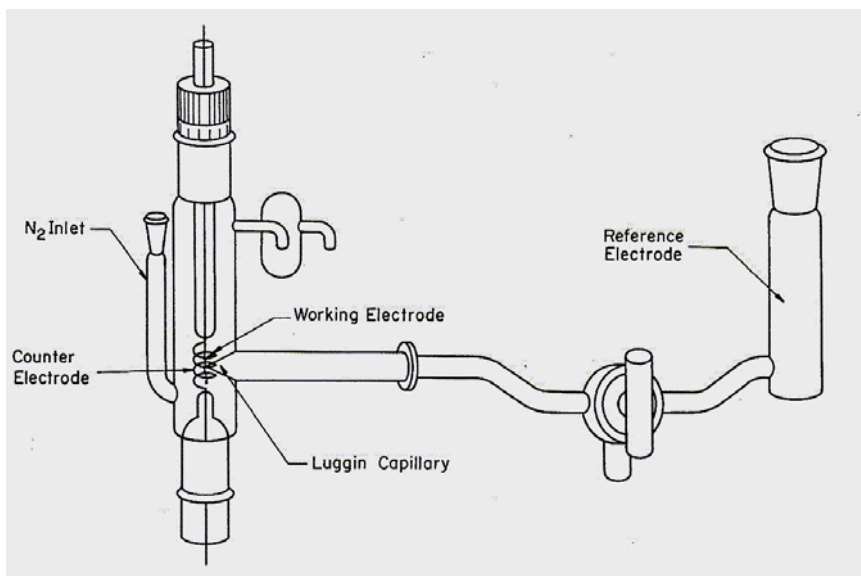


Figure 2.2 Cyclic voltammetry cell

### 2.3.1 Nuclear Magnetic Resonance Spectrometer ( $^1\text{H}$ -NMR and $^{13}\text{C}$ -NMR)

NMR spectra of samples were taken by Bruker Instrument-NMR Spectrometer (DPX-400).

### 2.3.2 Fourier Transform Infrared Spectrophotometry (FTIR)

FTIR is a useful method for the characterization of conducting polymers because it does not require polymers to be soluble. It is primarily used for the detection of functional groups, but analysis of spectra in the lower frequency finger print region can give evidence of degree of polymerization, the extent of mislinking within the polymer and the effect of substituents on the electronic properties of the polymer backbone. In this work, FTIR spectra of the polymers were recorded on a Nicolet 510 FT-spectrophotometer.

### **2.3.3 Gel Permeation Chromatography (GPC)**

For determination of molecular weight of insulating precursor polymers (dissolved in tetrahydrofuran), GPC were conducted using a Waters 510 liquid chromatography pump (1 mL/min) equipped with columns in series with 410 Waters differential refractometer. Molecular weights were determined on the basis of polystyrene standards.

### **2.3.4 Thermal Analysis**

Thermal characterization of polymers was carried out using a DuPont modular thermal analyzer system in conjunction with 951 thermal gravimetric analyzer and 910 differential scanning calorimeter. Thermal gravimetry analysis (TGA) experiments were performed under a dry nitrogen purge. A constant heating rate of 10 °C/min was using during differential scanning calorimetry (DSC) experiments.

### **2.3.5 UV-Vis Spectrophotometry**

A Shimadzu UV-1601 model spectrophotometer was employed in determination of activities of both free and immobilized enzyme

### **2.3.6 Scanning Electron Microscopy (SEM)**

SEM is a surface analytical technique which is employed to study the morphology of conducting polymer film surfaces and provides valuable information on the structure of the monomer, the nature of dopant and the thickness of the film. SEM of both copolymer and enzyme entrapped films was performed using a JEOL model JSM-6400 scanning electron microscope at 20kV with varying levels of magnification. With this aim, polymer films were peeled back from Pt electrode and glued to copper holder, and then they were coated by

sputtering with a thin gold film to avoid charge build-ups because of their low conductivity.

### 2.3.7 Conductivity Measurements

Among available conductivity techniques, four probe methods have several advantages for measuring electrical properties of conducting polymers. First, four probe techniques eliminate errors caused by contact resistance, since the two contacts measuring the voltage drop are different from the contacts applying the current across the sample. Second, this technique allows for conductivity measurements over a broad range of applied currents, usually varying between 1  $\mu\text{A}$  and 1mA for conducting polymers studied in this work. These current values produce potential differences ranging from 10  $\mu\text{V}$  to 10 V, depending on the resistance and thickness of the sample.

There are three types of four probe conductivity techniques that can be employed in the study of conducting polymers: Van der Pauw [160], four-wire [161] and four-point probe (Signatone) [162] and their use depends on the instrumentation available as well as sample quality and geometry.

Figure 2.3 shows the simplest form of a four-point probe measurement setup. A row of pointed electrodes touches the surface of a polymer film taped or spin cast on an insulating substrate. A known current  $I$  is injected at the electrode 1 and is collected at the electrode 4, while the potential difference  $\Delta V$  between contacts 2 and 3 is measured. Conductivity is calculated from the following equation:

$$\sigma = \ln 2 / (\pi R t)$$

where  $R$  is the resistance of the sample, and  $t$  is the thickness.

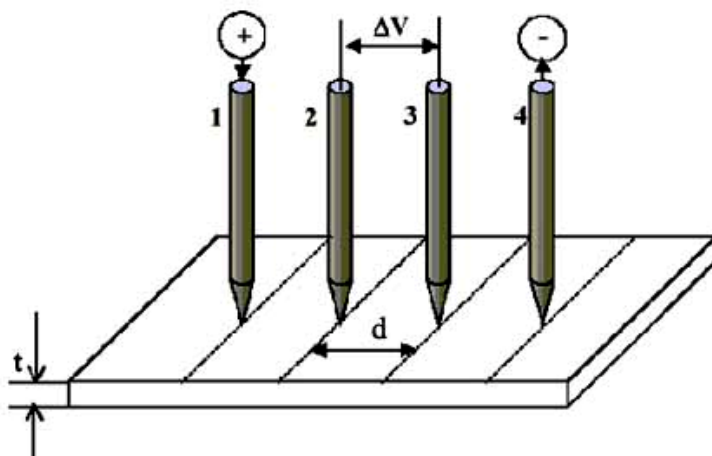


Figure 2.3 Four-probe conductivity measurement

## 2.4 Synthesis of Conducting Copolymers

### 2.4.1 Conducting Graft Copolymers of Poly (3-Methylthienyl Methacrylate) with Pyrrole and Thiophene

#### 2.4.1.1 Synthesis of 3-Methylthienyl Methacrylate (MTM)

5.7 g (50 mmol) of 3-thiophene methanol, 7.3 g (71 mmol) of dry triethylamine and a small amount of CuCl were dissolved in 35 mL of dry diethyl ether. 5.35 gr (51 mmol) of freshly distilled methacryloyl chloride in 35 mL of dry diethyl ether were added slowly at 0 °C. The mixture was stirred for two hours. The triethylammonium chloride was filtered off through a silica gel column. After solvent evaporation, the residue was stirred overnight in a 1:1 mixture of methylene chloride and 2 M NaOH. The organic layer was separated, washed twice with water and dried over CaCl<sub>2</sub>. Following solvent evaporation the residue was distilled in vacuum over a Vigreux column.

b.p.(1 mm-Hg) : 90 °C; yield: 70 %

<sup>1</sup>H-NMR (CDCl<sub>3</sub>) : δ = 1,9 (s; CH<sub>3</sub>), 5,1 (s; OCH<sub>2</sub>), 5,5 (s; vinyl H), 6,1 (s; vinyl H), 7,06 (m; ring H), 7,2 (m; ring H).

#### **2.4.1.2 Bulk Polymerization of 3-Methylthienyl Methacrylate**

Poly (3-methylthienyl methacrylate) (PMTM) was prepared by free-radical polymerization with the use of AIBN as the initiator. At the end of the polymerization, the reaction mixture was poured into methanol. The precipitated polymer was filtered off, dried in vacuum and purified by repeated precipitations.

#### **2.4.1.3 Cyclic Voltammetry (CV)**

A thin layer of the PMTM2 was deposited on a platinum working electrode by casting from dichloromethane solution. Ag wire was used as the reference and Pt foil as the counter electrodes. The voltammograms were recorded in ACN-TBAFB solvent-electrolyte couple using a system consisting of a potentiostat (Wenking POS 73) and an X-Y recorder at room temperature under nitrogen atmosphere.

#### **2.4.1.4 Synthesis of Copolymers with Pyrrole by Electrochemical Polymerization**

PMTM2/PPy graft copolymers were prepared by the electrochemical polymerization of pyrrole on PMTM2 coated electrodes. Electrochemical polymerization of pyrrole was carried out in distilled water and acetonitrile containing 0.02 mol/L pyrrole and 0.05 mol/L supporting electrolyte (PTSA, SDS and TBAFB) at the oxidation potential of pyrrole (1.0 V) vs Ag/Ag<sup>+</sup> reference electrode. The electrolysis was allowed to proceed until sufficiently thick films were obtained. After electrolysis, anode was removed from cell and immersed in dichloromethane for several hours to remove the ungrafted precursor polymer.

#### **2.4.1.5 Synthesis of Copolymers with Thiophene by Electrochemical Polymerization**

For the grafting process with thiophene, Pt electrode was coated with PMTM2 and used as the anode for the copolymerization. The electrolysis cell contained 0.02 mol/L thiophene and 0.05 mol/L TBAFB in acetonitrile. The electrolyses were carried out at 1.9 V for 60 min under nitrogen atmosphere. As a second route for the copolymer synthesis, 40 mg PMTM2 and 0.02 M thiophene were dissolved in dichloromethane and electrolyses were carried out at +1.9 V for 30 min at 0 °C. For both cases black films were peeled off from the working electrode surface and dried under vacuum.

#### **2.4.1.6 Oxidative Polymerization of PMTM1 with FeCl<sub>3</sub> (CPMTM1)**

78 mg of PMTM1 was dissolved under a blanket of N<sub>2</sub> in 5 mL dichloromethane. A solution of 10 gr FeCl<sub>3</sub> in 15 mL nitromethane was added dropwise to the solution of PMTM1. After a 24-h reaction time, the gray product was precipitated in methanol. It was washed several times with methanol and water. Product was dried to constant weight under vacuum.

#### **2.4.1.7 Oxidative Polymerization of PMTM1 by Constant Current Electrolysis (GPMTM1)**

Propylene carbonate and dichloromethane were used as the solvents for galvanostatic polymerization of PMTM1. 0.2M TBAFB was used as the supporting electrolyte. Platinum foils were used as the working and counter electrodes. For the self-polymerization of PMTM1, platinum electrode was coated with PMTM1 and electrolyses were carried out in propylene carbonate (GPMTM1P). As the second route for the oxidative polymerization of PMTM1, 50 mg of PMTM1 was dissolved in dichloromethane. The electrolyses were

carried out at 50 mA for 30 min at 0 °C under inert atmosphere. Black films were peeled from the anode and dried under vacuum (GPMTM1D).

## **2.4.2 Synthesis and Characterization of Conducting Copolymers of Thiophene-3-yl Acetic Acid Cholesteryl Ester with Pyrrole**

### **2.4.2.1 Synthesis of Cholesteryl Containing Thiophene Monomer (CM)**

a) A mixture of 3-thiophene acetic acid (14.217 g, 0.1 mol) in 50 mL dry benzene and thionyl chloride (35.69 g, 0.3 mol) was refluxed for 16 h. The solvent and unreacted thionyl chloride were removed by distillation. The residual liquid product was purified by distillation under reduced pressure.

<sup>1</sup>H-NMR in CDCl<sub>3</sub> (δ, ppm): 7.33, 7.21, 7.01 (3H, thiophene ring), 4.16 (2H, CH<sub>2</sub>).

b) To a solution of 1.966 g (0.005 mol) cholesterol in 10 mL dichloromethane containing 0.505 g (0.005 mol) triethylamine (TEA), was added dropwise in 0.5 h, by cooling in ice bath and nitrogen atmosphere onto 0.883 g 3-thiophene acetyl chloride (0.0055 mol). The esterification was carried out for over night at room temperature. Then the white solid of triethylamine chlorine hydrate was filtered off and the solution was washed with HCl 1% solution (three times) and water (three times). The organic layer was dried over MgSO<sub>4</sub> and the solvent was removed via rotaevaporator. The crude product was purified by chromatography through a silicagel column using a mixture of hexane/ethyl acetate (9/1 v/v) as the eluent. Twice recrystalization from ethanol provided 1.88 g of white crystals (yield 74 %).

#### **2.4.2.2 Cyclic Voltammetry (CV)**

The oxidation/reduction behavior of the monomer in the presence of pyrrole and thiophene was investigated by CV. The system consists of a potentiostat (HEKA), an X-Y recorder and a CV cell containing Pt foil working and counter electrodes, and a Ag/Ag<sup>+</sup> reference electrode. Measurements have been carried out under N<sub>2</sub> atmosphere in acetonitrile and water at room temperature.

#### **2.4.2.3 Potentiostatic Polymerization of CM**

##### **2.4.2.3.1 Self Polymerization of CM**

For the self-polymerization of CM, electrolysis cell was prepared by precoating the working electrode with 1 w/v % solution of CM in dichloromethane, 0.05 M PTSA and/or SDS in distilled water. Constant potential electrolyses were carried out at 1.1 V for 2 h. Electrolyses were also performed in AN-TBAFB, solvent electrolyte couple by precoating the Pt electrode with CM in 0.05 M or 0.1 M TBAFB at 2.0 V and 2.5 V for 2 h. Separate electrolyses were also performed by dissolving 50 mg of CM in dichloromethane and 0.05 M TBAFB at 2.5 V at 0°C.

##### **2.4.2.3.2 Synthesis of Copolymers of CM with Pyrrole**

1 w/v % solution of CM in dichloromethane was deposited onto Pt electrode. This electrode was used as the working electrode after the evaporation of the solvent. Electrolyses were performed in the presence of 0.02 M pyrrole; 0.05 M PTSA or SDS in water at 1.1 V. Separate electrolyses were also carried out 0.05 M TBAFB in acetonitrile at 1.3 V for 80 min by depositing the CM on the electrode. Then, the polymer film was peeled off from the electrode surface.

#### **2.4.2.3.3 Synthesis of Copolymers of CM with Thiophene**

For the synthesis of copolymers of CM, thiophene was used as the comonomer. The electrolysis cell was prepared by dissolving 0.05 M TBAFB and 0.02 M thiophene in acetonitrile was added and electrolyses were carried out at 1.9 V for 80 min.

#### **2.4.2.4 Chemical Polymerization of CM (PCM1) and Doping with Iodine**

Chemical polymerization of CM was carried out in both NM/CCl<sub>4</sub> (3:1) [163] and CHCl<sub>3</sub> under constant flow of nitrogen. 100 mg of CM was dissolved in CCl<sub>4</sub> and placed in three-necked flask. Polymerization was achieved by dropwise addition of FeCl<sub>3</sub> solution in NM (2.5 M) to a solution of monomer at 0 °C. The reaction was run for 24 h with constant stirring. Methanol was added to precipitate the gray solid. It was washed with water and methanol several times to remove excess ferric chloride. Then, the solid (PCM1) filtered dried under vacuum. The yield is 71 %.

For the polymerization of CM in CHCl<sub>3</sub> both monomer and FeCl<sub>3</sub> were dissolved in CHCl<sub>3</sub>. The reaction was performed in an inert atmosphere with constant stirring at room temperature [164].

Doping was achieved by using vapour phase doping technique. After known weight of PCM1 (20 mg) was placed into the tube, iodine was suspended to the test tube for one week. Conductivity of I<sub>3</sub><sup>-</sup> doped polymer was measured by using four-probe technique.

#### **2.4.2.5 Galvanostatic Polymerization of CM (PCM2), (PCM3), (PCM4)**

Constant current electrolyses (CCE) were carried out in AN-TBAFB, CH<sub>2</sub>Cl<sub>2</sub>-TBAFB and water-PTSA, solvent-electrolyte couples in one-compartment cell equipped with two electrodes; the working and counter electrodes. For water-PTSA system, stainless steel was used as the working (4x5 cm<sup>2</sup>) and a steel mesh as the counter electrode (4x5 cm<sup>2</sup>). 1 w/v % solution of monomer was deposited on the working electrode and electrolysis was performed by passing constant current of 100 mA. Electrolysis was also carried out in AN-TBAFB at room temperature at 300 mA. After electrolyses, a black precipitate (PCM2) was obtained from the solution by filtering. It was washed with acetonitrile several times and dried under vacuum. CCE was also performed in dichloromethane-TBAFB system at 0 °C at 200 mA with 50 mg monomer and 0.05 M TBAFB in 60 mL of dichloromethane. A green product (PCM3) was obtained from the solution. CCE was also performed for the same system by using Pt foils (1x1 cm<sup>2</sup>) as the working and counter electrodes. 0.2 M TBAFB and 50 mg of CM were dissolved in 15 mL dichloromethane. In this case, gray product (PCM4) was obtained both from the electrode surface and the solution.

#### **2.4.2.6 Synthesis of Block Copolymers of PCM1 with Pyrrole and Thiophene (PCM1/PPy and PCM1/PTh)**

For the copolymerization, chemically synthesized polymer (PCM1) was deposited on the electrode and electrolyses were carried out in acetonitrile-TBAFB, water-PTSA and water-SDS systems.

#### **2.4.2.7 Synthesis of Block Copolymers of PCM4 with Pyrrole and Thiophene (PCM4/PPy and PCM4/PTh)**

The synthesis of block copolymers of PCM4, were achieved in 1 w/v % PCM4 solution prepared in dichloromethane by coating the both sides of the electrode with PCM4. Electrolyses in the presence of pyrrole were done at room temperature for water-PTSA and water-SDS media since excess applied potentials cause the electrolysis of water, which leads to the loss of PCM4 on the anode. Application of +1.3 V in acetonitrile-TBAFB system, however, is possible and enhances the rate of production of the resultant copolymer. As to the polymerization of thiophene on PCM4 electrode, oxidation potential of thiophene was applied in AN-TBAFB solvent-electrolyte couple.

### **2.5 Immobilization Enzyme**

#### **2.5.1 Immobilization of Invertase in Conducting Copolymers of 3-Methylthienyl Methacrylate**

##### **2.5.1.1 Preparation of Enzyme Electrodes: 1-PPy/SDS, 2-PMTM/PPy/SDS, 3-(PMTM/PPy)/SDS, 4-(PMTM/PTh)/PPy/SDS and 5-(PTh)/PPy/SDS.**

Immobilization of invertase was accomplished by electropolymerization of pyrrole either on bare or previously PMTM coated platinum (Pt) electrode (enzyme electrodes 1 and 2). The electrolyses were carried out at +1.0 V in buffer that contains invertase, sodium dodecyl sulfate (SDS) and pyrrole. For the preparation of enzyme electrode 3, PMTM/PPy copolymer was prepared in acetonitrile-TBAFB solvent-electrolyte couple at +1.0 V for 60 min; then it was reduced in the same system at +0.1 V for 30 min. The reduced copolymer film was immediately moved into the buffer containing invertase and SDS, and oxidized at +1.0 V for 100 min. As to the enzyme electrodes 4 and 5 (Table II), PMTM/PTh copolymer and PTh films were again prepared in acetonitrile-

TBAFB, solvent-electrolyte pair at +1.9 V for 30 min, since thiophene is not soluble in buffer. Then, freshly prepared films were transferred into another cell containing 15 mL acetate buffer, 0.6 mg/mL SDS, 0.6 mg/mL invertase and 0.01 M pyrrole. Electrolyses were performed at +1.0 V for 100 min. Immobilization was performed in a one compartment cell, consisting of Pt working and counter electrodes and a Ag/Ag<sup>+</sup> reference electrode. A potentiostat Wenking POS-73 model potentiostat was used for electropolymerization. All electrolyses were carried out at room temperature and under nitrogen atmosphere. After immobilization was achieved, electrodes were removed and washed several times with distilled water to remove the supporting electrolyte. Next, the electrode was placed in acetate buffer for 10 minutes and solution was examined for the enzyme activity due to unbound enzyme. This procedure was repeated for several times with the acetate buffer until no activity was observed. Electrodes were stored in acetate buffer at 4 °C when not in use.

### **2.5.1.2 Activity Determination of Invertase**

#### **2.5.1.2.1 Preparation of Nelson's Reagent**

Nelson's Reagent was composed of 2 solutions, namely, reagent A and reagent B, for the preparation of Nelson reagent A, sodium carbonate (25 g), sodium potassium tartarate (25 g), sodium bicarbonate (20 g), sodium sulfate (200 g) were dissolved in distilled water and diluted to 1000 mL. Nelson reagent B was prepared by dissolving copper sulfate (15 g) in 100 mL distilled water. Reagent A and reagent B were mixed in 25:1 (v/v) prior to activity assay [140].

#### **2.5.1.2.2 Preparation of Arsenomolibdate Reagent**

Arsenomolibdate reagent was prepared by dissolving ammonium heptamolibdate (25 g), in 450 mL distilled water and by adding 21 mL concentrated sulfuric acid. Another solution, prepared by dissolving sodium

hydrogen arsenate (3 g) in distilled water, was added to the above solution. After incubation of resultant solution for 24-48 hours at 37 °C, it was stored in dark [140].

#### **2.5.1.2.3 Activity Assay**

The activities of immobilized invertase were determined by using Nelson's Method [165]. Different concentration of sucrose solutions prepared in acetate buffer (pH 7) were placed in test tubes and moved to water bath at 25 oC for 10 min. Enzyme electrode (EE) was immersed in the test tubes and shaken in the water bath for 2 min. The electrodes were removed; 1 mL aliquots were drawn and added to 1 mL Nelson's reagent to terminate the reaction. The tubes were then placed in boiling water bath for 20 min, cooled and 1 mL arsenomolybdate was added. Finally, 7 mL of distilled water was added to each test tube and mixed well by vortexing. After mixing, absorbances for the blank and the solutions were determined at 540 nm with a double beam spectrophotometer (Shimadzu Model, UV-1601). One unit of invertase activity was defined as the amount of enzyme required to release 1  $\mu$ mol glucose equivalents per minute under the assay conditions.

#### **2.5.1.3 Determination of Kinetic Parameters**

The kinetic studies of the reaction catalyzed by immobilized invertase were performed at varying concentrations of sucrose by keeping assay conditions constant (pH 4.8, at 25 °C). Activity assay was performed according to Section 2.4.3.2.3.

#### **2.5.1.4 Determination of Optimum Temperature**

For optimum temperature determination, incubation temperature was changed between 10 °C and 80 °C at the optimum pH of the immobilized

invertase by keeping sucrose concentration ( $\sim 10 K_m$ ) constant. For the activity measurement, the procedure described above was applied.

#### **2.5.1.5 Determination of Operational Stability**

One of the most important parameters to be considered in enzyme immobilization is operational stability. The stability of enzyme electrodes in terms of repetitive uses was studied.

#### **2.5.1.6 Morphologies of Films**

For investigation of morphology of enzyme entrapped polymer films, enzyme immobilization procedure was carried out until obtaining free standing films. After peeling of the films from electrode and washing with buffer solution for several times to remove unbound enzyme and supporting electrolyte from the surface of the film, SEM analysis was performed.

### **2.5.2 Immobilization of Cholesterol Oxidase in Conducting Copolymer of Thiophene-3-yl Acetic Acid Cholesteryl Ester with Pyrrole**

#### **2.5.2.1 Synthesis of Copolymer**

Electropolymerization of thiophene-3-yl acetic acid cholesteryl ester (CM) with pyrrole is given in Figure 2.4.

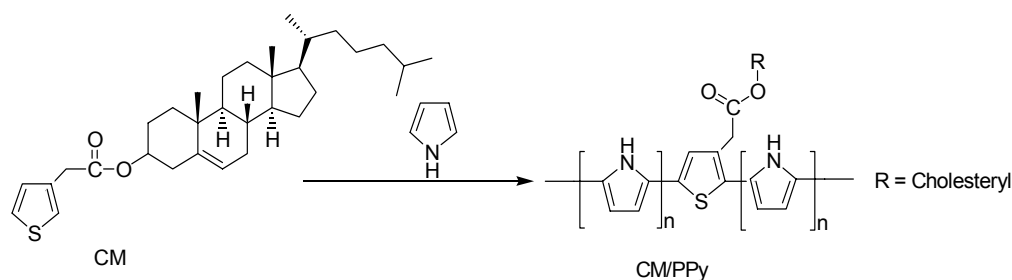


Figure 2.4 Electrochemical synthesis route for copolymerization

### 2.5.2.2 Preparation of Enzyme Electrodes (PPy/COD, CM/PPy/COD)

The electropolymerization process was carried out using a potentiostat Wenking POS-73 model potentiostat with a three-electrode configuration consisting of platinum foil as the working and counter electrode and Ag wire as the reference electrode. A 10 mL solution of 0.1M phosphate buffer (pH 7.0) containing 0.2 M pyrrole, 6 mg mL<sup>-1</sup> PTSA as the supporting electrolyte, 1 mg mL<sup>-1</sup> COD were used for immobilization via electropolymerization. For the preparation of CM/PPy/COD electrode, Pt electrode was coated with CM and used as the anode for the electropolymerization. Electrolyses were performed at room temperature under nitrogen atmosphere at the oxidation potential of pyrrole (+1.0 V). After immobilization was achieved, electrodes were removed and washed several times with distilled water to remove the supporting electrolyte. Next, the electrode was placed in phosphate buffer for 10 minutes and solution was examined for the enzyme activity due to unbound enzyme. This procedure was repeated for several times with the phosphate buffer until no activity was observed. Electrodes were stored in phosphate buffer at 4 °C when not in use.

### 2.5.2.3 Preparation of Cholesterol Solution

Cholesterol is insoluble in water. However, it is soluble in alcohols and also in the presence of surfactants [149,156,166,167]. The cholesterol was

dissolved in phosphate buffer, isopropanol and Triton X-100 (t-Octylphenoxy polyethoxy ethanol) in a weight ratio of 86:10:4. The surfactant and isopropanol were used due to the poor solubility of cholesterol in pure water. The cholesterol solutions were prepared daily by dissolving the cholesterol in isopropanol, then adding Triton X-100 and finally, the phosphate buffer (pH=7.0).

#### **2.5.2.4 Enzyme Activity Measurements**

The activity of cholesterol oxidase was determined spectrophotometrically by the method of Kumar et al. [149]. One unit will convert 1.0  $\mu\text{mol}$  of cholesterol to 4-cholesten-3-one per minute at pH=7.0 at 25 °C. 4 mL of cholesterol solution was incubated at 37 °C for 5 min. A 1 mL aliquot of cholesterol oxidase solution (2 mg in 50 mL phosphate buffer, pH 7.0) were added to a cholesterol solution. After the reaction, a 3 mL solution containing 4-aminoantipyrine ( $158 \text{ mg mL}^{-1}$ ), phenol ( $146 \text{ mg mL}^{-1}$ ) and peroxidase (HRP) ( $10 \text{ mg dL}^{-1}$ ) was added. The appearance of quinoneimine dye formed by coupling with 4-aminoantipyrine, phenol and peroxide was measured at 500 nm with a double beam spectrophotometer (Shimadzu Model, UV-1601). One unit of activity was defined as the formation of 1  $\mu\text{mol}$  of hydrogen peroxide per minute at 37 °C and pH 7.0. The  $V_{\text{max}}$  and  $K_{\text{m}}$  values were estimated from Lineweaver-Burk plots. Reaction mixtures composed of 0-5 mM substrate solution were used to calculate kinetic parameters.

#### **2.5.2.5 Kinetic Studies of Free and Immobilized COD**

Kinetic studies of the free and immobilized cholesterol oxidase were performed at various concentrations of cholesterol. Maximum velocity,  $V_{\text{max}}$ , and the apparent Michaelis-Menten constant,  $K_{\text{m}}$ , were found from the Lineweaver-Burk plot.

#### **2.5.2.6 Operational Stability of Immobilized COD**

Operational stability is an important consideration for an immobilized enzyme. To determine this parameter, activities of the enzyme electrodes were checked for 25 successive measurements.

#### **2.5.2.7 Surface Morphologies of Enzyme-entrapped Film**

For investigation of morphology of cholesterol oxidase entrapped free standing films, SEM analysis was performed.

## CHAPTER III

### RESULTS AND DISCUSSION

#### 3.1 Conducting Copolymers

##### 3.1.1 Conducting Graft Copolymers of Poly (3-Methylthienyl Methacrylate) with Pyrrole and Thiophene

###### 3.1.1.1 Bulk Polymerization of 3-Methylthienyl Methacrylate

Thiophene functionalized methacrylate monomer (MTM) was synthesized via esterification of the 3-thiophene methanol with methacryloyl chloride [168]. The methacrylate monomer was polymerized by free radical polymerization in the presence of AIBN as the initiator (Figure 3.1). The results of the polymerization were presented in Table 3.1 (PMTM1 and PMTM2).

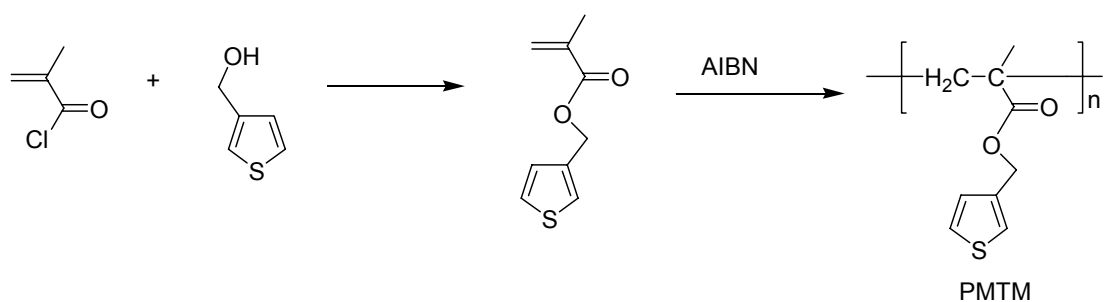


Figure 3.1. PMTM synthesis route

Table 3.1. Synthesis of poly (3- methylthienyl methacrylate)

Code	Monomer (mol L <sup>-1</sup> )	Conversion(%)	$M_n^a$	$M_w/M_n^a$
PMTM1	6	33	73000	2
PMTM2	6	21	133000	2.1

[AIBN] =  $5 \cdot 10^{-3}$  mol L<sup>-1</sup>, T = 65 °C.

<sup>a</sup> by GPC based on PS standards.

### 3.1.1.2 Cyclic Voltammetry (CV)

Cyclic Voltammetry experiments were carried out in ACN-TBAFB system under N<sub>2</sub> atmosphere. Figure 3.2 depicts the redox behavior of pyrrole, thiophene and PMTM2 in the presence of thiophene and pyrrole. In the cyclic voltammogram of pristine polymer, PMTM2, no detectable redox peak was observed. However, in the presence of thiophene, an increasing redox peak appeared at +2.0 V with increasing scan number. The CV behavior of thiophene on a bare Pt electrode was completely different. This is an indication of a reaction between PMTM2 and thiophene. In the same manner, upon addition of pyrrole, PMTM2 exhibited different electroactivity compared to that of pyrrole. This reveals a possible interaction between pyrrole and PMTM2.

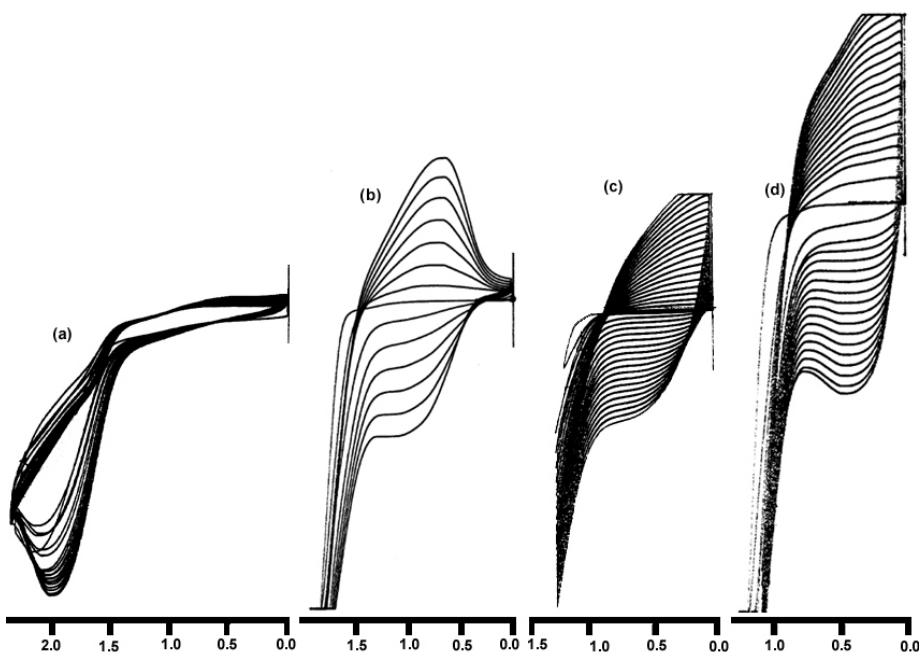


Figure 3.2 Cyclic voltammograms of (a) PMTM2 in the presence of thiophene (b) thiophene on a bare Pt electrode (c) PMTM2 in the presence of pyrrole (d) pyrrole on a bare Pt electrode.

### 3.1.1.3 Oxidative Polymerization of PMTM1

Polymerization of PMTM1 was accomplished by chemical oxidation and constant current electrolysis techniques (Figure 3.3). FTIR spectra of PMTM1 show a sharp intense peak at  $1725\text{ cm}^{-1}$ , which can be attributed to the presence of C=O stretching vibrations (Figure 3.4). The broad peak ranging from  $1250$  to  $1000\text{ cm}^{-1}$  is due to C-O (ester group) stretching vibrations. The band at  $780\text{ cm}^{-1}$  is the result of the presence of thiophene units. After the oxidative polymerization of precursor polymer with  $\text{FeCl}_3$ , new bands appeared at  $1570\text{ cm}^{-1}$  and  $1625\text{ cm}^{-1}$ , indicating conjugation (Figure 3.5). Moreover, the intensity of band at  $780\text{ cm}^{-1}$  decreased and the intensity of band at  $832\text{ cm}^{-1}$  which is responsible for the 2,3,5 trisubstituted thiophene ring increased. As to the galvanostatical polymerization of PMTM1, an intense peak was observed at about  $1074\text{ cm}^{-1}$  due to the dopant anion (Figure 3.6). The absorption at  $1790\text{ cm}^{-1}$  was attributed to the formation of

anhydride structure for GPMTM1P [169,170]. There were also absorption bands that are related to the pristine polymer, 1725  $\text{cm}^{-1}$ , 1472  $\text{cm}^{-1}$ , 1390  $\text{cm}^{-1}$ , 1260  $\text{cm}^{-1}$ , and 790  $\text{cm}^{-1}$ . A shoulder at 1621  $\text{cm}^{-1}$  was also appeared in GPMTM1P and GPMTM1D.

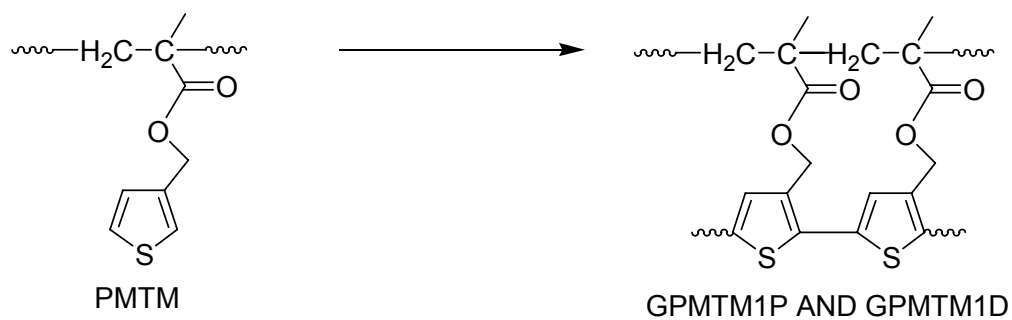


Figure 3.3. Galvanostatic polymerization route

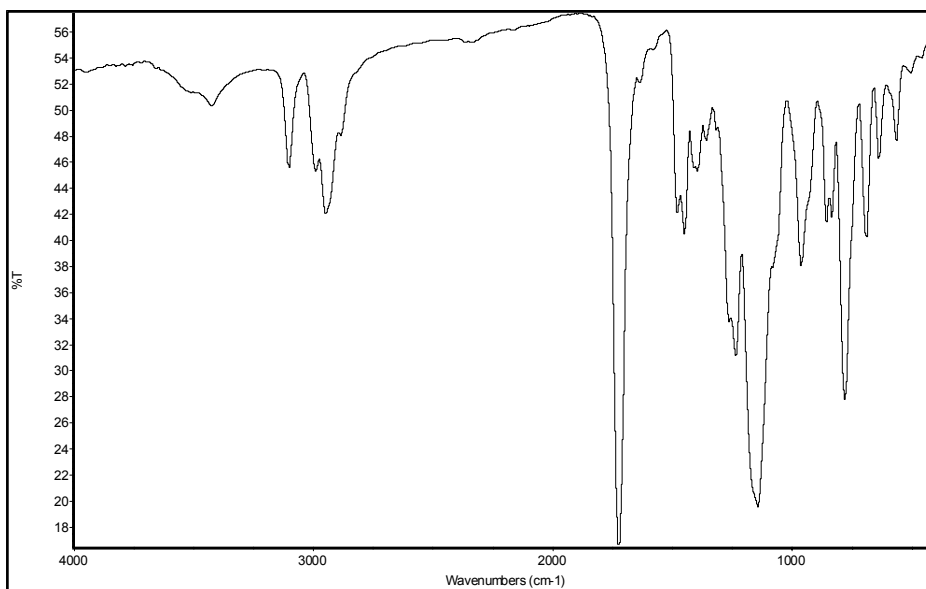


Figure 3.4 FTIR spectra of PMTM

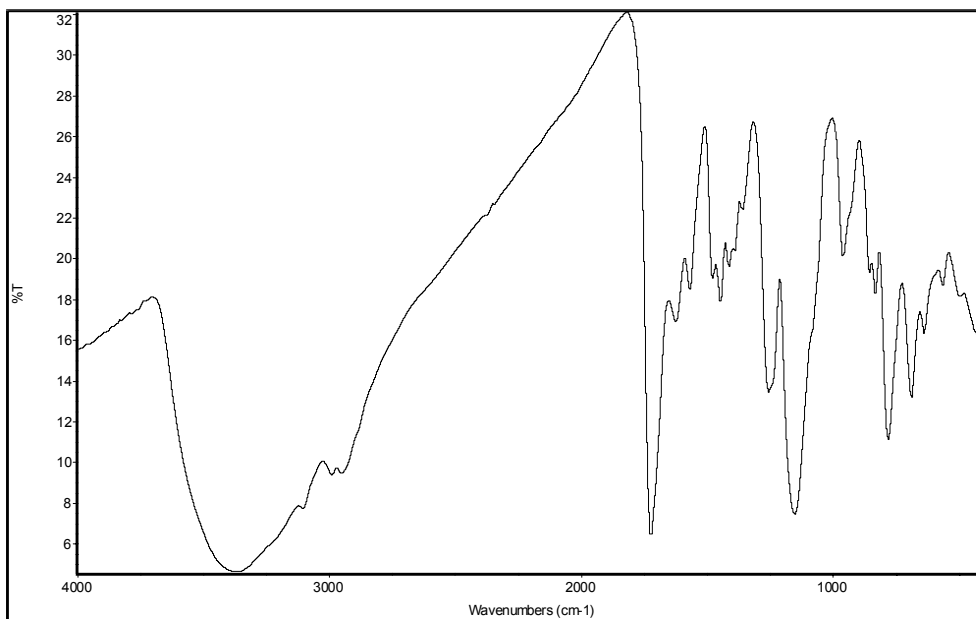


Figure 3.5 FTIR spectra of CPMTM

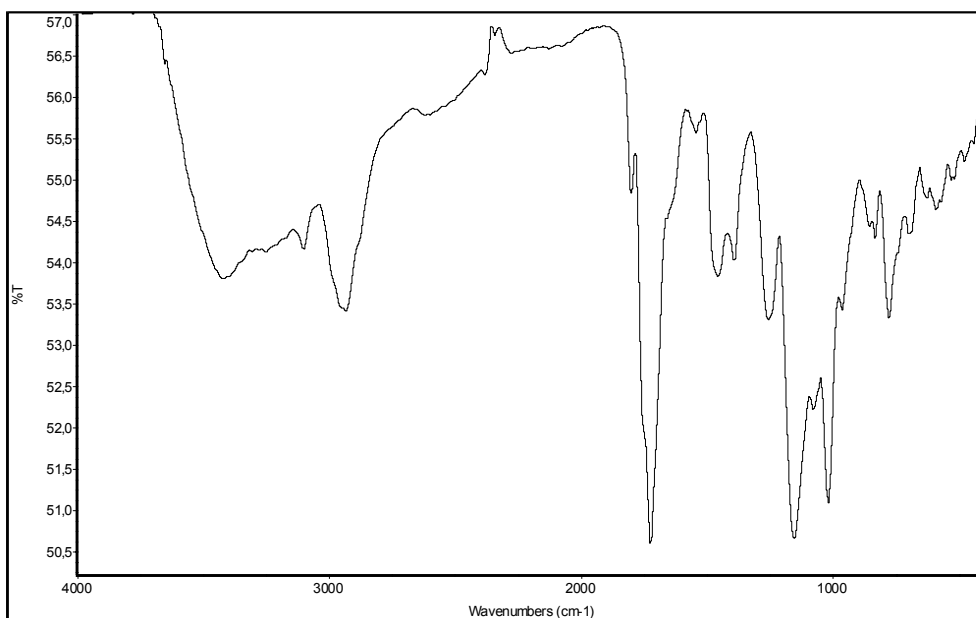


Figure 3.6 FTIR spectra of GPMTM

### 3.1.1.4 Synthesis of Copolymers

Electropolymerization of PMTM2 was achieved in the presence of pyrrole and thiophene by constant potential electrolysis (Figure 3.7).

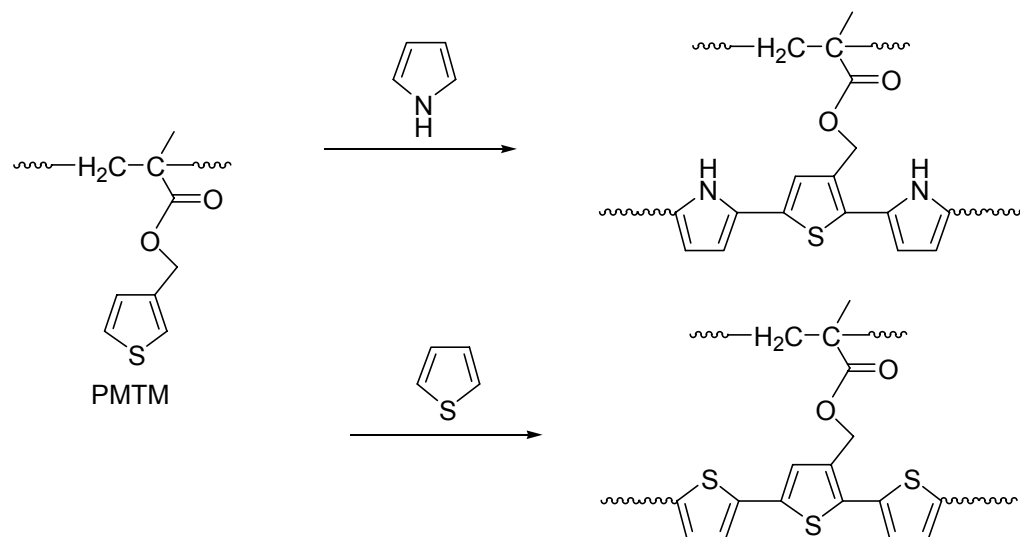


Figure 3.7 Electrochemical synthesis route for copolymerization

FTIR spectra of  $\text{PTS}^-$ , SDS and  $\text{BF}_4^-$  doped PMTM2/PPy showed peaks at 3400, 1440, 1310, 1180  $\text{cm}^{-1}$  due to C-N and C-C stretchings which are characteristic for PPy. A characteristic peak at 1725  $\text{cm}^{-1}$  belonging to carbonyl group of pristine PMTM2 was also observed (Figure 3.8). These results indicated that the polymerization of pyrrole occurred through PMTM2 chain. The absorption bands at 1725, 1636, 1471, 1400, 1302, 1074 and 780  $\text{cm}^{-1}$  were observed on the FTIR spectra of  $\text{BF}_4^-$  doped PMTM2/PTh copolymer synthesized either in acetonitrile or dichloromethane (Figure 3.9). The most intense band at 1074  $\text{cm}^{-1}$  is related to the dopant anion and the band at 1725  $\text{cm}^{-1}$  was attributed to the PMTM2.

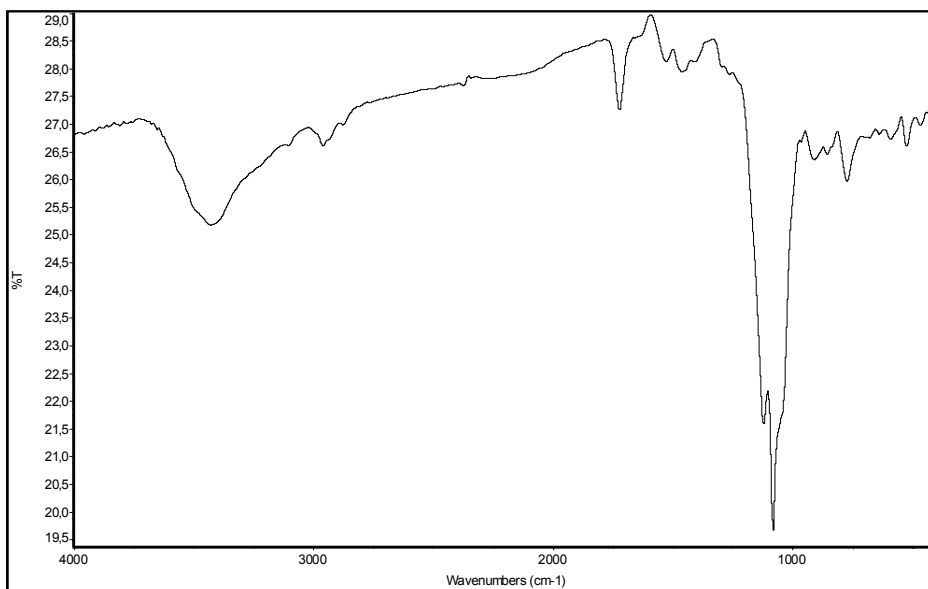


Figure 3.8 FTIR spectra of PMTM/PPy doped with  $\text{BF}_4^-$

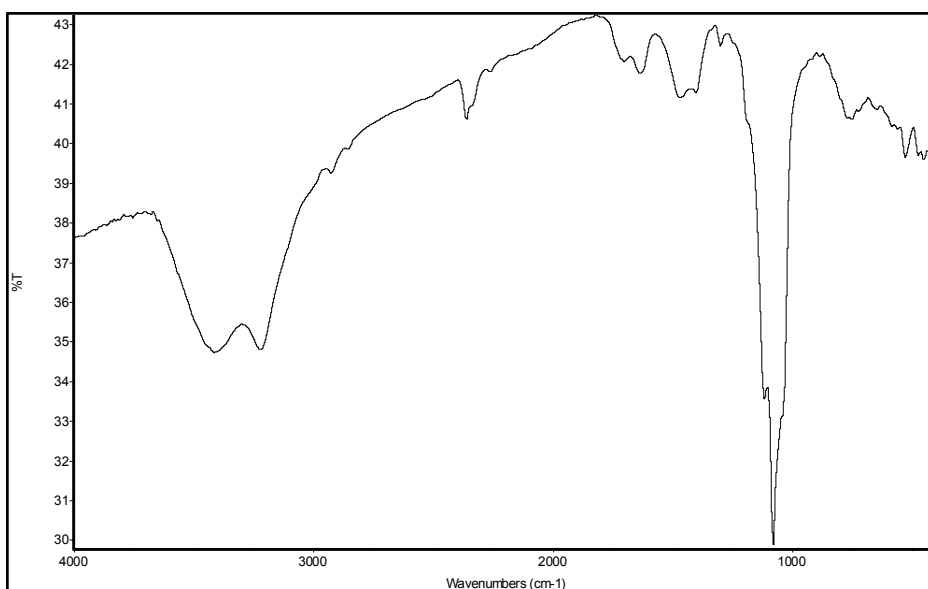


Figure 3.9 FTIR spectra of PMTM/PTh doped with  $\text{BF}_4^-$

### 3.1.1.5 Conductivities of PMTM2/PPy and PMTM2/PTh Films

Electrical conductivity measurements were carried out by using the standard four probe technique. Conductivities of graft copolymers, PMTM2/PPy, (doped with any one of PTS<sup>-</sup>, SDS, BF<sub>4</sub><sup>-</sup>) were 0.6-3 S/cm (Table 3.2). Upon washing with dichloromethane no marked changes were measured in conductivity. In the case of PTh graft copolymers, conductivities were in the order of 10<sup>-3</sup> S/cm. The conductivities of both electrode and solution sides were also in the same order of magnitude, which reveals the homogeneity of the films.

Table 3.2 Conductivities of the films

Sample	Conductivity (S/cm)
PMTM2/PPy (PTS <sup>-</sup> doped)	3.0
PMTM2/PPy (SDS <sup>-</sup> doped)	0.8
PMTM2/PPy (BF <sub>4</sub> <sup>-</sup> doped)	0.6
PMTM2/PTh (BF <sub>4</sub> <sup>-</sup> doped)	6x10 <sup>-3</sup>

### 3.1.1.6 Thermal Properties

DSC thermograms of both precursor polymer and copolymers were examined in the range 30 °C to 500 °C at a heating rate of 10 °C /min (Figure 3.10). DSC thermogram of PMTM2 exhibited two thermal events; a glass transition (T<sub>g</sub>) at about 70 °C and a decomposition at about 360 °C. Thermal behavior of PMTM1 and PMTM2 are similar. In CPMTM1, two endothermic peaks appeared at 93 °C and 231 °C. As for the GPMTM1P, two thermal transitions were observed at 103 °C may be due to removal of solvent and 350 °C may be attributed to decomposition of the sample. In the case of GPMTM1D, a glass transition at 97 °C and two endothermic transitions at 208 °C and 368 °C, which were probably as a result of dopant loss or decomposition, were appeared. DSC thermogram of PMTM2/PTh, synthesized in acetonitrile-TBAFB solvent-

electrolyte couple, showed three endothermic transitions at 79 °C, 105 °C which could be due to the loss of solvent and decomposition at 243 °C. The PTS<sup>-</sup> doped PMTM2/PPy showed three endothermic peaks at about 74 °C, 201 °C, 333 °C. As far as the DS<sup>-</sup> doped copolymer films were concerned, two endothermic peaks at about 75 °C and 251 °C were noticeable. These results reveal the presence of high polypyrrole content in the resultant copolymers.

Thermal behavior of the samples was investigated by using a Du Pont 2000 Thermal Gravimetry Analyser. TGA curve of the samples was shown in Figure 3.11. The thermogravimetry scan of the precursor polymer, PMTM2, revealed huge weight losses at 412 °C and 450 °C. TGA curve for PMTM1 (425 °C and 468 °C) indicated that thermal degradation occurs again in two steps similar to PMTM2. Only 5.8 % of the polymers remained after 450 °C. In the case of GPMTM1D, a weight loss of about 20 % occurs at 112 °C which may be due to the removal of the solvent from the polymer matrix. A maximum weight loss of about 37 % at 358 °C was observed. A third weight loss was observed at 428 °C. Second and third weight losses were due to decomposition of polymer. TGA curve for GPMTM1P showed weight losses at 94 °C, 326 °C and 460 °C. The weight loss at 94 °C could be due to the removal of solvent. Last two weight losses were responsible for the decomposition of sample. The most striking difference is the char residue. Only 5.8 % of the samples remained for the precursor polymer whereas 19.5 % remnant was found for GPMTM1P. As far as the PPy/ PMTM2 is concerned, this weight loss is observed at 351 °C for PTS<sup>-</sup> doped films and at 245 °C for DS<sup>-</sup> doped films. Higher resistance to heat is observed in PTS<sup>-</sup> doped films; about 60 % of the polymer was remained after 600 °C; whereas, % 42 of the polymer remained in the DS<sup>-</sup> doped films. Thermogram for the PMTM2/PTh synthesized in acetonitrile-TBAFB, solvent-electrolyte couple exhibited two transitions at 266 °C and 435 °C. First transition may be attributed to the removal of the dopant anion from the matrix and second one may be responsible for the degradation of the copolymer.

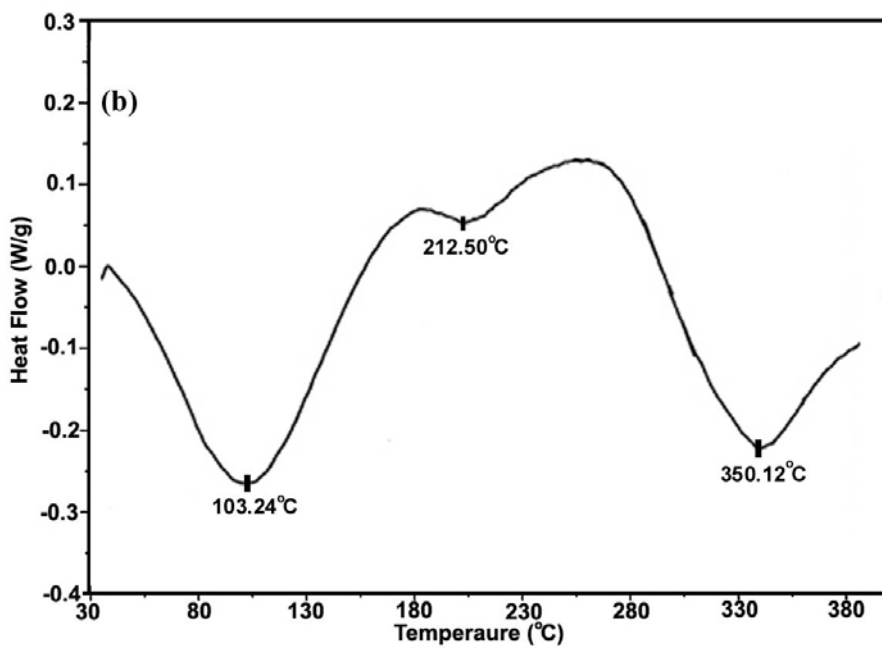
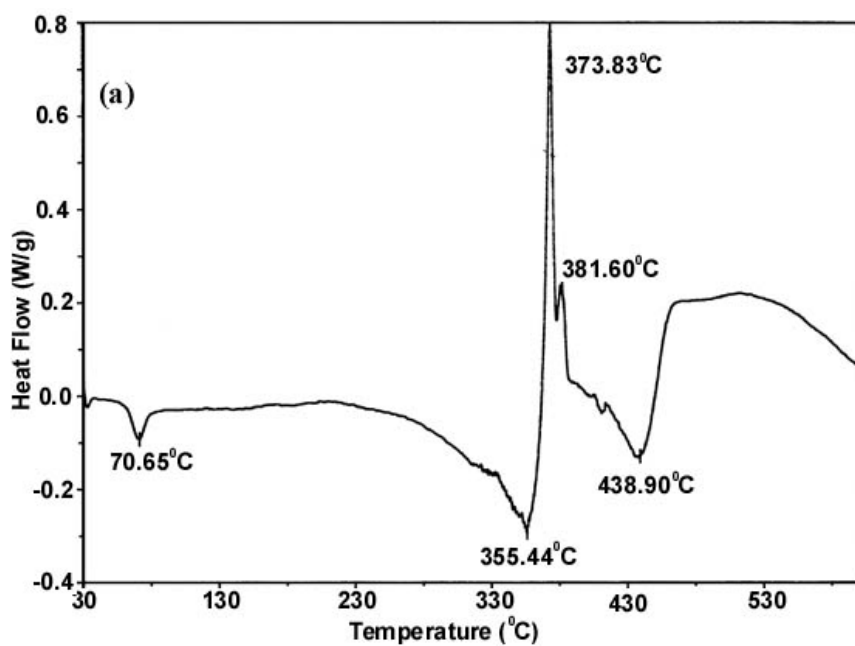


Figure 3.10 DSC thermograms of (a) PMTM2 (b) GPMTM1P (c) GPMTM1D (d) PMTM2/PTh ( $\text{BF}_4^-$  doped).

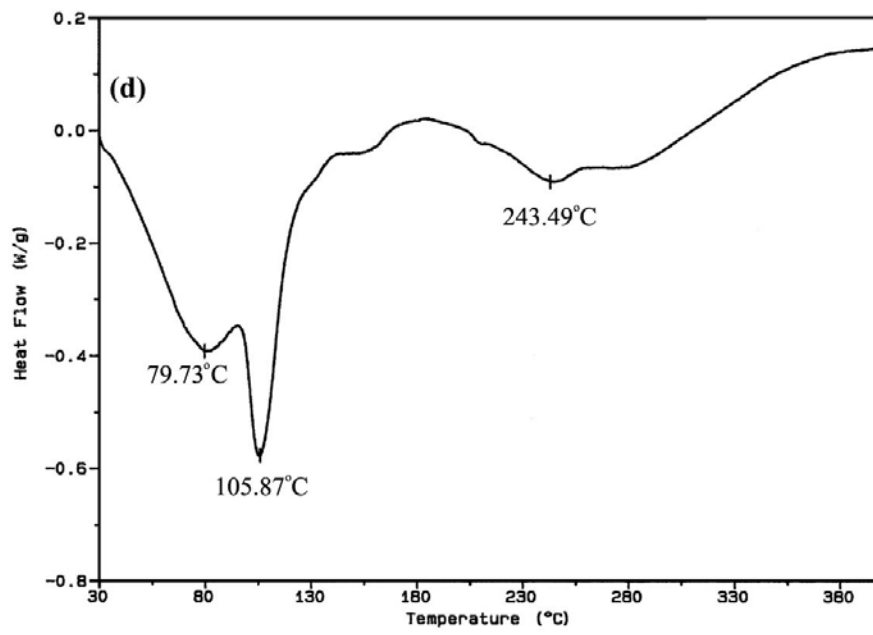
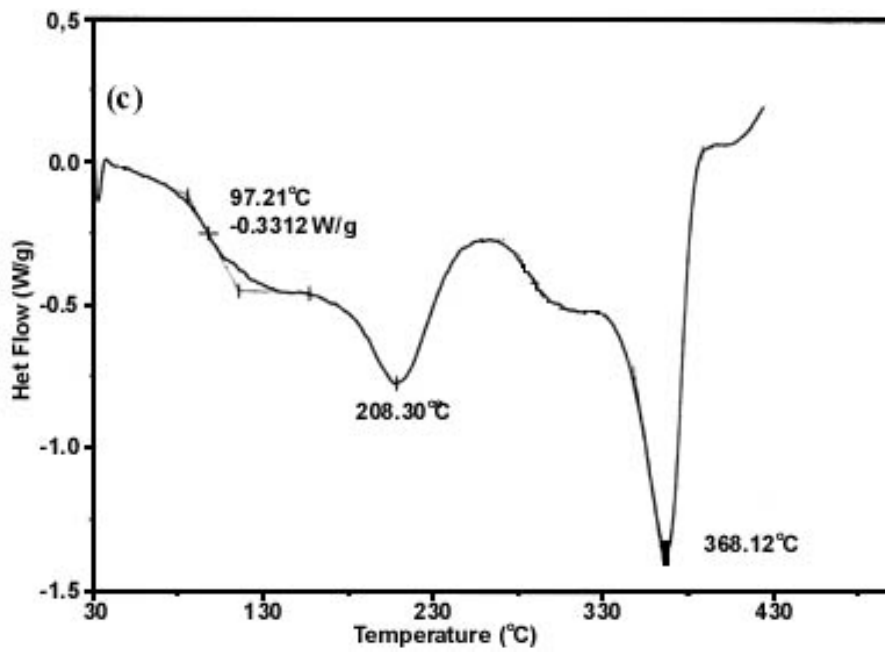


Figure 3.10 cont.

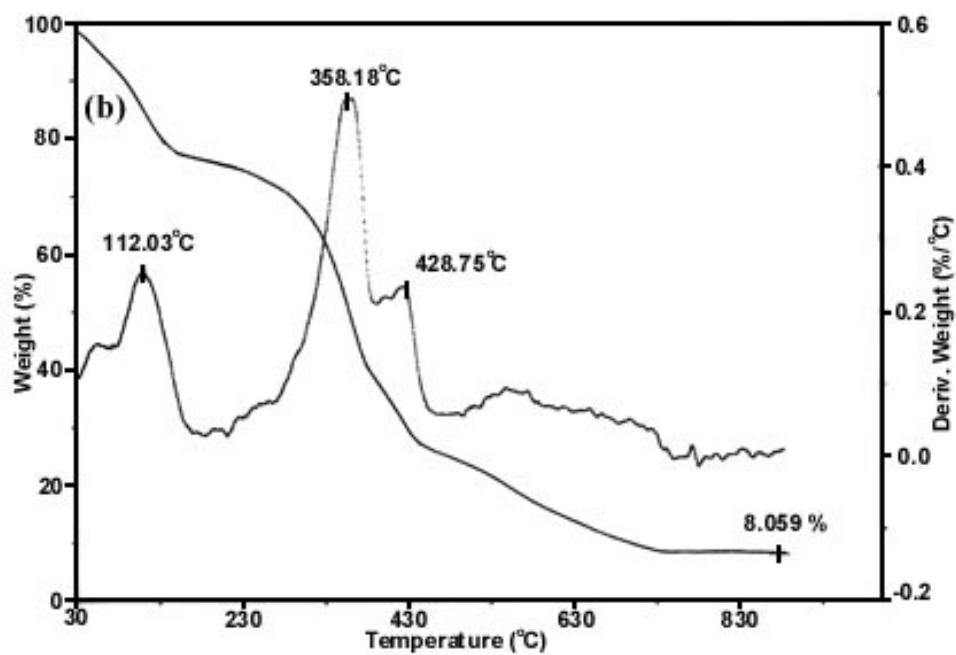
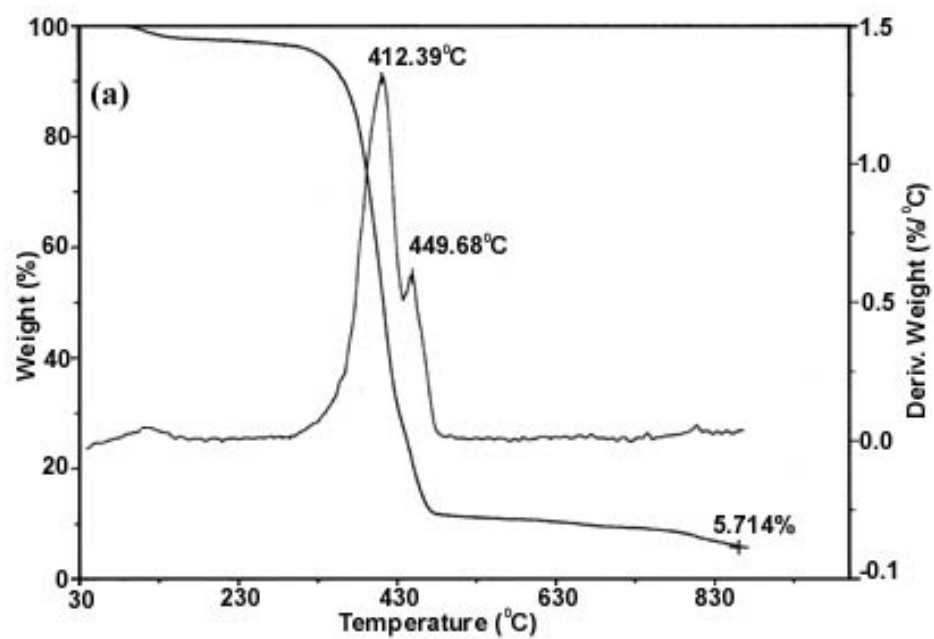


Figure 3.11 TGA curves for (a) PMTM2 (b) GPMTM1D (c) GPMTM1P (d) PMTM2/PTh ( $\text{BF}_4^-$  doped).

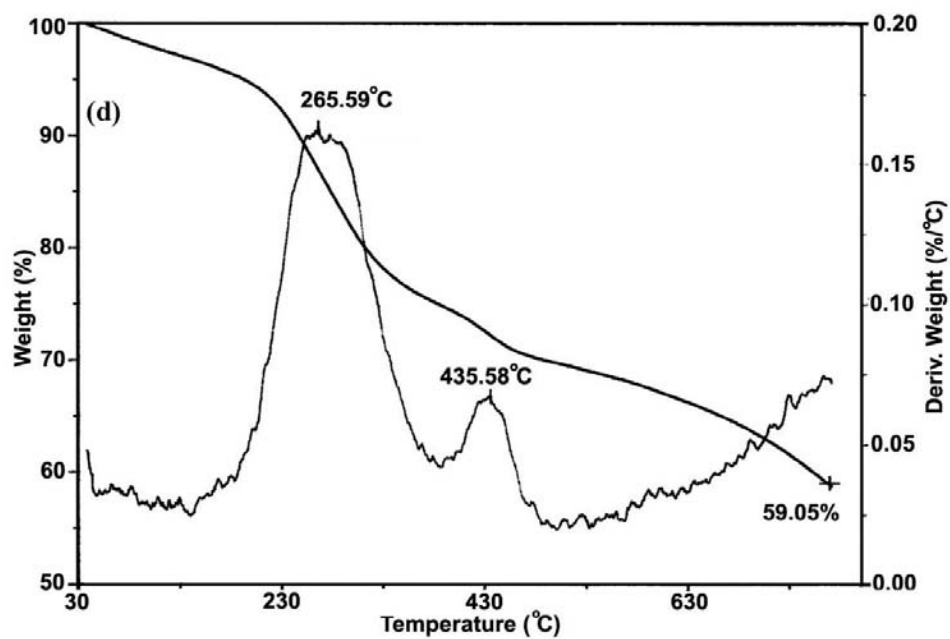
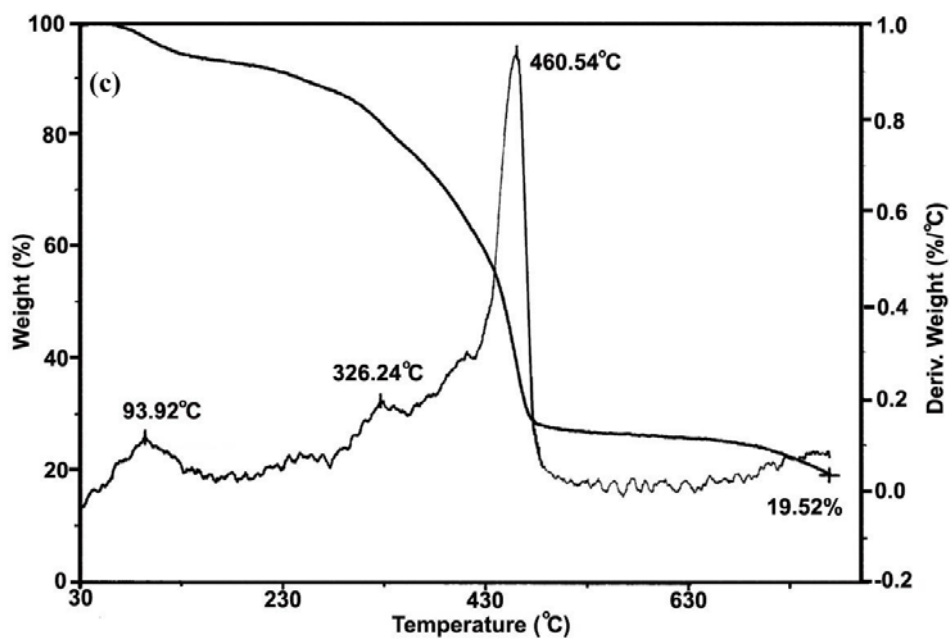


Figure 3.11 cont.

### 3.1.1.7 Morphologies of the Films

The morphologies of the copolymer films were investigated by Scanning Electron Microscopy (SEM) studies (JEOL JSM-6400). The surface morphology of the solution sides of PMTM2/PPy (either  $\text{PTS}^-$  or  $\text{DS}^-$  doped) copolymers showed cauliflower-like structures which is characteristic for pristine polypyrrole. However, the electrode side of the PMTM2/PPy films was different from that of polypyrrole (Figure 3.12 (a) and (b)). Figure 3.12 (c) and (d) shows the SEM micrographs of solution side of unwashed and washed PMTM2/PPy ( $\text{BF}_4^-$  doped) film. Some irregularities can be seen on the unwashed solution side of PMTM2/PPy film. After washing process, some of the irregularities are removed. However, there is no significant change in the morphology of the film. With the same synthesis conditions, PPy was synthesized and both sides of the film were examined. Typical cauliflower-like structure was observed for the solution side of PPy films. Presence of PMTM2 changes the film morphologies and that may be due to the polymerization of pyrrole through precursor polymer. Different morphological properties were observed with different supporting electrolytes.

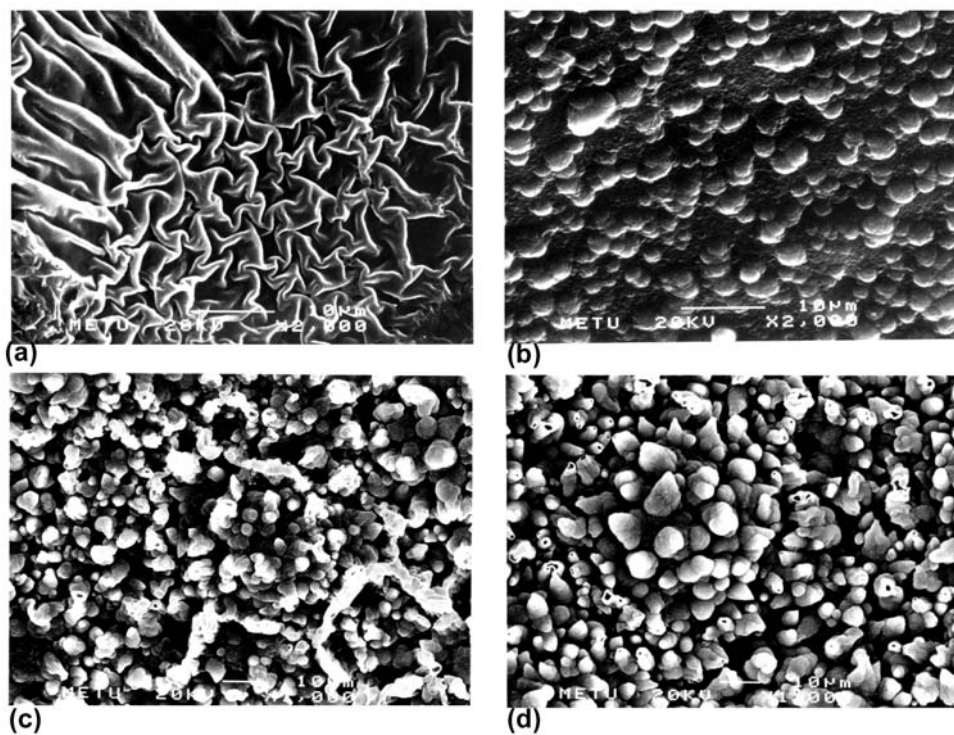


Figure 3.12 SEM micrographs of

- (a) Electrode side of washed PMTM2/PPy film ( $\text{PTS}^-$  doped)
- (b) Electrode side of washed PMTM2/PPy film ( $\text{DS}^-$  doped)
- (c) Solution side of unwashed PMTM2/PPy film ( $\text{BF}_4^-$  doped)
- (d) Solution side of washed PMTM2/PPy film ( $\text{BF}_4^-$  doped)

### 3.1.2 Synthesis and Characterization of Conducting Copolymers of Thiophene-3-yl Acetic Acid Cholesteryl Ester with Pyrrole

The aim of this attempt was the synthesis and characterization of a new monomer containing an ester group derived from 3-thiophene acetic acid and cholesterol [171] (Figure 3.13). In addition, both chemical and galvanostatical polymerizations of CM were studied. Copolymers of both monomer and chemically or galvanostatically synthesized polymers with pyrrole were synthesized by using two different supporting electrolytes in aqueous medium, namely, *p*-toluene sulfonic acid (PTSA) and sodium dodecyl sulfate (SDS).

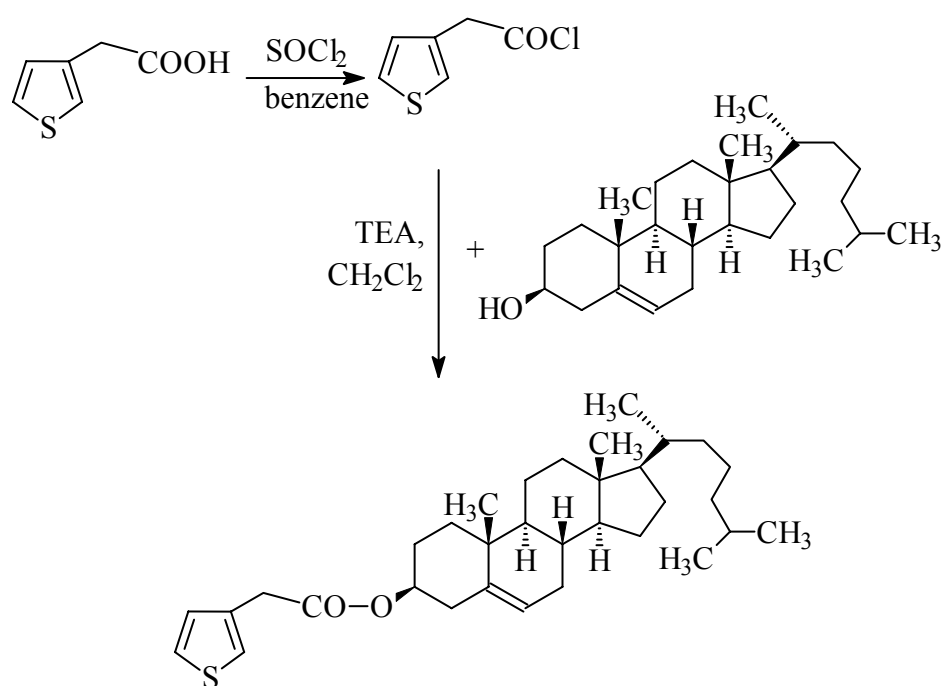


Figure 3.13 Synthesis scheme of CM

#### 3.1.2.1 Cyclic Voltammetry

Cyclic voltammetry experiments were performed in acetonitrile-TBAFB, solvent-electrolyte couple. In the cyclic voltammogram of CM, no detectable

redox peaks were observed (Figure 14a). Thus, it was concluded that CM was not electroactive. However, with the addition of pyrrole, a redox peak, which revealed increasing height with increasing scan number, was observed at +0.75 (Figure 14b). This potential value was somewhat different from the oxidation potential of pure polypyrrole, which was obtained as +0.65 V after 33 scans (Figure 14c). The shift to higher potential value may serve as an indication for the copolymer formation.

In the presence of thiophene, a redox peak was observed at + 1.25 V (Figure 14d). The same redox peak appeared for the thiophene on a bare Pt electrode (Figure 14e). This observation may reflect that there is no noticeable interaction between CM and thiophene.

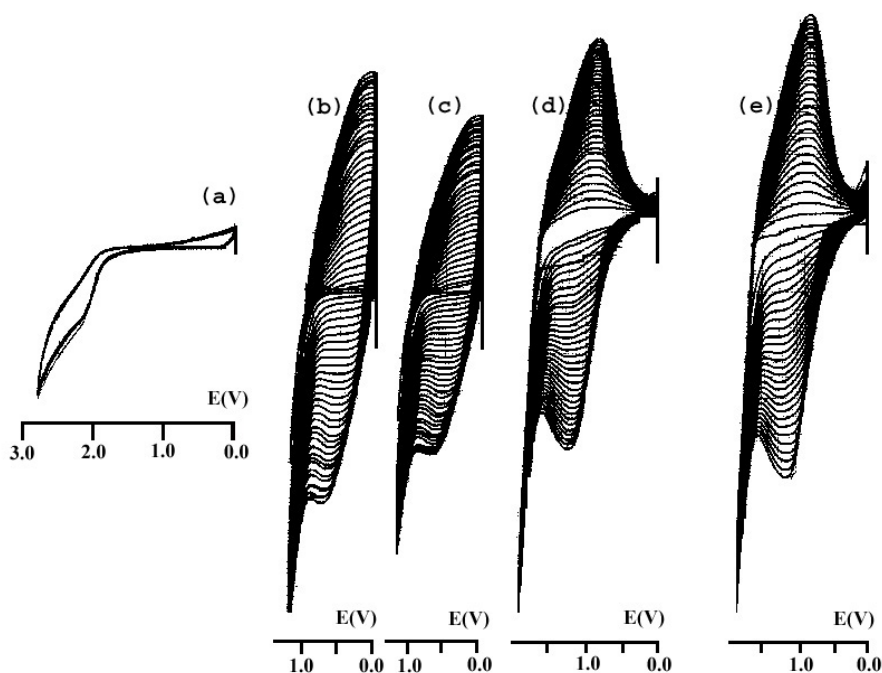


Figure 3.14 Cyclic voltammograms of (a) monomer (CM), (b) CM in the presence of pyrrole, (c) pyrrole on a bare Pt electrode, (d) CM in the presence of thiophene and (e) thiophene on a bare Pt electrode.

### 3.1.2.2 Characterization

For the self-polymerization of CM by constant potential electrolysis, no product formation was observed on the electrode surface for AN-TBAFB, dichloromethane-TBAFB, water-PTSA and water-SDS systems. However, self-polymerizations of CM were achieved both by chemical polymerization ( $\text{FeCl}_3$ ) and galvanostatic polymerization (CCE) methods successfully. Via constant current electrolysis, desired product was obtained only in the dichloromethane-TBAFB system at  $0^\circ\text{C}$  by using a single compartment cell and Pt foil electrodes. As for the other systems, target product was not obtained. Electropolymerizations of CM, PCM1 and PCM4 with pyrrole and thiophene were shown in Figure 3.15. Only pyrrole seemed to be appropriate for the polymerization.

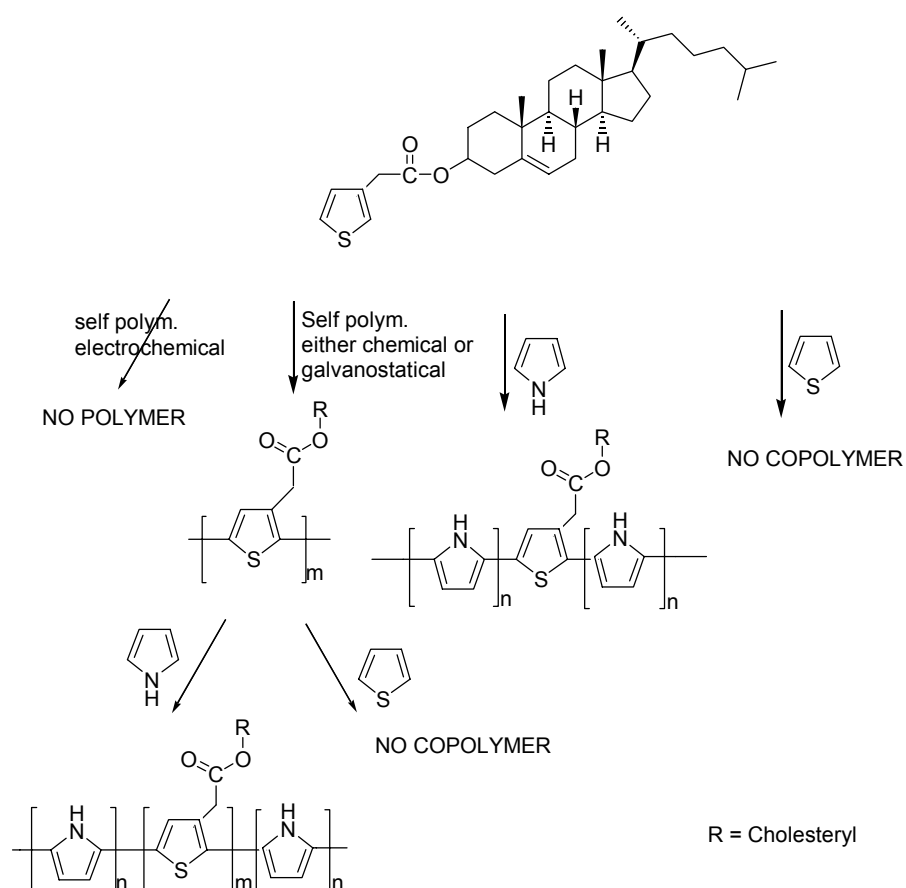


Figure 3.15 Reactions with CM

### 3.1.2.3 <sup>1</sup>H NMR and FT-IR Characterization

<sup>1</sup>H-NMR spectrum of the monomer and PCM1 were taken by using a Bruker-Instrument-NMR Spectrometer (DPX-400) with CDCl<sub>3</sub> as the solvent and tetramethylsilane as the internal standard. <sup>1</sup>H-NMR data for the monomer: <sup>1</sup>H-NMR(δ, ppm): 7.27 (s, 1H), 7.15(s, 1H), 7.05 (s, 1H), from 3-thienyl ring, 5.37 (s, 1H) C=CH from cholesteryl 4.65 (s, 1H), COO-CH- in cholesteryl), 3.62 (s, 2H), Th-CH<sub>2</sub>-COO-, 0.67-2.40 (m, 44H), cholesteryl (Figure 3.16). In the <sup>1</sup>H-NMR spectra of the PCM1, a wide signal in the region of 6.75 to 7.10 ppm was assigned to thiophene hydrogens (Figure 3.17). Dominant signal at 7.00 ppm was assigned to head to tail, head to head linkage structure [172,173]. Other signals were remained unchanged but broadened due to polymerization.

IR spectrum was recorded on a Nicolet 510 FTIR spectrometer. The absorption bands at 768 and 3106 cm<sup>-1</sup> are due to the thienylene C-H<sub>α</sub> stretching modes in the monomer (Figure 3.18). As to the CM and PCM1, the bands related to the carbonyl group and to C-O-C stretching are present at about 1725 and in the 1000-1265 cm<sup>-1</sup> region respectively [174]. There are several peaks, which are attributed to the cholesteryl group. These are 2933, 2863, 1462, 1377, 1010, 955, 803 and 740 cm<sup>-1</sup>. After the chemical polymerization of CM, a new band appears at 1626 cm<sup>-1</sup> indicating the conjugation [175] (Figure 3.19). Moreover, the band at 768 cm<sup>-1</sup> is very much attenuated in the polymers (PCM1 and PCM4), which is the proof of 2,5 disubstitution on the thiophene ring (Figure 3.19 and 3.20). Doping PCM1 with iodine, took on a noticeable change in the IR spectra. At 500-1500 cm<sup>-1</sup> strong and broad doping-induced bands are present, which are related to the presence of free charge carriers.

Electrochemically synthesized copolymers; CM/PPy, PCM1/PPy and PCM4/PPy contain an absorption band at around 1710 cm<sup>-1</sup> for the water-SDS and water-PTSA systems (Figure 3.21 and 3.22). This proves the presence of CM in the resultant polymers, since the carbonyl is specific to the monomer. The

possibility of overoxidation of pyrrole, this carbonyl on the ring, has been eliminated via studying the IR of PPy produced under the same conditions. Moreover, it was concluded that copolymerization was not achieved in AN-TBAFB system with pyrrole and/or thiophene due to the lack of carbonyl absorption band in the IR spectrum. In other words, in these cases pure PPy and PTh were obtained.

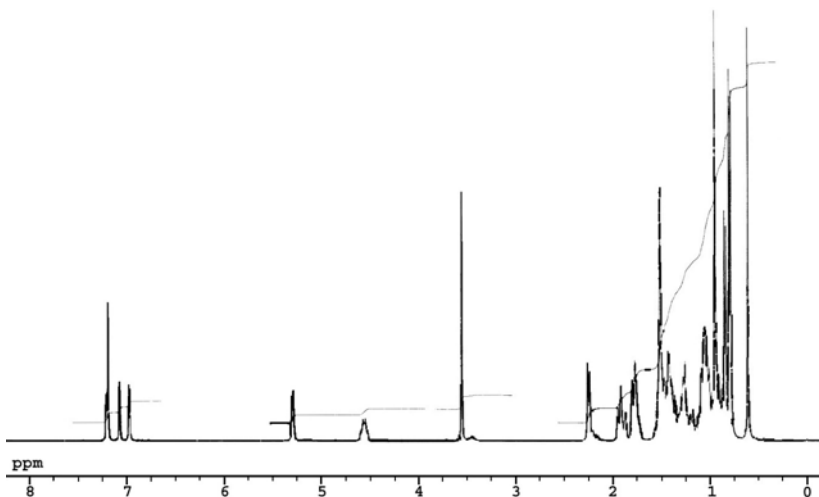


Figure 3.16 H-NMR spectra of CM

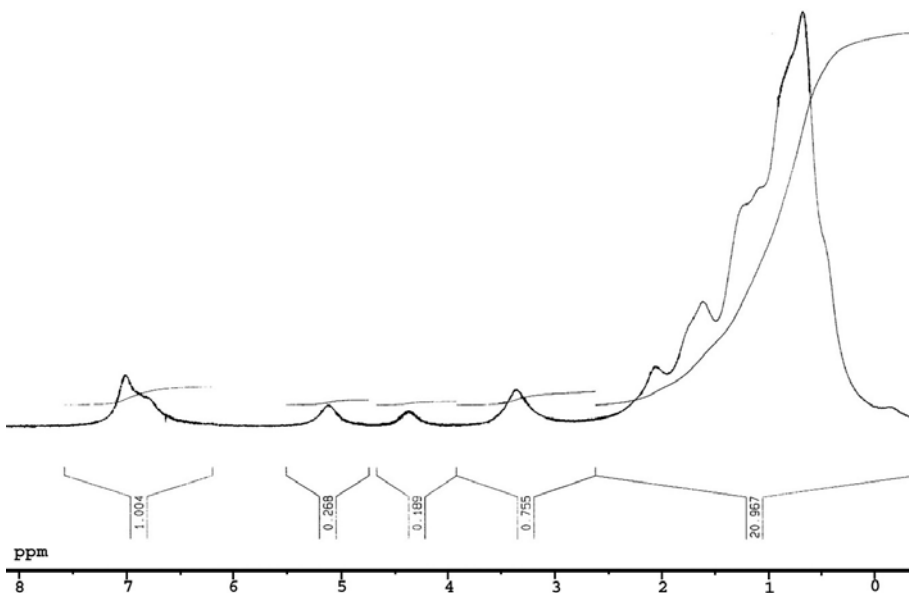


Figure 3.17 H-NMR spectra of PCM

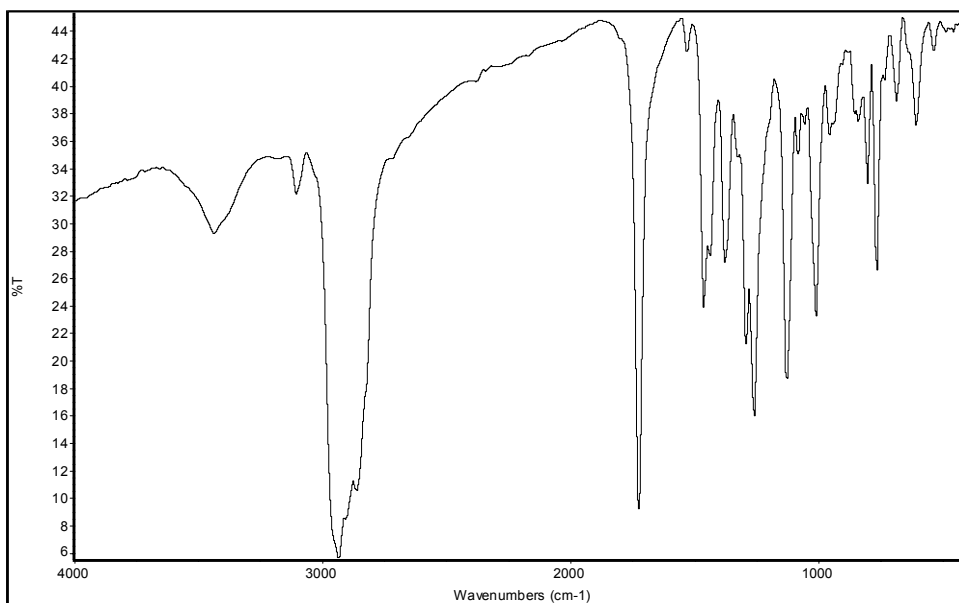


Figure 3.18 FTIR spectra of CM.

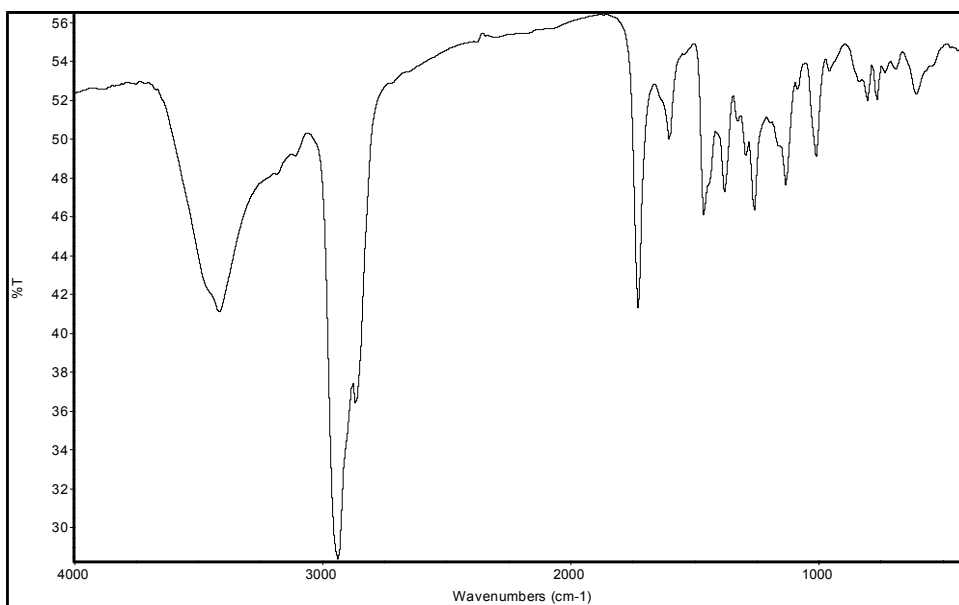


Figure 3.19 FTIR spectra of PCM.

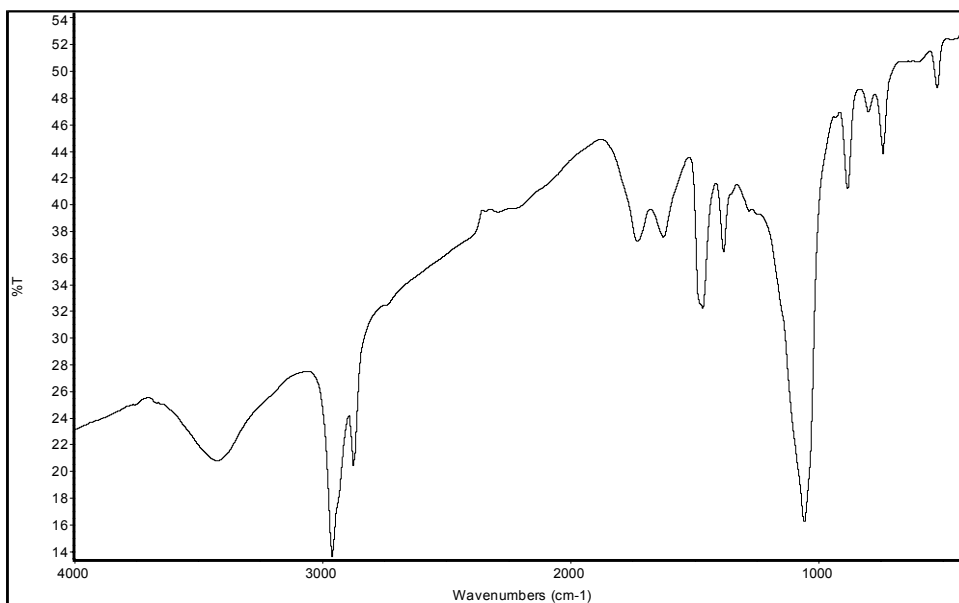


Figure 3.20 FTIR spectra of PCM4.

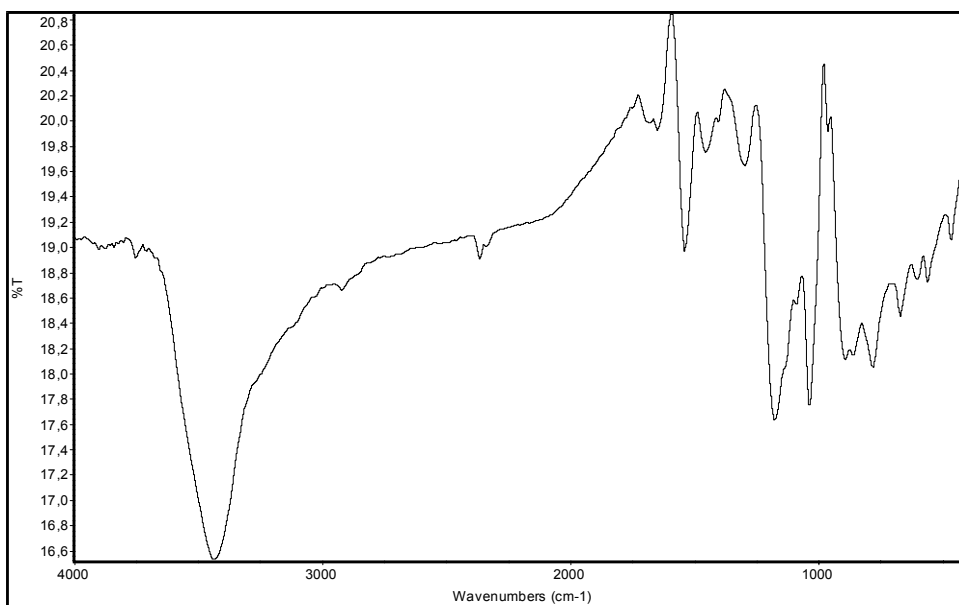


Figure 3.21 FTIR Spectra of PCM/PPy copolymer doped with PTS<sup>-</sup>.

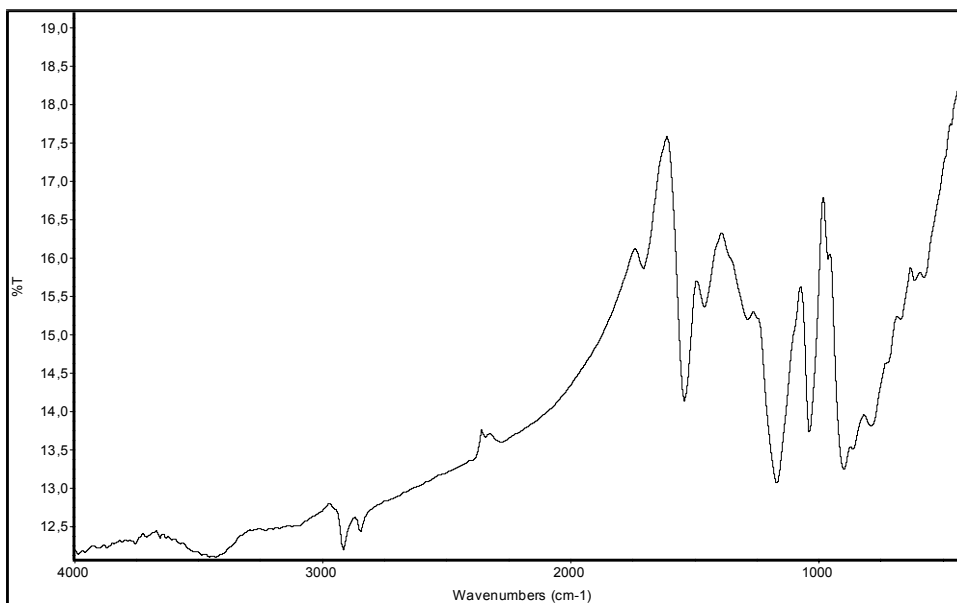


Figure 3.22 FTIR spectra of PCM/Py copolymer doped with DS<sup>-</sup>.

### 3.1.2.4 Thermal Analysis

Thermal behavior of the samples was investigated by using a Du Pont 2000 Thermal Gravimetry Analyser and Differential Scanning Calorimetry. TGA thermogram of the monomer (CM) showed a weight loss at 384.4 °C (Figure 3.23 (a)) whereas for the PCM1, a weight loss was observed at 328.7 °C (Figure 3.23 (b)). The most striking difference is the char residue. Only 4% of the samples remained for the monomer whereas 23.4 % remnant was found for PCM1. Thermogram for the CM/PPy (PTS<sup>-</sup> doped) revealed four transitions at 73 °C, 226.8 °C, 362 °C and 490 °C (Figure 3.24 (a)). However, three thermal transitions were observed at 114 °C, 235 °C and 500 °C for CM/PPy (DS<sup>-</sup> doped) film (Figure 3.24 (b)). PTS<sup>-</sup> doped polymer is more thermally stable than the DS<sup>-</sup> doped film. Thermograms of PCM1/PPy (PTS<sup>-</sup> doped) and PCM4/PPy (PTS<sup>-</sup> doped) are nearly the same with the CM/PPy (PTS<sup>-</sup> doped). This is due to high percentage of the pyrrole content in the copolymer matrix. This argument is also valid for PCM1/PPy (DS<sup>-</sup> doped) and PCM4/PPy (DS<sup>-</sup> doped) samples.

DSC thermogram of monomer shows a sharp melting point at 106.3 °C and it is stable up to 224 °C (Figure 3.25 (a)). PCM1 exhibits three endothermic transitions at 172.5 °C, 223.2 °C and 265 °C (Figure 3.25 (b)). Same experiment was performed by heating the sample up to 200 °C with 10 °C/min rate in the first run and cooling back to room temperature and heating again up to 400 °C. Only two transitions were observed at 223.2 °C and 265 °C. These are due to the decomposition of the samples. For the copolymers, CM/PPy (PTS<sup>-</sup> doped) and CM/PPy (DS<sup>-</sup> doped) thermograms are shown in Figure 3.26 (a) and (b) respectively. Two transitions were observed for CM/PPy (PTS<sup>-</sup> doped) at 91.1 °C and 334.4 °C. First transition is due to the removal of the water from the polymer matrix. Second one is responsible for the decomposition of the sample. DSC curves of PCM1/PPy (PTS<sup>-</sup> doped) (two transitions at 82.4 °C and 334.7 °C) and PCM4/PPy (PTS<sup>-</sup> doped) (at 101.3 °C and 344 °C) are nearly the same as CM/PPy (PTS<sup>-</sup> doped), which is probably due to the long chains of PPy in the copolymer matrix. The DS<sup>-</sup> doped CM/PPy shows also two transitions at 89.2 °C and 265.1 °C. Similarly, the first one is attributed to the removal of the adsorbed water and second one is related to the dopant ion leaving the matrix. It can be concluded that PTS<sup>-</sup> doped copolymers are thermally more stable than DS<sup>-</sup> doped copolymer. Thermograms of PCM1/PPy (DS<sup>-</sup> doped) (85.2 °C and 260.1 °C) and PCM4/PPy (DS<sup>-</sup> doped) (72.9 °C and 251.2 °C) are similar to that of CM/PPy.

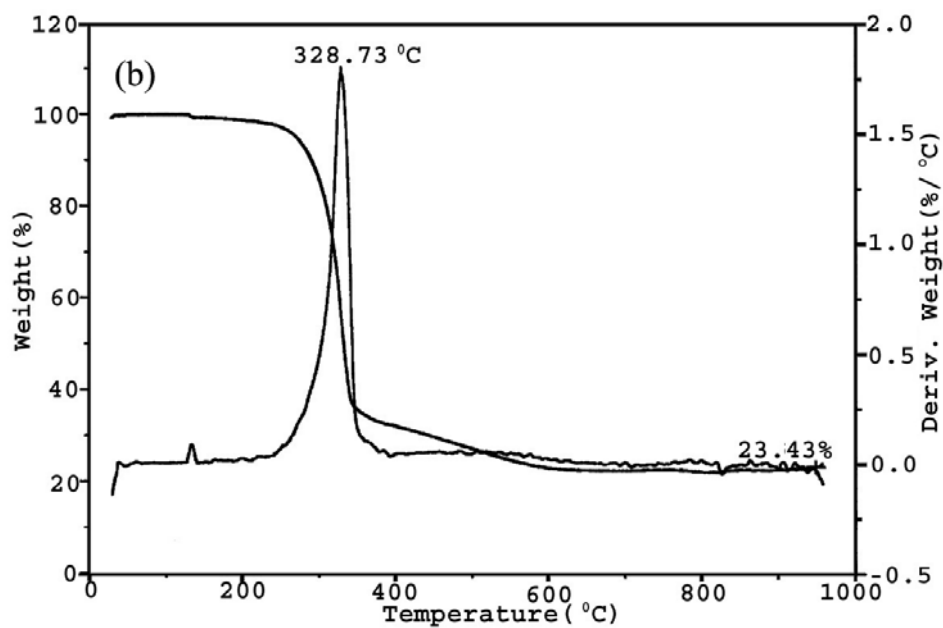
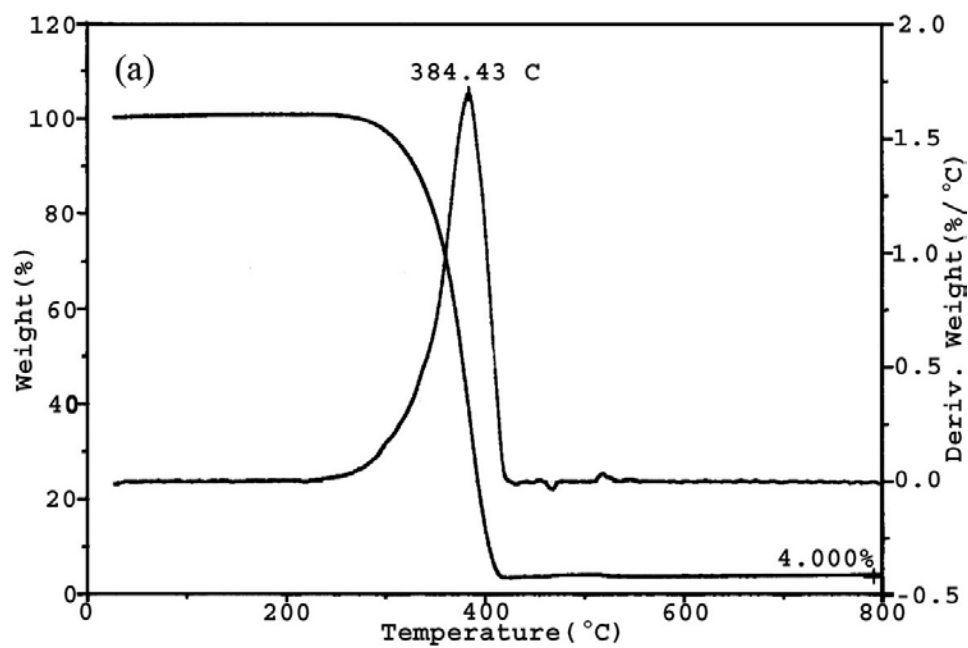


Figure 3.23 TGA thermograms of (a) CM and (b) PCM1.

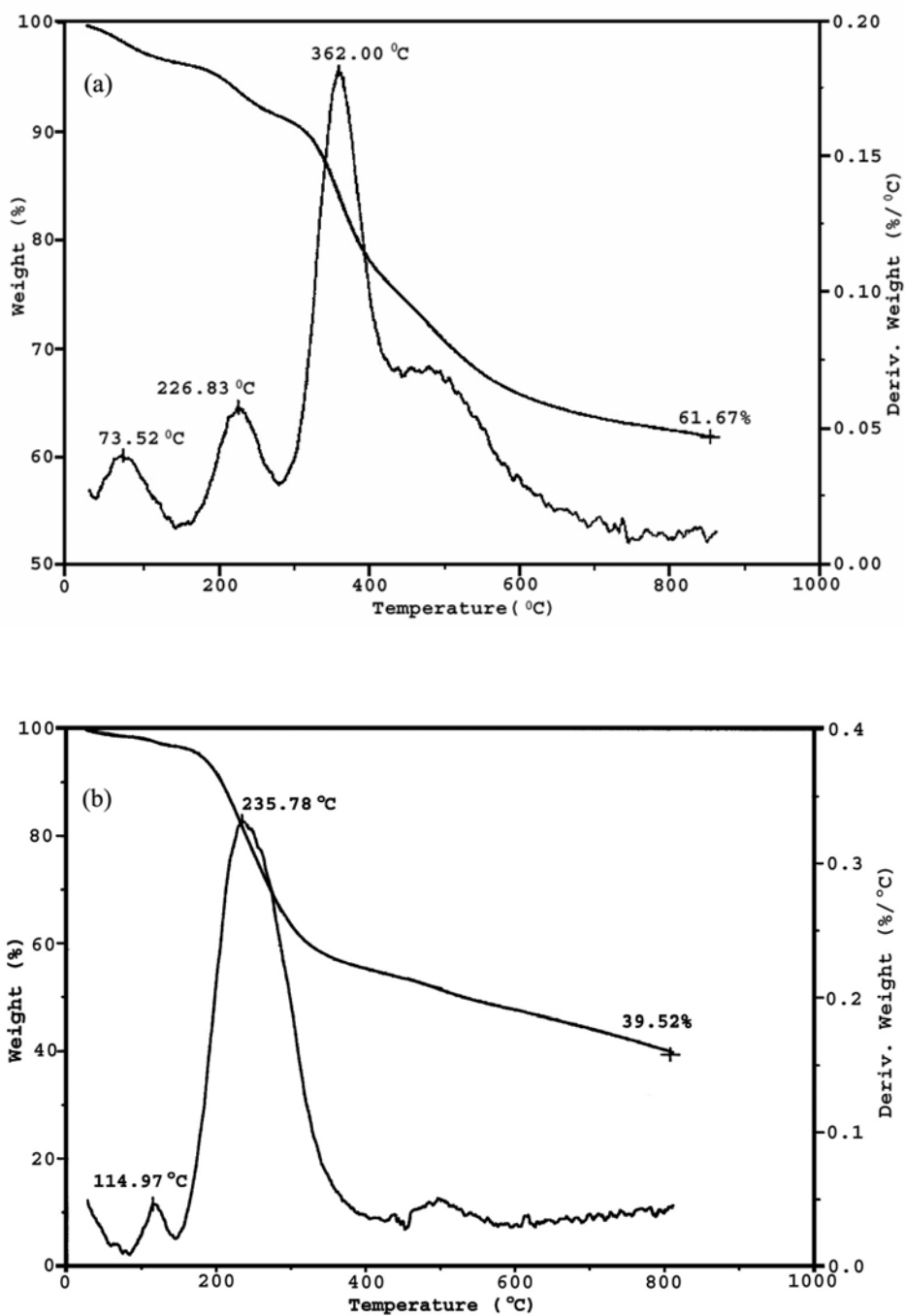


Figure 3.24 TGA thermograms of (a) PPy/CM (PTSA doped) and (b) PPy/CM (DS<sup>-</sup> doped).

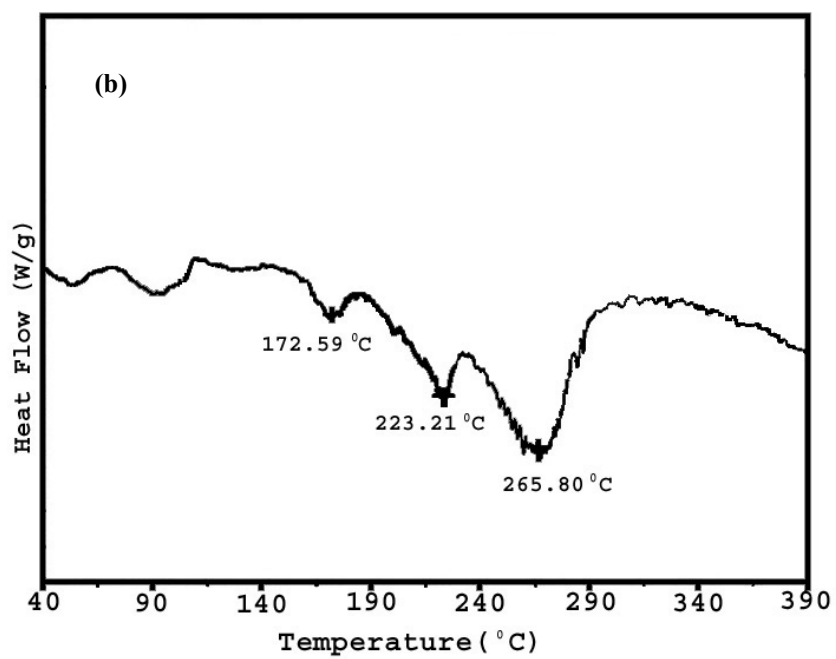
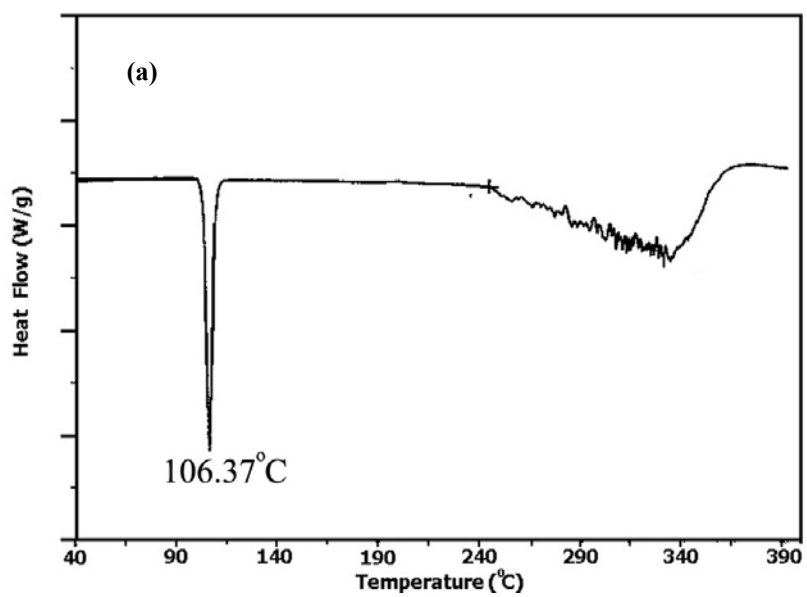


Figure 3.25 DSC thermograms of (a) CM and (b) PCM1.

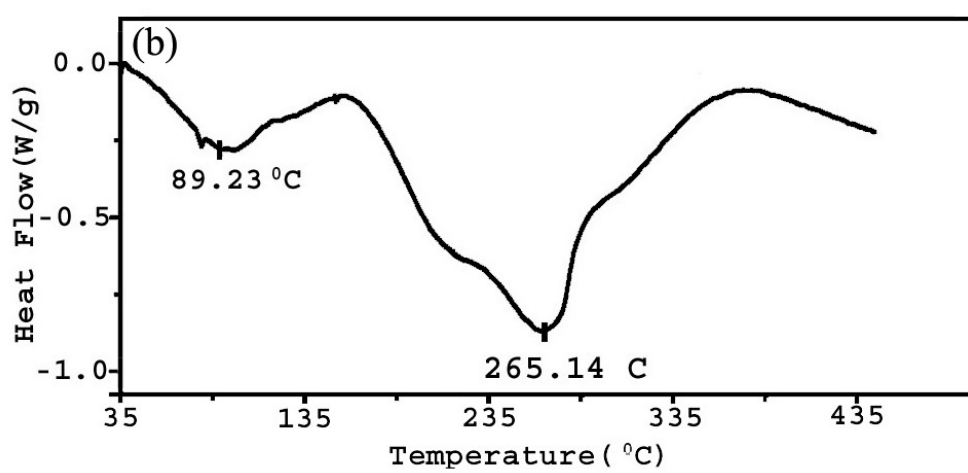
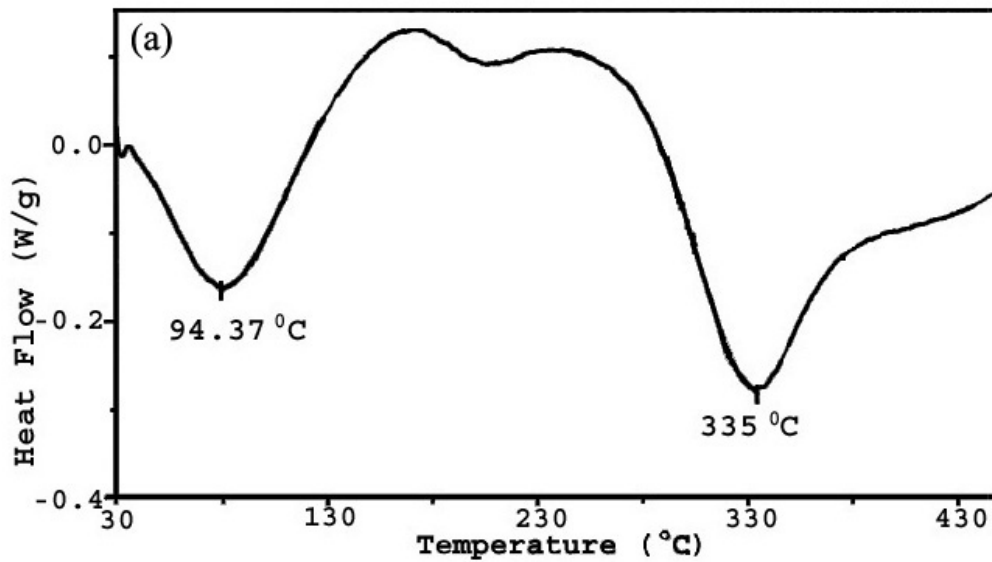


Figure 3.26 DSC thermograms of (a) PPy/CM (PTSA doped) and (b) PPy/CM (DS<sup>-</sup> doped).

### 3.1.2.5 Conductivity Measurements

Electrical conductivity measurements were carried out by using the standard four-probe technique. Conductivities of the copolymers doped with either  $\text{PTS}^-$  or  $\text{DS}^-$ , were 0.2-6 S/cm (Table 3.3). There was no significant difference between the conductivity of washed and unwashed samples. The conductivities of both the electrode and solution sides were also in the same order of magnitude that reveals the homogeneity of the films. To impart electrical conductivity to the PCM1, vapor phase doping process was applied ( $\text{I}_2$ : acceptor). The conductivity was measured as  $5 \times 10^{-2}$  S/cm.

Table 3.3 Conductivities of the films.

Polymer	Electrode Side	Solution Side
PCM1 (pellets)	$5 \times 10^{-2}$	$5 \times 10^{-2}$
CM/PPy ( $\text{PTS}^-$ doped)	0.2	3.3
CM/PPy ( $\text{DS}^-$ doped)	0.3	0.4
PCM1/PPy ( $\text{PTS}^-$ doped)	5.0	6.0
PCM1/PPy ( $\text{DS}^-$ doped)	0.3	0.5
PCM4/PPy ( $\text{PTS}^-$ doped)	0.4	1.0
PCM4/PPy ( $\text{DS}^-$ doped)	0.3	0.6

### 3.1.2.6 Scanning Electron Microscopy (SEM)

The morphologies of the copolymer films were investigated by SEM studies (JEOL JSM-6400). As far as the SEM micrographs of PPy/CM films are concerned, electrode side morphologies of both  $\text{PTS}^-$  doped (Figure 3.27 (a)) and  $\text{DS}^-$  doped (Figure 3.27 (b)) species are significantly different from that of pure PPy. This may be yet another indication of the polymerization of pyrrole on CM.  $\text{PTS}^-$  doped PPy/CM's electrode side had small globules like droplets, on the

other hand,  $DS^-$  doped one had larger and more denser globules. Micrographs of  $DS^-$  doped unwashed PPy/PCM4 (Figure 3.27 (c)) and washed (Figure 3.27 (d)) electrode sides of PPy/PCM4 films revealed that surface appearance of films was altered by washing process. However, washed PPy/PCM4 film had quite different morphology compared to pure PPy that indicates the interaction between PCM4 and pyrrole.

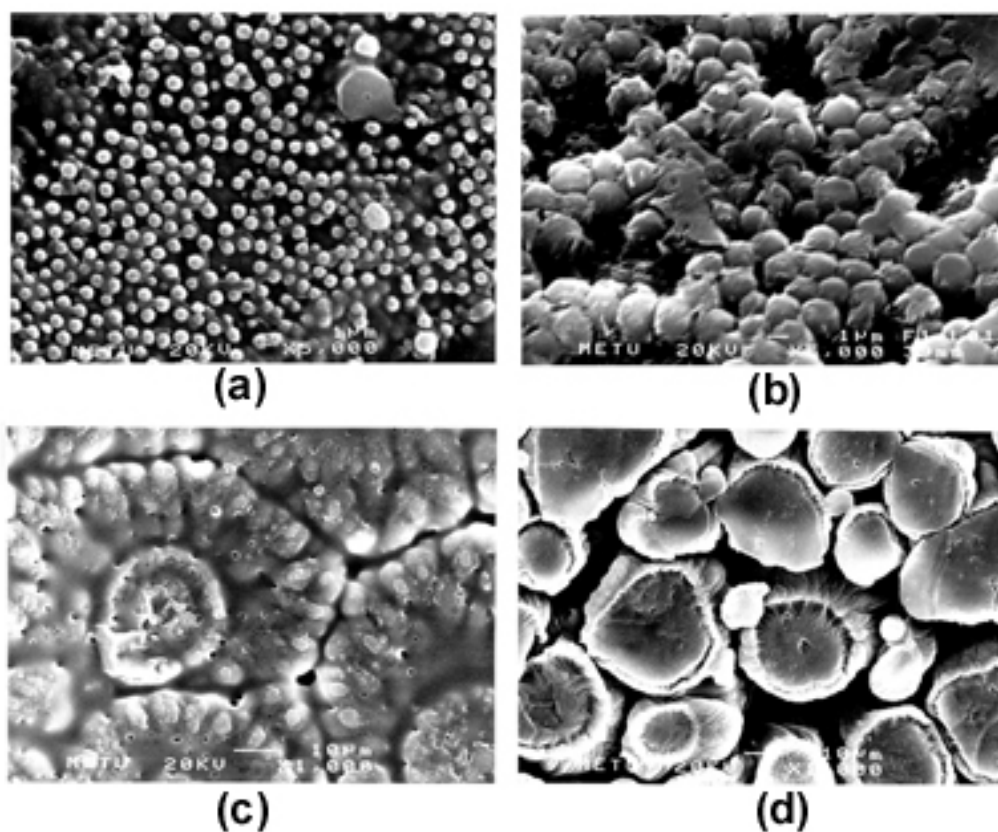


Figure 3.27 SEM micrographs of (a) electrode side of washed PPy/CM (PTSA doped), (b) electrode side of washed PPy/CM ( $DS^-$  doped), (c) electrode side of unwashed PPy/PCM4 ( $DS^-$  doped) and (d) electrode side of washed PPy/PCM4 ( $DS^-$  doped).

## 3.2 Immobilization of Enzymes

### 3.2.1 Immobilization of Invertase in Conducting Copolymers of 3-Methylthienyl Methacrylate

During the electropolymerization of pyrrole, enzyme molecules were carried by pyrrole and supporting electrolyte. In order to understand which one was the predominant enzyme carrier, enzyme electrodes 2 and 3 were prepared. Their activities were determined at the same concentration of substrate (Table 3.4). In the case of EE3, since pyrrole polymerization was carried out before immobilization step; the only enzyme carrier was the supporting electrolyte. For EE2, both pyrrole and supporting electrolyte carry enzyme to the electrode surface. As seen from Table 3.4, the invertase activity of enzyme electrode 2 was ten times higher than that of enzyme electrode 3. In addition to this, enzyme electrode 2 exhibited higher  $V_{\max}$  compared to EE3. One can conclude that enzymes are mostly carried to electrode surface by the diffusion of pyrrole [176]. Higher activity of invertase immobilized on the EE2 films also means more enzyme molecules entrapped compared to enzyme electrode 3.

Table 3.4 Invertase activities in PMTM/PPy/SDS and (PMTM/PPy)/SDS polymer matrices.

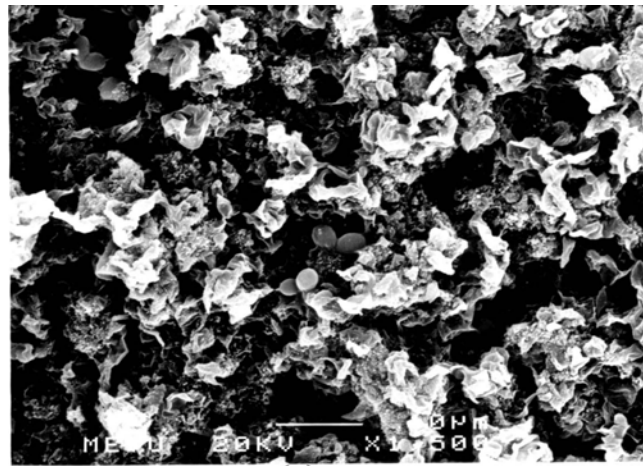
Polymer matrix	Activity ( $\mu\text{mol per min per electrode}$ )
PMTM/PPy/SDS	2.053
(PMTM/PPy)/SDS	0.188

Whether immobilized invertase is removed or not by the reduction of polymer synthesized in the presence of invertase was investigated. Firstly, enzyme electrode was prepared and invertase activity was calculated. After that, enzyme electrode was put into the electrolysis cell containing acetate buffer and SDS as

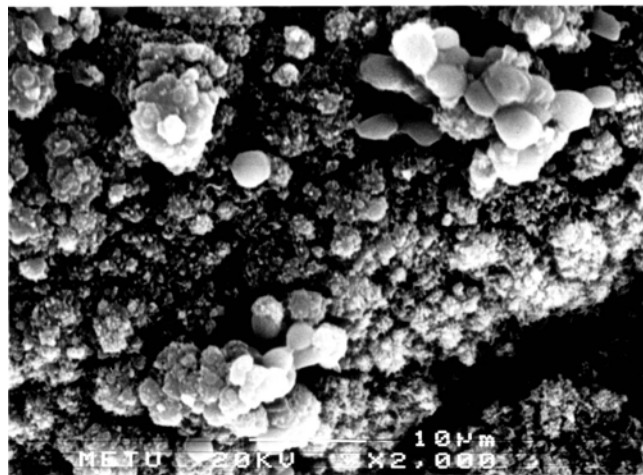
the supporting electrolyte. It was reduced for 60 min. Activity of enzyme electrode was again determined. Immobilized invertase activity was not changed before and after the reduction process. No enzyme activity was found in the electrolysis solution. As a result, removal of immobilized invertase from the matrix is not possible by a simple electrochemical reduction process.

### **3.2.1.1 Morphologies of the Films**

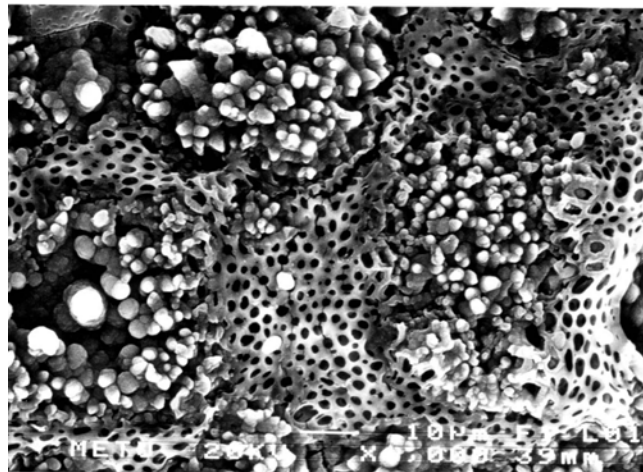
Scanning electron microscopy (SEM) (JEOL JSM-6400) was used to examine the surface morphologies of the polymer films where enzyme was entrapped. The surface morphologies of these films were completely different compared to the films prepared in the absence of invertase. Cauliflower-like structure was noticeably damaged when invertase was entrapped in the matrix (Figure 3.28). Moreover, invertase clusters were observed in the solution side of the films, especially for electrode 2 (Figure 3.28 (a)) and electrode 4 (Figure 3.28 (b)). On the other hand, the original structure of electrode 3 was not significantly damaged (Figure 3.28 (c)), as supported by lower kinetic parameters.



(a)



(b)



(c)

Figure 3.28 Scanning electron micrographs of (a) solution side of EE2 (b) solution side of EE4 (c) solution side of EE3

### 3.2.1.2 Kinetic Studies of Immobilized Invertase

Kinetic studies of the immobilized invertase were performed at various concentrations of sucrose. Maximum velocity,  $V_{\max}$ , and the apparent Michaelis-Menten constant,  $K_m$ , [177] were found from the Lineweaver-Burk plot [178]. The calculated parameters are given in Table II. Although different matrices were used, the  $K_m$  values were in the same order. The highest  $V_{\max}$  was observed for electrode 1. The values obtained for electrodes 2, 4 and 5 are comparable with that of 1. In contrast,  $V_{\max}$  value of electrode 2 was about 3.5 times lower than that of EE1.

Table 3.5 Kinetic parameters for hydrolytic breakdown of sucrose to glucose and fructose

Polymer matrix	$K_m$ (mM)	$V_{\max}$ ( $\mu\text{mol min}^{-1}$ electrode $^{-1}$ )
(EE1) PPy/invertase	28.2	4.17
(EE2) PMTM/PPy/SDS/invertase	30.2	3.15
(EE3) Pt(PMTM/PPy)/SDS/inv	26.2	1.16
(EE4)Pt(PMTM/PTh)/PPy/SDS/inv	22.5	3.17
(EE5) Pt(PTh)/PPy/SDS/inv	27.3	3.88

### 3.2.1.3 Operational Stability of the Enzyme Electrodes

One of the most important parameters to be considered in enzyme immobilization is operational stability. The stability of enzyme electrodes in terms of repetitive uses was studied. Applying more than 20 successive measurements revealed very small losses in the activity (Figure 3.29). The enzyme activities were almost stable during the 20 experiments performed at 25°C, on the day of immobilization.

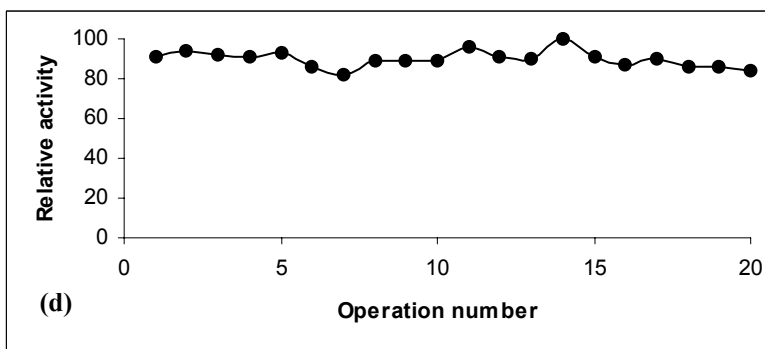
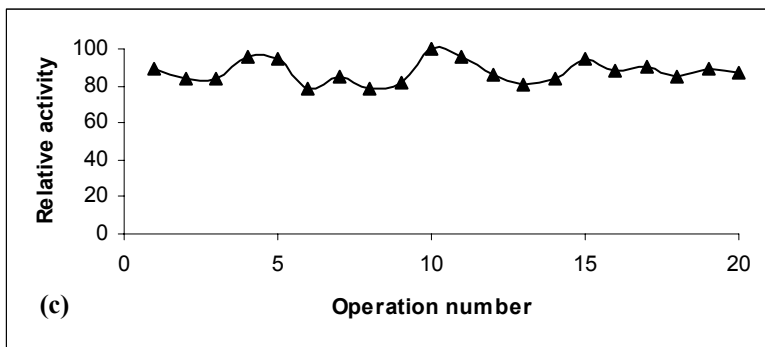
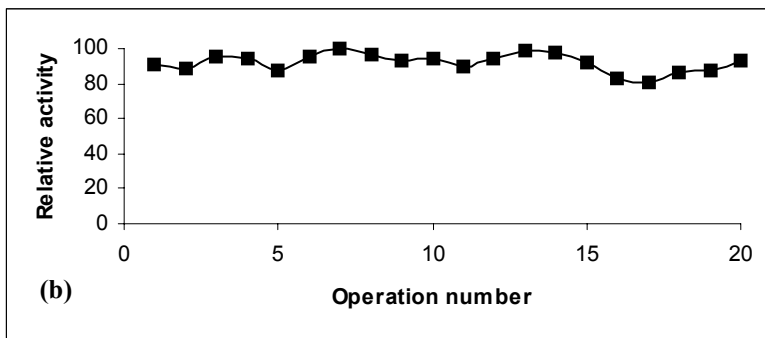
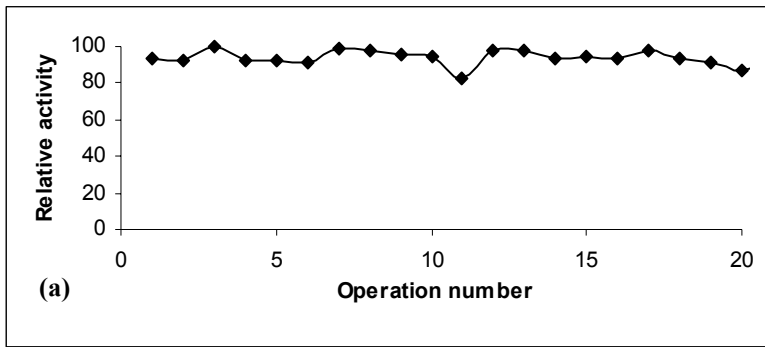


Figure 3.29 Operational stability of (a) EE2, (b) EE3, (c) EE4 and (d) EE5.

### 3.2.1.4 Effect of Temperature on the Enzyme Electrode Response

The activity of the invertase is strongly dependent on temperature, with the optimum temperature being observed between 50 and 60°C. As the temperature increases continuously after the optimum temperature the structure of the enzyme becomes altered and its catalytic properties are reduced and eventually destroyed. The effect of temperature on enzyme electrodes was investigated and is given in Figure 3.30. Maximum activity was found at 50°C for enzyme electrode 3. However, optimum temperature of immobilized invertase was shifted to the 60°C for enzyme electrodes 2, 4 and 5.

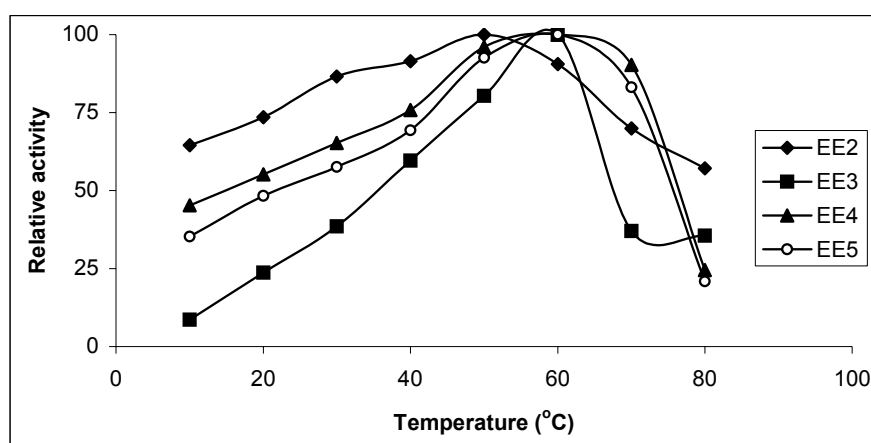


Figure 3.30 Optimum temperature of enzyme electrodes.

### 3.2.2 Immobilization of Cholesterol Oxidase in Conducting Copolymer of Thiophene-3-yl Acetic Acid Cholesteryl Ester with Pyrrole

In this study, CM/PPy and PPy were used as the supporting materials to immobilize cholesterol oxidase [179]. Immobilization was achieved by electrochemical polymerization. The presence of the cholesteryl group on the monomer (CM) was investigated in terms of enzyme activity.

This study describes a procedure involving the use of cholesterol oxidase enzyme for determination of cholesterol; the hydrogen peroxide generated by COD is measured by the oxidative coupling of 4-aminoantipyrine and phenol. The sequence of reaction is shown in Figure 3.31.

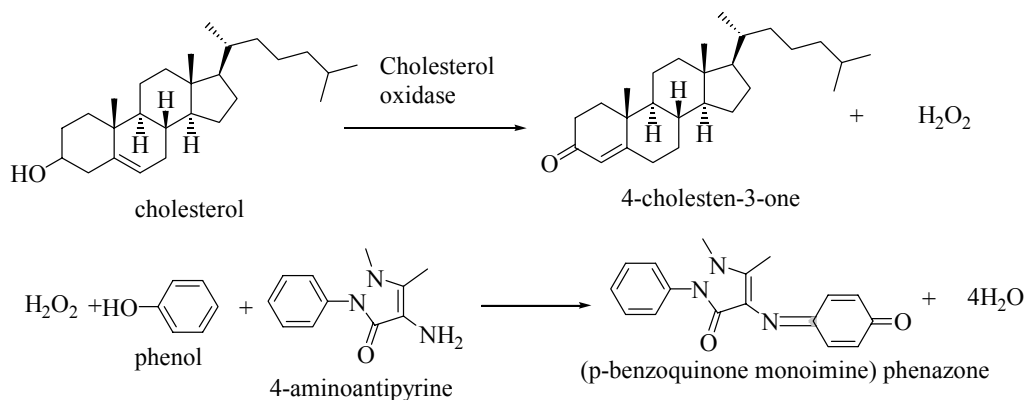


Figure 3.31 Reaction scheme for the enzymatic measurement of cholesterol.

### 3.2.2.1 Kinetic Studies of Free and Immobilized COD

Kinetic studies of the immobilized COD were performed at various concentrations of cholesterol. Maximum velocity,  $V_{\text{max}}$ , and the apparent Michaelis-Menten constant,  $K_M$ , were found from the Lineweaver-Burk plot. Kinetic constants for the oxidation of cholesterol by free and immobilized cholesterol oxidase are given in Table 3.6. There is usually a decrease in activity of an enzyme upon insolubilization, and this can be attributed to denaturation of the enzymic protein caused by the coupling process. Once an enzyme has been insolubilized, however, it finds itself in a microenvironment that is; may be drastically different from that existing in free solution. The new microenvironment might be a result of the physical and chemical character of the support matrix alone, or it may result from interactions of the matrix with substrates or products involved in the enzymatic reaction. The Michaelis constant has been found to decrease by more than one order of magnitude when substrate of opposite charge to the carrier matrix was used. Again, this only happened at

low ionic strengths, and when neutral substrates were used. The diffusion of substrate from the bulk solution to the micro-environment of an immobilized enzyme can limit the rate of the enzyme reaction. The rate at which substrate passes over the insoluble particle affects the thickness of the diffusion film, which in turn determines the concentration of substrate in the vicinity of the enzyme and hence the rate of reaction. The molecular weight of the substrate has also significant effect. Diffusion of large molecules will obviously be limited by steric interactions with the matrix, and this is reflected in the fact that the relative activity of bound enzymes towards high molecular weight substrates has been generally found to be lower than towards low molecular weight substrates. Although the different matrices were used, the  $K_m$  and  $V_{max}$  values were in the same order. This means that cholesteryl group on monomer does not affect the kinetic parameters of the immobilized COD enzyme.

Table 3.6 Kinetic parameters of free and immobilized enzyme.

	$V_{max}$	$K_m$ (mol L <sup>-1</sup> )
Free COD	$3.0 \times 10^{-1}$ <sup>a</sup>	$2.6 \times 10^{-4}$
PPy//PTSA/COD	$4.0 \times 10^{-3}$ <sup>b</sup>	$8.2 \times 10^{-5}$
CM/PPy/PTSA/COD	$7.0 \times 10^{-3}$ <sup>b</sup>	$7.8 \times 10^{-5}$

<sup>a</sup>  $\mu \text{ mol min}^{-1} \text{ mL}^{-1}$

<sup>b</sup>  $\mu \text{ mol min}^{-1} \text{ electrode}^{-1}$

### 3.2.2.2 Operational Stability of Immobilized COD

Operational stability is an important consideration for an immobilized enzyme. To determine this parameter, activities of the enzyme electrodes were checked for 25 successive measurements. Figure 3.32 and 3.33 shows the operational stability of the PPy/PTSA/COD and CM/PPy/PTSA/COD electrodes respectively. The response of the electrodes did not significantly change. Slight

increase in the response of PPy/PTSA/COD enzyme electrode is related to the swelling of the polymer structure and reorganization of the enzyme molecules in the PPy matrix (Figure 3.32). Slight decrease in the response is due to desorption of the enzyme molecules initially adsorbed on the CM/PPy layer (Figure 3.33). Hence enzyme retains their catalytic activity for a 25 measurements.

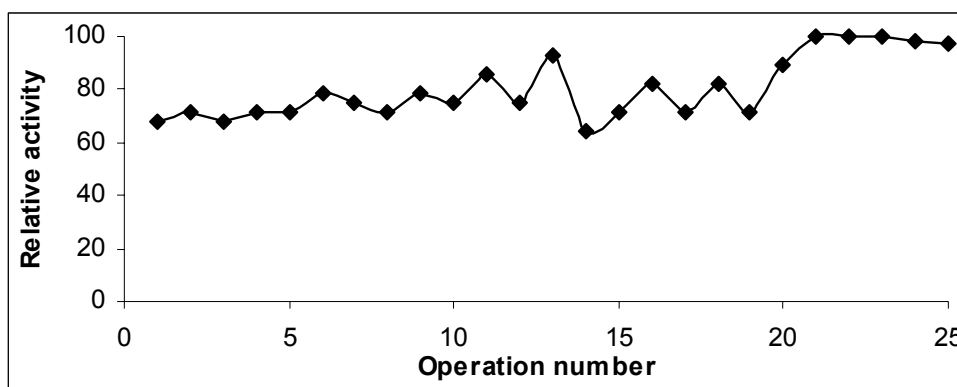


Figure 3.32 Operational stability of the PPy/PTSA/COD electrode

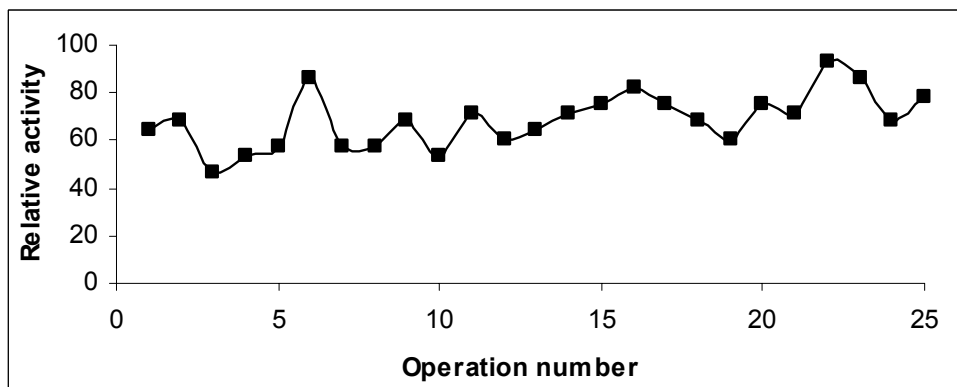


Figure 3.33 Operational stability of the CM/PPy/PTSA/COD electrode

### 3.2.2.3 Surface Morphologies of Enzyme-Entrapped Film

Scanning electron microscopy (SEM) (JEOL JSM-6400) was used to observe the surface changes of the films when the enzyme was anchored. The films were washed before analysis in order to remove unbound enzymes. The surface morphologies of these films were completely different compared to the films produced in the absence of COD. On the solution sides of the films, the cauliflower-like structure was significantly damaged when COD was anchored in each polymer matrix (Figure 3.34 (a) and (c)). Enzyme clusters, however, could not be observed on the electrode side (Figure 3.34 (b) and (d)). Small islands were observed for the electrode side of CM/PPy/PTSA film in the presence of cholesterol oxidase enzyme. In the absence of COD enzyme, electrode side of CM/PPy/PTSA film exhibited different morphology [171].

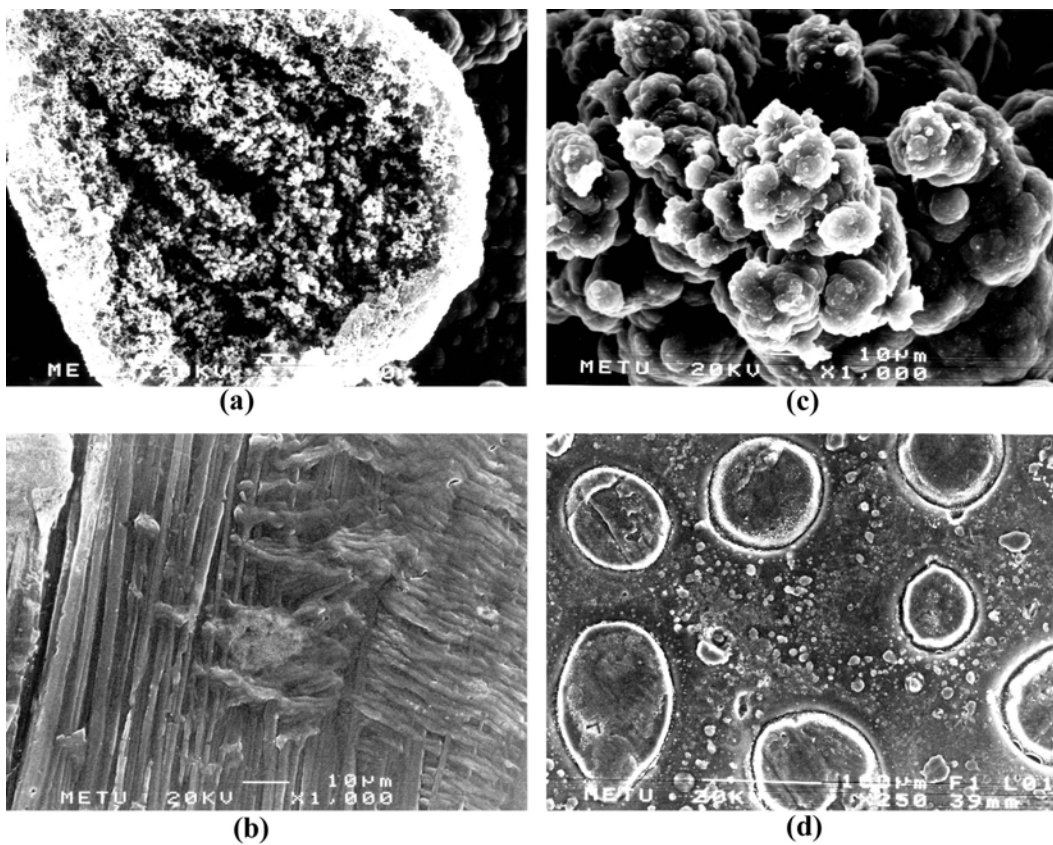


Figure 3.34 Scanning electron micrographs of (a) solution side of PPy/PTSA/COD electrode (b) electrode side of PPy/PTSA/COD electrode (c) solution side of CM/PPy/PTSA/COD electrode (d) electrode side of CM/PPy/PTSA/COD electrode.

## CHAPTER IV

### CONCLUSION

The synthesis of graft copolymers of PMTM2 with pyrrole and thiophene were achieved in the presence different solvent and supporting electrolytes. Oxidative polymerization of PMTM1 was also accomplished via both chemical and constant current electrolysis methods. Thermally stable and electrically conducting polymer films were obtained. Use of different dopants resulted in different thermal behaviors and surface morphologies.

Chemical polymerization of CM via controlled addition of  $\text{FeCl}_3$  was achieved at low temperature. Moreover, polymerization of CM was also accomplished by CCE. The syntheses of copolymers of thiophene-3-yl acetic acid cholesteryl ester (CM), PCM1 and PCM4 with pyrrole were achieved by using two different solvent-electrolyte pairs (water-PTSA and water-SDS).

Immobilization of both invertase and cholesterol oxidase enzyme in conducting copolymer matrices were achieved by electrochemical polymerization procedures. The major enzyme carrier during immobilization was determined as the pyrrole monomer. It was also shown that enzymes can be entrapped in conducting polymers, here polythiophene, which cannot be synthesized in aqueous medium. The effect of reduction on the removal of immobilized invertase activity was also investigated. Kinetic parameters, operational stability, optimum temperature and morphology of enzyme electrodes were investigated.

## REFERENCES

1. H. Shirakawa, E.J. Louis, A.G. MacDiarmid, C.K. Chiang, A.J. Heeger, J. Chem. Soc. Chem. Commun. (1977) 578.
2. C.K. Chiang, C.R. Fischer, Y.W. Park, A.J. Heeger, H. Shirakawa, E.J. Louis, S.C. Gau, A.G. MacDiarmid, Phys. Rev. Letters, 39 (1977) 1098.
3. H. Shirakawa, in Handbook of Conducting Polymers, 2nd ed.; T.A. Skotheim, R.L. Elsenbaumer, J.R. Reynolds, Eds.; Marcel Dekker: New York, 1998, pp.197-208.
4. J.C.W. Chien, Polyacetylene: Chemistry, Physics, and Materials Science, Academic: Orlando, 1984.
5. A.F. Diaz, Chem. Scr. 17 (1981) 142.
6. G. Tourillon, F.J. Garnier, J. Electroanal. Chem. 135 (1982) 173.
7. A.F. Diaz, K.K. Kanazawa, G.P. Gardini, J. Chem. Soc., Chem. Commun. (1979) 635.
8. G. Grem, G. Leditzky, B. Ullrich, G. Leising, Adv. Mater. 4 (1992) 36.
9. J.H. Burroughes, D.D.C. Bradley, A.R. Brown, R.N. Marks, K. MacKay, R.H. Friend, P.L. Burn, A.B. Holmes, Nature 347 (1990) 539.
10. J. Rault-Berthelot, J. Simonet, J. Electrochem. Soc. 182 (1985) 187.
11. A.G. MacDiarmid, A.J. Epstein, Faraday Discuss. Chem. Soc. 88 (1989) 317.
12. A.J. Heeger, S. Kivelson, J.R. Schrieffer, W.P. Su, Reviews of Modern Physics, 60 (1988) 781.
13. A. Johansson, S. Stafstrom, Physical Review B, (2002) 6504 art. no.-045207.
14. J.L. Bredas, D. Beljonne, J. Cornil, J.P. Calbert, Z. Shuai, R. Silbey, Synthetic Metals, 125 (2001) 107.

15. J.-L. Brédas, G.B. Street, *Acc. Chem. Res.* 18 (1985) 309.
16. S.N. Hoier, S.-M. Park, *J. Phys. Chem.* 96 (1992) 5188.
17. J.F. Oudard, R.D. Allendoerfer, R.A. Osteryoung, *J. Electroanal. Chem.* 241 (1988) 231.
18. K. Fesser, A.R. Bishop, D.K. Campbell, *Phys. Rev. B* 27 (1983) 4804.
19. M.G. Hill, J.F. Penneau, B. Zinger, K.R. Mann, L.L. Miller, *Chem. Mater* 4 (1992) 1106.
20. P. Bäuerle, W. Segelbacher, A. Maier, M. Mehring, *J. Am. Chem. Soc.* 115 (1993) 10217.
21. Y. Furukawa, *J. Phys. Chem.* 100 (1996) 15644.
22. J.J. Apperloo, R.A.J. Janssen, *Synth. Met.* 101 (1999) 373.
23. J.J. Apperloo, L. Groenendaal, H. Verheyen, M. Jayakannan, R.A.J. Janssen, A. Dkhissi, D. Beljonne, R. Lassaroni, J.L. Brédas, *Chem. Eur. J.* 8 (2002) 2384.
24. D. Kumar, R.C. Sharma, *Eur. Polym. J.*, 34 (1998) 1053
25. S. Asavapiriyonont, G.K. Chandler, G.A. Gunawardena, D. Pletcher, *J. Electroanal. Chem.*, 177 (1984) 229.
26. E. Genies, G. Bidan, A.F. Diaz, *J. Electroanal. Chem.*, 149 (1983) 113.
27. A.F. Diaz, J. Bargon, In *Handbook of Conducting Polymers; Vol. 1; T.A. Skotheim, Ed.; Marcel Dekker: New York, 1986, p 82.*
28. C. Pinzino, R. Angelone, F. Benvenuti, C. Carlini, A.M.R. Galletti, G. Sbrana, *J. Polym. Chem., Polym. Phys.* 36 (1986) 1901.
29. T. Okada, T. Ogata, M. Ueda, *Macromolecules* 40 (1996) 3963.
30. R. Sugimoto, S. Takeda, H.B. Gu, K. Yoshino, *Chem. Express* 1 (1986) 635.
31. N. Toshima, S. Hara, *Prog. Polym. Sci.* 20 (1995) 155.
32. P. Kovacic, M.B. Jones, *Chem. Rev.* 87 (1987) 357.
33. R.H. Baughman, J.L. Brédas, R.R. Chance, R.L. Elsenbaumer, L.W. Shacklette, *Chem. Rev.* 82 (1982) 209.
34. M. Salmon, K.K. Kanazawa, A.F. Diaz, M. Krounbi, *J. Polym. Sci.* 20 (1982) 187.

35. J.R. Reynolds, J.P. Ruiz, A.D. Child, K. Navak, D.S. Marynick, *Macromolecules* 24 (1991) 678.
36. J.R. Reynolds, A.D. Child, J.P. Ruiz, S.Y. Hong, D.S. Marynick, *Macromolecules* 26 (1993) 2095.
37. K. Doblhofer, K. Rajeshwar, In *Handbook of Conducting Polymers*; 3rd ed.; T.A. Skotheim, R.L. Elsenbaumer, J.R. Reynolds, Eds.; Marcel Dekker: New York, 1998.
38. H. Abruna, *Coordination Chemistry Reviews*, 86 (1998) 135.
39. R.F. Lane, A.T. Hubbard, *J. Phys. Chem.*, 77 (1973) 1401.
40. E. Laviron, *J. Electroanal. Chem.*, 39 (1972) 1.
41. M. De Paoli, R.J. Waltman, A.F. Diaz, J. Bargon. *J. Polym. Sci., Polym. Chem. Ed.*, 23 (1985) 1687.
42. O. Niwa, T. Tamamura, M. Kakuchi. *Macromolecules*, 20 (1987) 749.
43. H.L. Wang, L. Toppare, J.E. Fernandez, *Macromolecules*, 23 (1990) 1053.
44. E. Kalaycioglu, L. Toppare, U. Akbulut. *J. Appl. Polym. Sci.*, 61 (1996) 1067.
45. C.O. Yoon, M. Reghu, D. Moses, A.J. Heeger, Y. Cao, *Synth. Met.*, 63 (1994) 47.
46. S.A. Ghen, G.W. Hwang, *Polymer*, 38 (1997) 3333.
47. F.L. VanNice, F.S. Bates, G.L. Baker, P.J. Carroll, G.D. Patterson, *Macromolecules* 27 (1984) 2626.
48. J. Roncali, F. Garnier, *J. Chem. Soc., Chem. Comm.*, (1986) 783.
49. M.S. Kim, K. Levon, *ACS Polymer Prep.*, 37 (1996) 111.
50. M.S. Kim, K. Levon, *J. Polym. Sci. B*, 35 (1997) 1025.
51. M. Aldissi, *Chem. Soc. Chem. Comm.*, (1984) 1347.
52. M. Aldissi, A.R. Bishop, *Polymer*, 26 (1985) 622.
53. G.L. Baker, F.S. Bates, *Macromolecules*, 17 (1984) 2619.
54. S.P. Armes, B. Vincent, J.W. White, *J. Chem. Soc., Chem. Comm.*, (1986) 1525.
55. B. Francois, G. Widawski, M. Rawiso, *Synth. Met.*, 69 (1995) 491.
56. X.F. Zhong, B. Francois, *Makromol. Chem.*, 292 (1991) 2277.

57. B. Francois, G. Widawski, M. Rawiso, *Synth. Met.*, 69 (1995) 491.
58. H.S. Nalwa, *Synth. Met.*, 35 (1990) 387.
59. B. Cesar, M. Rawiso, A. Mathis, B. Francois, *Synth. Met.*, 84 (1997) 241.
60. N. Kızılyar, L. Toppare, A. Önen, Y. Yağcı, *J. Appl. Polym. Sci.*, 71 (1999) 713.
61. F.S. Bates, G.L. Baker, *Macromolecules*, 16 (1983) 704.
62. M.L. Hallensleben, F. Hollwedel, D. Stanke, *Macromol. Chem. Phys.*, 196 (1995) 3535.
63. A.I. Nazzal, G.B. Street, *Chem. Soc. Chem. Comm.*, (1985) 375.
64. D. Stanke, M.L. Hallensleben, L. Toppare, *Synth. Met.*, 55 (1993) 1108.
65. D. Stanke, M.L. Hallensleben, L. Toppare, *Synth. Met.*, 72 (1993) 89.
66. T. Olinga, B. Francois, *Makromol. Chem., Rapid Comm.*, 12 (1991) 575.
67. D. Stanke, M.L. Hallensleben, L. Toppare, *Macromol. Chem. Phys.*, 196 (1995) 75.
68. D. Stanke, M.L. Hallensleben, L. Toppare, *Synth. Met.*, 72 (1995) 89.
69. D. Stanke, M.L. Hallensleben, L. Toppare, *Macromol. Chem. Phys.*, 196 (1995) 1697.
70. N. Balci, U. Akbulut, L. Toppare, D. Stanke, M.L. Hallensleben, *Mater. Res. Bull.*, 32 (1997) 1449.
71. A.A. Argun, A. Cirpan, J.R. Reynolds, *Adv. Mater.*, 15 (2003) 1338.
72. A. Cirpan, A.A. Argun, C.R.G. Grenier, B.D. Reeves, J.R. Reynolds, *J. Mater. Chem.*, 13, (2003) 2422.
73. J.L. Boehme, D.S.K. Mudigonda and J.P. Ferraris, *Chem. Mater.*, 13 (2001) 4469.
74. I. Schwendeman, J. Hwang, D.M. Welsh, D.B. Tanner and J.R. Reynolds, *Adv. Mater.*, 13 (2001) 634.
75. I. Schwendeman, R. Hickman, G. Sonmez, P. Schottland, K. Zong, D.M. Welsh and J.R. Reynolds, *Chem. Mater.*, 14 (2002) 3118.
76. W.A. Gazotti, G. Casalbore-Miceli, A. Geri, A. Berlin and M.A. DePaoli, *Adv. Mater.*, 10 (1998) 1523.

77. H. Pages, P. Topart and D. Lemordant, *Electrochim. Acta.*, 46 (2001) 2137.
78. P. Chandrasekhar, B.J. Zay, G.C. Birur, S. Rawal, E.A. Pierson, L. Kauder and T. Swanson, *Adv. Funct. Mater.*, 12 (2002) 2137.
79. M.A. DePaoli, W.A. Gazotti, *J. Braz. Chem. Soc.*, 13(4) (2002) 410.
80. P. May, *Phys. World*, 8 (1995) 52.
81. N. S. Sariciftci, L. Smilowitz, A.J. Heeger, F. Wudl, *Science*, 258 (1992) 1474.
82. N.S. Sariciftci, D. Braun, C. Zhang, V.I. Srdanov, A.J. Heeger, G. Stucky, F. Wudl, *Appl. Phys. Lett.*, 62 (1993) 585.
83. Z. Bao, *Adv. Mater.*, 12 (2000) 227.
84. G. Horowitz, *Adv. Mater.*, 10 (1998) 365.
85. R.H. Friend, R.W. Gymer, A.B. Holmes, J.H. Burroughes, R.N. Marks, C. Taliani, D.D.C. Bradley, D.A. Dos Santos, J.L. Brédas, M. Lögdlund, W.R. Salaneck, *Nature*, 397 (1999) 121.
86. A. Kraft, A.C. Grimsdale, A.B. Holmes, *Angew. Chem. Int. Ed.*, 37 (1998) 402.
87. M.T. Bernius, M. Inbasekaran, J. O'Brien, W. Wu, *Adv. Mater.*, 12 (2000) 1737.
88. G. Yu, J. Wang, J. McElvain, A.J. Heeger, *Adv. Mater.*, 10 (1998) 1431.
89. M. Granström, K. Petritsch, A.C. Arias, A. Lux, M.R. Andersson, R.H. Friend, *Nature*, 395 (1998) 257.
90. G.G. Wallace, P.C. Dastoor, D.L. Officer, C.O. Too, *Chem. Innov.*, 30 (2000) 14.
91. L. Chen, D.W. McBranch, H. Wang, R. Helgeson, F. Wudl, D.G. Whitten, *Proc. Natl. Acad. Sci. USA*, 96 (1999) 12287.
92. D. Moses, *Appl. Phys. Lett.*, 60 (1992) 3215.
93. F. Hide, M.A. Díaz-García, B.J. Schwartz, M.R. Andersson, Q. Pei, A.J. Heeger, *Science*, 273 (1996) 1833.
94. M.D. McGehee, A.J. Heeger, *Adv. Mater.*, 12 (2000) 1655.
95. M.L. Renak, G.C. Bazan, D. Roitman, *Synth. Met.*, 97 (1998) 17.

96. T. Hebner, C. Wu, D. Marcy, M. Lu, J. Sturm, *Appl. Phys. Lett.*, 72 (1998) 519.
97. S. Chang, J. Liu, J. Bharathan, Y. Yang, J. Onohara, J. Kido, *Adv. Mater.*, 11 (1999) 734.
98. T. Granlund, T. Nyberg, L.S. Roman, M. Svensson, O. Inganäs, *Adv. Mater.*, 12 (2000) 269.
99. F. Pschenitzha, J.C. Sturm, *Appl. Phys. Lett.*, 74 (1999) 1913.
100. J.A. Rogers, Z. Bao, L. Dhar, *Appl. Phys. Lett.*, 73 (1998) 294.
101. G. Gustafsson, Y. Cao, G.M. Treacy, F. Klavetter, N. Colaneri, A.J. Heeger, *Nature*, 357 (1992) 477.
102. A. Cornish-Bowden, *Principles of Enzyme Kinetics* Butterworth Co. Ltd. London, (1976).
103. L. Michaelis, M. L. Menten, *Biochem. Z.*, 49 (1913) 333.
104. G. E. Briggs, J. B. S. Haldane, *Biochem. J.*, 19 (1925) 338.
105. H. Lineweaver, D. Burk, *J. Am. Chem. Soc.*, 56 (1934) 658.
106. G.F. Bickerstaff, *Genet. Engineer Biotechnologist*, 15 (1995) 13.
107. G.F. Bickerstaff, *Enzymes in Industry and Medicine*, E. Arnold, London, UK (1987).
108. G.F. Bickerstaff, Applications of immobilized enzymes to fundamental studies on enzyme structure and function, in *Topics in Enzyme and Fermentation Biotechnology*, E. Horwood, Chichester, UK, 9 (1984) 162.
109. R.A. Messing, Adsorption and inorganic bridge formations, in *Methods in Enzymology*, vol. XLIV, Academic, New York, (1976) 148.
110. J. Woodward, Immobilized enzymes: adsorption and covalent coupling, in *Immobilized Cells and Enzymes: A Practical Approach*, IRL, Oxford, (1985) 3.
111. J. Porath, R. Axen, (1976) Immobilization of enzymes to agar, agarose and Sephadex supports, in *Methods in Enzymology*, K. Mosbach, ed.; Academic, New York, XLIV (1976) 19.

112. J. M. S. Cabral, J.F. Kennedy, Covalent and coordination immobilization of proteins, in *Protein Immobilization* (R.F. Taylor, ed.), Marcel Dekker, New York (1991) 73.
113. P. A. Srrere, K. Uyeda, Functional groups on enzymes suitable for bind-to matrices, in *Methods in Enzymology*, K. Mosbach, ed.; Academic, New York, XLIV (1976) 11.
114. C.A. White, J.F. Kennedy, *Enzyme Microb. Technol.*, 2 (1980) 82.
115. P. Gemeiner, (1992) Materials for enzyme engineering, in *Enzyme Engineering* (P. Gemeiner, ed.; Ellis Horwood, New York, (1992) 13.
116. C. Bucke, *Phil. Trans. R. Soc. B*, 300 (1983) 369.
117. K. Nilsson, *Trends Biotechnol.*, 5 (1987) 73.
118. A. Groboillot, D.K. Boadi, D. Poncelot, R.J. Neufeld, *Crit. Rev. Biotechnol.*, 14 (1994) 75.
119. G. B. Broun, in *Methods in Enzymology*, K. Mosbach, ed.; Academic, New York, XLIV (1976) 263.
120. N.C. Foulds, C.R. Lowe, *J. Chem. Soc. Faraday Trans.*, 82 (1986) 1259.
121. P.N. Bartlett, J.M. Cooper, *J. Electroanal. Chem.*, 363 (1993) 1.
122. W. Schuhmann, *Mikrochim. Acta.*, 121 (1995) 1.
123. S. Cosnier, *Electroanalysis*, 9 (1997) 894.
124. P.N. Bartlett, D.J. Caruana, *Analyst*, 117 (1992) 1287.
125. S. Cosnier, B. Galland, C. Gondran, A. Le Pellec, *Electroanalysis* 10 (1998) 808.
126. C. Kranz, H. Wohlschlager, H.L. Schmidt, W. Schuhmann, *Electroanalysis*, 10 (1998) 546.
127. M. Umana, J. Waller, *Anal. Chem.*, 58 (1986) 2979.
128. M.D. Trevan, *Immobilized Enzymes: An introduction and applications in biotechnology*, John Wiley and sons (1980).
129. O. Zaborsky, *Immobilized Enzymes*, CRC press (1974).
130. A.I. Laskin, *Enzymes and Immobilized cells in Biotechnology*, Edited by Benjamin/Cummings publishing company (1985).

131. A.A.A. Queiroz, M. Vitolo, R.C. Oliveira, O.Z. Higa, *Radiat. Phys. Chem.*, 47(6) (1996) 873.
132. Y. Chen, E.T. Kang, K.G. Neoh, K.L. Tan, *Eur. Polym. J.*, 36 (2000) 2095.
133. P. Monsan, O. Combes, *Biotech. Bioeng.*, 26 (1984) 347.
134. U. Akbulut, S. Sungur, S. Pekyardimci, *Macromol. Rep. A*, 28 (1991) 239.
135. M. Marek, O. Valentova, J. Kas, *Biotech. Bioeng.*, 26 (1984) 1223.
136. J. Mansfeld, M. Förster, A. Schellenberger, H. Dautzenberg, *Enzyme Microb. Technol.*, 13 (1991) 240.
137. P. A. Dickensheets, L. F. Chen, G. T. Tsao, *Biotechnol. Bioeng.*, 19 (1977) 365.
138. C. Simioneseu, M. Popa, S. Dumitru, *Biotechnol. Bioeng.*, 28 (1987) 198.
139. K. Imai, T. Shiami, K. Uchida, M. Miya, *Biotechnol. Bioeng.*, 28 (1986) 198.
140. F. Selampinar, U. Akbulut, M.Y. Özden, L. Toppare, *Biomaterials* 18 (1997) 1163.
141. N. Kizilyar, U. Akbulut, M.Y. Özden, L. Toppare, Y. Yağcı, *Synth. Met.*, 104 (1999) 45.
142. S. Alkan, L. Toppare, Y. Yağcı, Y. Hepuzer, *J. Biomater. Sci. Polymer Edn.*, 10 (12) (1999) 1223.
143. C.H. Huang, J.T. Mason, *Biochim. Biophys. Acta.*, 864 (1986) 423.
144. R. Bittman, Has nature designed the cholesterol side chain for optimal interaction with phospholipids, in *Cholesterol: Its Functions and Metabolism in Biology and Medicine*, R. Bittman, Editor., Plenum Press: New York. (1997) 145.
145. H.K. Kimetberg, *Prog, Surf. Sci.*, (1973) 141.
146. F.J. Zeelen, *Medicinal Chemistry of Steroids*; Elsevier: New York, (1990) 43.
147. G.F. Gibbons, K.A. Mitropoulos, N.B. Myant, *Biochemistry of Cholesterol*; Elsevier Biomedical Press: New York, (1982).
148. J.R. Sabine, *Cholesterol*; Marcel Dekker, Inc.: New York, (1977) 245.

149. A. Kumar, R. Malhotra, B.D. Malhotra, S.K. Grover, *Anal. Chim. Acta.* 414 (2000) 43.
150. H. Wang, S. Mu, *Sensors and Actuators B*, 56 (1999) 22.
151. J.C. Vidal, E. Garcia, J.R. Castillo, *Anal. Chim. Acta.*, 385 (1999) 213.
152. J.C. Vidal, E. Garcia, J.R. Castillo, *Sensors and Actuators B*, 57 (1999) 219.
153. J.C. Vidal, E. Garcia, J.R. Castillo, *J. Pharmaceutical and Biomedical Analysis*, 24 (2000) 51.
154. W. Trettnak, I. Lioni, M. Mascini, *Electroanalysis*, 5 (1993) 753.
155. I. Karube, K. Hara, H. Matsuoka, S. Suzuki, *Anal. Chim. Acta.*, 139 (1982) 127.
156. W. Trettnak, O.S. Wolfbeis, *Anal. Biochem.*, 184 (1990) 124.
157. C.E. Hall, D. Datta, E.A.H. Hall, *Anal. Chim. Acta.*, 323 (1996) 87.
158. C.S.P. Suman, *Current Applied Physics*, 3 (2003) 129.
159. C.C. Lin, M.C. Yang, *Biomaterials*, 24 (2003) 549.
160. L.J. van der Pauw, *Philips Technical Review*, 20 (1958) 220.
161. A.R. Blythe, *Polymer Testing*, 4 (1984) 195.
162. F.M. Smits, *Bell System Technical Journal*, 37 (1958) 711.
163. S. C. Ng, Y. F. Ma, H. S. O. Chan, Z. L. Dou, *Synt. Met.*, 100 (1998) 269.
164. M. Liu, R. V. Gregory, *Synt. Met.*, 72 (1995) 45.
165. E.G. Griffin, J. M. Nelson, *J. Am. Chem. Soc.*, 38 (1916) 722.
166. M. Masoom, A. Townshend, *Anal. Chim. Acta.*, 174 (1985) 293.
167. L. Charpentier, N. Murr, *Anal. Chim. Acta.*, 318 (1995) 89.
168. A.Cirpan, S. Alkan, L. Toppare, Y. Hepuzer, Y. Yağcı, *J. Polym. Sci. Polym. Chem.*, 40 (2002) 4131.
169. C.R.E. Mansur, E.E.C. Monteiro, *J. Appl. Polym. Sci.*, 68 (1998) 345.
170. D.H. Grant, N. Grassie, *Polymer* 1 (1960) 125.
171. A.Cirpan, S. Alkan, L. Toppare, I. Cianga, Y. Yağcı, *J. Material Sci.*, 37 (2002) 1767.
172. M. Sato, H. Morii, *Macromolecules* 24 (1991) 1196.
173. X. Hu, L. Xu, *Polymer* 41 (2000) 9147.

174. E.R. Blout, M. Fields, R. Karplus, J. Amer. Chem. Soc., 70 (1984) 194.
175. X. Qiao, X. Wang, Z. Mo, Synt. Met., 118 (2001) 89.
176. A.Cirpan, S. Alkan, L. Toppare, Y. Yağcı, Y. Hepuzer, Bioelectrochemistry, 59 (2003) 29.
177. L. Michaelis, M. L. Menten, Biochem. Z., 49 (1913) 333.
178. H. Lineweaver, D. Burk, J. Am. Chem. Soc., 56 (1934) 658.
179. A.Cirpan, S. Alkan, L. Toppare, I. Cianga, Y. Yagci, Designed Monomers & Polymers, 6 (2003) 237.

## VITA

Ali Çırpan was born on January 1, 1973 in Ordu. He graduated from Middle East Technical University (METU), Department of Chemistry in 1998. He began his MS studies at Chemistry Department of METU where he became a research assistant. During this time, he worked on synthesis, characterization and electrical conductivity of poly (p-phenylene vinylene) under the supervision of Prof. Dr. Zuhâl Küçükyavuz. He began PhD studies in 2000 with Professor Levent Toppare in the area of electrochemical polymerization, conducting polymers and enzyme immobilization. He worked as a visiting graduate student at University of Florida in Prof. Dr. Reynolds' group on electrochromic devices for six months. He published ten papers in international journals, and submitted another seven.

- 1) A.Cirpan, S. Alkan, L. Toppare, G. David, Y. Yağcı, "Synthesis and electroactivity of pyrrole end-functionalized poly(2-methyl-2-oxazoline)." *European Polym. J.* 37, 2225-2229 (2001).
- 2) A.Cirpan, S. Alkan, L. Toppare, I. Cianga, Y. Yağcı, "Synthesis and characterization of conducting copolymers of thiophene-3-yl acetic acid cholesteryl ester with pyrrole." *J. Material Sci.* 37, 1767-1775 (2002).
- 3) A.Cirpan, S. Alkan, L. Toppare, Y. Hepuzer, Y. Yağcı, "Synthesis and characterization of conducting copolymers of poly(3-methyl thienyl methacrylate) with pyrrole and thiophene." *J. Polym. Sci. Polym. Chem.* 40, 4131-4140, (2002).

- 4) A.Cirpan, S. Alkan, L. Toppare, Y. Yağcı, Y. Hepuzer, "Immobilization of invertase in conducting copolymers of 3-methylthienyl methacrylate Bioelectrochemistry, 59, 29-33,(2003)."
- 5) A. Cirpan, Z. Küçükyavuz, S. Küçükyavuz, "Synthesis, characterization and electrical conductivity of poly(paraphenylene vinylene)." Turkish Polym. J. 27, 135-143 (2003).
- 6) A.Cirpan, S. Alkan, L. Toppare, I. Cianga, Y. Yagci, Immobilization of cholesterol oxidase in conducting copolymer of thiophene-3-yl acetic acid cholesteryl ester with pyrrole." Designed Monomers & Polymers 6, 237-243 (2003).
- 7) A.A. Argun, A. Cirpan, J.R. Reynolds, "The First Truly All-Polymer Electrochromic Devices." Adv. Mater., 15, 1338-1341 (2003).
- 8) A. Cirpan, A. A. Argun, C. R. G. Grenier, B.D. Reeves, J.R. Reynolds, "Electrochromic Devices Based On New Soluble And Processable Conjugated Polymers." J. Mater. Chem. 13, 2422-2428 (2003).
- 9) M. Ertas, A. Cirpan, L. Toppare "Synthesis and characterization of conducting copolymers of succinic acid bis-(4-pyrrol-1-yl-phenyl) ester and their electrochromic properties." Synth. Met., (in press 2004).
- 10) A. Cirpan, Y. Guner, L. Toppare, "Synthesis and characterization of decanedioic acid bis-(4-pyrrol-1-yl-phenyl) ester and its polymers and copolymers." Mater. Chem. Phys. (in press 2004).
- 11) P.-H. Auberta, A. A. Arguna, A. Cirpan, D.B. Tanner, J. R. Reynolds, "Microporous Patterned Electrodes for Color Matched Electrochromic Displays." Chem. Mater. (Submitted 2004).

- 12) B.D. Reeves, C. R. G. Grenier, A. A. Argun, A. Cirpan, J.R. Reynolds, "Highly soluble and processable electrochromic alkyl and alkoxy derivatized propylenedioxythiophene polymers with high coloration efficiencies." *Macromolecules* (Submitted 2004).
- 13) Bahar Bingöl, Yusuf Güner, Ali Cirpan, Levent Toppare, "Synthesis and characterization of thiophen-3-yl acetic acid 4-pyrrol-1-yl phenyl ester and its conducting polymer". *Int. J. Polym. Mater.* (in press 2004).
- 14) P. Camurlu, A. Cirpan, L. Toppare, "Conducting Polymers of Octanoic acid 2-thiophen-3-yl-ethyl ester and Their Electrochromic Properties". *J. Polym. Sci. Part A: Polym. Chem.* (Submitted 2004).
- 15) P. Camurlu, A. Cirpan, L. Toppare, "Synthesis, Characterization and Electrochromic Properties of Conducting Poly(Hexanedioic acid bis-(2-thiophen-3-yl-ethyl ester) and Its Copolymers with Thiophene and Pyrrole". *Synth. Met.* (Submitted 2004)
- 16) P. Camurlu, A. Cirpan, L. Toppare, "Dual Type Complementary Colored Polymer Electrochromic Devices Utilized by 3- Ester Substituted Thiophenes". *J. Electroanal. Chem.* (Submitted 2004).
- 17) U. Bulut, A. Cirpan, "Dual-type electrochromic devices based on conducting copolymers of thiophene-functionalized monomers". *Sensors and Actuators B: Chemical* (Submitted 2004).